



<https://theses.gla.ac.uk/>

Theses Digitisation:

<https://www.gla.ac.uk/myglasgow/research/enlighten/theses/digitisation/>

This is a digitised version of the original print thesis.

Copyright and moral rights for this work are retained by the author

A copy can be downloaded for personal non-commercial research or study, without prior permission or charge

This work cannot be reproduced or quoted extensively from without first obtaining permission in writing from the author

The content must not be changed in any way or sold commercially in any format or medium without the formal permission of the author

When referring to this work, full bibliographic details including the author, title, awarding institution and date of the thesis must be given

Enlighten: Theses

<https://theses.gla.ac.uk/>  
[research-enlighten@glasgow.ac.uk](mailto:research-enlighten@glasgow.ac.uk)

PROPERTIES OF SINGLE INWARDLY RECTIFYING  
K CHANNELS IN SKELETAL AND CARDIAC MUSCLE.

A thesis presented for the degree of

Doctor of Philosophy

by

Francis Lindley Burton

Institute of Physiology  
Glasgow University

December 1990

ProQuest Number: 11007619

All rights reserved

INFORMATION TO ALL USERS

The quality of this reproduction is dependent upon the quality of the copy submitted.

In the unlikely event that the author did not send a complete manuscript and there are missing pages, these will be noted. Also, if material had to be removed, a note will indicate the deletion.



ProQuest 11007619

Published by ProQuest LLC (2018). Copyright of the Dissertation is held by the Author.

All rights reserved.

This work is protected against unauthorized copying under Title 17, United States Code  
Microform Edition © ProQuest LLC.

ProQuest LLC.  
789 East Eisenhower Parkway  
P.O. Box 1346  
Ann Arbor, MI 48106 – 1346

## SUMMARY

An important requirement of the patch clamp technique, by which the functional properties of a single ion channel in a cell membrane may be studied, is a tight seal between the membrane and the glass pipette electrode. Hitherto, the properties of ionic channels in mammalian skeletal muscle have been studied mostly in cultured cells which present a relatively clean surface membrane. Here a method is described by which the surface membrane (sarcolemma) of adult skeletal muscle, which is normally covered by a basement membrane, is made accessible for patch clamping. It is a simplified version of a procedure previously used for the production of membrane vesicles from frog muscle by treatment with a high KCl solution containing collagenase. The method has proved applicable to human muscle biopsy samples and so may be useful in clinical investigations.

In exploring sarcolemmal vesicles from rat and human muscles the following ion channels could be readily demonstrated in high KCl solution: (i) ATP-sensitive K channels, (ii) delayed rectifier K channels, (iii) Ca-activated K channels. In addition, the following channels could be found though more rarely: (iv) inwardly rectifying K channels, (v) a channel of small conductance, (vi) a chloride channel. In subsequent work, attention was focused on the inwardly rectifying K channel as that channel had hitherto been little studied.

The role of  $Mg^{2+}$  in producing inward rectification was demonstrated by comparing the properties of the channel in patches left attached to vesicles and detached into  $Mg^{2+}$ -free solution. In the presence of internal  $Mg^{2+}$  no current passes when an outward driving force is applied and the inward current flowing in response to a small

inside negative potential shows frequent interruptions (flickery block). In the absence of internal  $Mg^{2+}$ , flickery block disappears and current flows instantaneously as readily in outward as in inward direction. When  $Mg^{2+}$  does not block the channel the existence of an intrinsic gating process which operates so as to close the channel on depolarization becomes evident. The time and voltage dependence of this gating process is described. The relationship between channel open probability ( $P_o$ ) and voltage is a steep one with a slope factor of 4.13mV. These results are compared with the already known properties of inwardly rectifying K channels in cardiac muscle.

With the patch clamp technique, membrane patches may be detached from cells or vesicles so as to allow access to the inner surface of the membrane. The effect of changes in the composition of the "intracellular" solution on channel activity may therefore be studied. To change the composition of the internal solution, detached patches were exposed to a stream of flowing solution of variable composition. Under such conditions it was found that the kinetic properties of the inwardly rectifying K channel were influenced by flow itself. This entirely new phenomenon was found also in patches detached from dispersed muscle fibres from rat flexor digitorum brevis. Analysis of the new phenomenon showed that as a result of flow, the maximum open probability is decreased and the midpoint of the  $P_o$ -voltage relation is shifted to the right by more than 20mV. No evidence could be found for the existence of a local concentration gradient sensitive to flow. Application of suction to the patch pipette showed the inwardly rectifying channels not be sensitive to membrane stretch. The possibility is contemplated that shear stress upon the inner face of the patch modulates the kinetic behaviour of the channel.

From experiments on whole cells, it is known that the inwardly rectifying K conductance is sensitive to changes in intracellular pH ( $\text{pH}_i$ ). This effect was studied at the single channel level on patches excised from rat sarcolemmal vesicles and subjected to changes in  $\text{pH}_i$  under conditions of constant flow. When  $\text{pH}_i$  was lowered from 7.4 to 6.9, 6.5 or 6.0, the channel continued to show transitions between open and short closed states, but this activity became interrupted by long lasting closures, the more so the lower  $\text{pH}_i$ . On exposure to  $\text{pH}_i$  5.0, the channel soon closed down until  $\text{pH}_i$  was returned to 7.4. During the periods of channel activity at  $\text{pH}_i$  below 7.4,  $P_o$  decreased in graded fashion the lower  $\text{pH}_i$ . This reduction in  $P_o$  during the periods of channel activity was not obviously voltage dependent and cannot therefore be attributed to a shift in the  $P_o$ -voltage relation. The current through *single* inwardly rectifying channel decreased with lowered  $\text{pH}_i$ . This effect was also not obviously voltage dependent. The decrease in  $P_o$  due to the changed kinetics whilst the channel remains active, and to the entry of the channel into a prolonged closed state, was combined with the decrease in single channel current to yield the expected reduction in macroscopic current when  $\text{pH}_i$  falls. This relation is compared with that reported in the literature.

In cardiac muscle, intracellular acidification occurs during ischaemia. It was therefore of interest to study the effect of lowered  $\text{pH}_i$  also on patches detached from guinea pig ventricular myocytes. As in skeletal muscle,  $P_o$  fell with lowered  $\text{pH}_i$ , but this time almost entirely as a result of the channel entering into a long lasting closed state. In addition, the single channel conductance fell, again as in skeletal muscle. Surprisingly, the  $K_{inw}$  channel in cardiac muscle was not sensitive to flow. This striking difference between the channel in membrane patches detached from the two tissues remains unexplained.

## CONTENTS

|                            |      |
|----------------------------|------|
| Contents . . . . .         | i    |
| List of Figures . . . . .  | iv   |
| List of Tables . . . . .   | vi   |
| Acknowledgements . . . . . | vii  |
| Declaration . . . . .      | viii |

|                        |   |
|------------------------|---|
| INTRODUCTION . . . . . | 1 |
|------------------------|---|

### CHAPTER 1

#### Materials and Methods

|                                  |    |
|----------------------------------|----|
| Sarcolemmal vesicles . . . . .   | 6  |
| Dispersed muscle cells . . . . . | 8  |
| Myocardial cells . . . . .       | 8  |
| Pipettes . . . . .               | 10 |
| Dishes . . . . .                 | 12 |
| Microscope . . . . .             | 12 |
| Electrodes . . . . .             | 13 |
| Solution change . . . . .        | 14 |
| Electrical recording . . . . .   | 15 |
| Analysis . . . . .               | 16 |

### CHAPTER 2

#### Single channel activity in skeletal muscle vesicles: an overview

|  |    |
|--|----|
| Methods . . . . .                                  | 22 |
| Results: ATP-sensitive potassium channel . . . . . | 23 |
| Delayed rectifier . . . . .                        | 23 |
| Ca-activated K channel . . . . .                   | 26 |
| Small conductance channel . . . . .                | 35 |
| Chloride channel . . . . .                         | 35 |
| Chloride channels in frog muscle . . . . .         | 39 |

CHAPTER 3

Properties of inwardly rectifying K channels:  
role of intracellular Mg and of intrinsic gating

|  |    |
|--|----|
| Introduction . . . . .   | 43 |
| Methods . . . . .  | 43 |
| Results . . . . .  | 45 |
| Ion selectivity and conductance of the open channel . . . .              | 47 |
| Block by foreign cations . . . . .                                       | 50 |
| Mechanism of inward rectification . . . . .                              | 50 |
| Kinetics in the absence of Mg <sup>2+</sup> : intrinsic gating . . . . . | 55 |

CHAPTER 4

Sensitivity of skeletal muscle inwardly rectifying K channels to flow

|   |    |
|---|----|
| Summary . . . . .   | 63 |
| Introduction . . . . .                                    | 64 |
| Methods . . . . .   | 64 |
| Results . . . . .   | 65 |
| Experiments in Mg <sup>2+</sup> -free solutions . . . . . | 69 |
| Selectivity of the flow effect . . . . .                  | 71 |
| Discussion . . . . .                                      | 74 |
| Chemical mechanisms . . . . .                             | 74 |
| Physical mechanisms . . . . .                             | 75 |

CHAPTER 5

Effect of lowering intracellular pH on  
inwardly rectifying K channels in skeletal muscle

|   |     |
|---|-----|
| Summary . . . . .   | 79  |
| Introduction . . . . .  | 80  |
| Methods . . . . .   | 82  |
| Results . . . . .   | 82  |
| Effect on channel kinetics . . . . .  | 84  |
| Effect on single channel current and leak current . . . . .   | 88  |
| Discussion: Comparison between the effects of<br>internal acidification as measured in single channel<br>and in 'intact' cell experiments . . . . . | 96  |
| Mode of action of lowered pH <sub>i</sub> . . . . .   | 99  |
| Possible physiological role of fall<br>in K <sub>inw</sub> conductance on intracellular acidification . . . .                                       | 102 |

CHAPTER 6

Sensitivity to  $pH_i$  of inwardly rectifying K channels in cardiac muscle

Summary . . . . . 105

Introduction . . . . . 107

Methods . . . . . 107

Results: Properties of inwardly rectifying  $K^+$  channel  
in cell-attached patches and in patches detached into  
solution of pH 7.4 . . . . . 108

Effects of lowering  $pH_i$  on inward rectifier . . . . . 115

Effect on channel kinetics . . . . . 117

Effect on single channel current and leak current . . . . . 122

Discussion . . . . . 130

Contribution of internal  $Mg^{2+}$   
and intrinsic gating to inward rectification . . . . . 130

Absence of inactivation . . . . . 131

Rarity of substates . . . . . 132

Absence of flow effect . . . . . 132

Effect of lowering  $pH_i$  on inwardly rectifying channel:  
decrease in single channel conductance . . . . . 133

Effects of  $pH_i$  on kinetic behaviour of cardiac channel . . . 134

Functional role of pH sensitivity  
of inwardly rectifying channels in cardiac muscle . . . . . 141

REFERENCES . . . . . 145

## List of Figures

|      |  |    |
|------|--|----|
| 2.1  | ATP-sensitive K channel . . . . .  | 24 |
| 2.2  | Transient opening of presumptive delayed rectifier . . . . .   | 25 |
| 2.3  | Calcium-activated K channel . . . . .  | 27 |
| 2.4  | Current-voltage relation of $K_{Ca}$ channel . . . . .   | 29 |
| 2.5  | Rectification of Ca-activated K channel<br>induced by blocking ions . . . . .  | 30 |
| 2.6  | $K_{Ca}$ channel activity showing substates<br>and variable gating kinetics . . . . .                                | 32 |
| 2.7  | Distributions of open and closed times<br>from recordings of $K_{Ca}$ channel activity . . . . .                     | 33 |
| 2.8  | Voltage dependence of $K_{Ca}$ channel kinetics . . . . .  | 34 |
| 2.9  | Small conductance channel . . . . .  | 36 |
| 2.10 | Chloride channel activity<br>in inside-out patch of human sarcolemma . . . . .                                       | 37 |
| 2.11 | Chart recordings of chloride channel activity . . . . .  | 38 |
| 2.12 | Giant chloride channel activity in an<br>inside-out patch detached from frog sarcolemmal vesicle . . . . .           | 40 |
| 3.1  | Effect of pH on magnesium buffering<br>in standard high K solution . . . . .   | 44 |
| 3.2  | Inwardly rectifying K channel and ATP-sensitive<br>K channel in vesicle-attached patch of human sarcolemma . . . . . | 46 |
| 3.3  | $K_{inw}$ channel in inside-out patch of rat sarcolemma . . . . .  | 48 |
| 3.4  | Conductance-voltage relation for $K_{inw}$ channel of Fig.3.3 . . . . .  | 49 |
| 3.5  | Foreign cations reduce open probability of $K_{inw}$ . . . . .   | 51 |
| 3.6  | Effect of lowering internal $[Mg^{2+}]$ on $K_{inw}$ channel . . . . .   | 52 |
| 3.7  | $K_{inw}$ channel in patch excised<br>into $Mg^{2+}$ -free symmetrical 140mM KCl solution . . . . .                  | 54 |
| 3.8  | Distributions of open and closed times<br>from recordings of $K_{inw}$ channel activity . . . . .                    | 56 |
| 3.9  | Distributions of open and closed times<br>from 150s recording at $V_h$ -60mV . . . . .                               | 57 |
| 3.10 | Rate constants at different holding potentials . . . . .   | 59 |
| 3.11 | Open probability-voltage relation for $K_{inw}$ channel . . . . .  | 60 |

|      |   |     |
|------|---|-----|
| 4.1  | Effect of flow on kinetic behaviour of single $K_{inw}$ channels  | 66  |
| 4.2  | Insensitivity of $K_{inw}$ channel<br>to stretch deformation of membrane produced by suction . .                                | 70  |
| 4.3  | Single-channel currents recorded from patch containing<br>two $K_{inw}$ channels in symmetrical $Mg^{2+}$ -free 140mM KCl . . . | 72  |
| 4.4  | Dependence of open probability<br>on membrane potential in static and flowing solution . . .                                    | 73  |
| 5.1  | Effects of lowering $pH_i$ on skeletal muscle $K_{inw}$ channels . .  | 83  |
| 5.2  | Overall open probability of $K_{inw}$ channel at different $pH_i$ . .   | 85  |
| 5.3  | Amplitude histograms of $K_{inw}$ currents at $pH_i$ 7.4 and 6.9 . .  | 89  |
| 5.4  | Reduction in open probability<br>of $K_{inw}$ channels with mild acidification . . . . .  | 90  |
| 5.5  | Amplitude histograms of $K_{inw}$ currents at $pH_i$ 7.4 and 6.0 . .  | 91  |
| 5.6  | Reduction in single $K_{inw}$ channel current at different $pH_i$ . .   | 93  |
| 5.7  | Reduction in single $K_{inw}$ channel current<br>at different holding potentials . . . . .                                      | 94  |
| 5.8  | Reduction of leak current on lowering $pH_i$ . . . . .  | 95  |
| 5.9  | Combined $P_o$ - $pH_i$ and $i$ - $pH_i$ relationships<br>for skeletal muscle $K_{inw}$ channel . . . . .                       | 97  |
| 6.1  | Inwardly rectifying K channel in cell-attached patch<br>of guinea pig ventricular myocyte . . . . .                             | 109 |
| 6.2  | Open probability-voltage relationship of $K_{inw}$ channel<br>in patch detached into $Mg^{2+}$ -free solution at pH 7.3 . . .   | 111 |
| 6.3  | Kinetic behaviour of $K_{inw}$ channel<br>in $Mg^{2+}$ -free solution at pH 7.4 . . . . .                                       | 113 |
| 6.4  | $K_{inw}$ channel activity in static and flow solutions . . . . .   | 114 |
| 6.5  | Subconductance states in cardiac $K_{inw}$ channel . . . . .  | 114 |
| 6.6  | $K_{inw}$ current activity with changes in $pH_i$ . . . . .   | 116 |
| 6.7  | Overall open probability of cardiac $K_{inw}$ at different $pH_i$ . .   | 118 |
| 6.8  | Kinetic analysis of $K_{inw}$ channel at $pH_i$ 7.3 and 6.0 . . . . .   | 120 |
| 6.9  | Effect on channel open probability of lowering $pH_i$ . . . . .   | 121 |
| 6.10 | Outward current activity of $K_{inw}$ channel at $pH_i$ 7.3 and 6.0 .   | 123 |
| 6.11 | Amplitude histograms of $K_{inw}$ currents at $pH_i$ 7.8 and 6.5 . .  | 125 |
| 6.12 | Amplitude histograms of $K_{inw}$ currents at $pH_i$ 7.3 and 6.0 . .  | 126 |
| 6.13 | Reduction in single $K_{inw}$ channel current when<br>$pH_i$ was lowered from 7.3 to 6.0 at different potentials .              | 127 |
| 6.14 | Single channel conductance at different $pH_i$ . . . . .  | 128 |

|  |     |
|--|-----|
| 6.15 Reduction in leak current when $pH_i$ was lowered<br>from 7.4 to 6.0 at different potentials . . . . .                | 129 |
| 6.16 Equations relating time constants and rate constants for<br>linear kinetic models with one open and two closed states | 136 |
| 6.17 Real and simulated activity at $pH_i$ 7.4 . . . . .   | 138 |
| 6.18 Real and simulated activity at $pH_i$ 6.0 . . . . .   | 140 |
| 6.19 Combined $P_o$ - $pH_i$ and $i$ - $pH_i$ relationships<br>for cardiac muscle $K_{inw}$ channel . . . . .              | 142 |

**Tables**

|   |     |
|---|-----|
| Table 1. Composition of solutions used in the preparation of<br>dispersed skeletal and myocardial cells . . . . .   | 9   |
| Table 2. Kinetics of inwardly rectifying $K^+$ channel<br>in static and flowing solution . . . . .                  | 68  |
| Table 3. Kinetics of inwardly rectifying $K^+$ channel<br>at $pH_i$ 7.4/5.0 and $pH_i$ 7.4/6.0 . . . . .            | 87  |
| Table 4. Rate constants derived from analysis<br>of $K_{inw}$ channel at $pH_i$ 7.3 . . . . .                       | 137 |
| Table 5. Kinetic analysis of real and simulated channel<br>activity at $pH_i$ 7.3 . . . . .                         | 137 |
| Table 6. Model rate constants for simulated activity at $pH_i$ 6.0 .  | 137 |
| Table 7. Mean open and closed times, and open probability of<br>real and simulated activity at $pH_i$ 6.0 . . . . . | 137 |

## **ACKNOWLEDGEMENTS**

I would like to thank Prof. Otto Hutter and Prof. Sheila Jennett for the use of facilities in the Institute of Physiology, Glasgow.

I am greatly indebted to Prof. Otto Hutter for his support and guidance throughout this work.

Many people have provided help. In particular, I would like to thank Anne Ward for her untiring technical support, and the people who have worked with me in the lab at one time or another: Ursula Dörstelmann, Tian Li Jun and Douglas Bovell.

During the course of this work, I was supported financially by the Medical Research Council, and the Muscular Dystrophy Association, USA.

## DECLARATION

Miss Ursula Dörstelmann was a visiting worker in the laboratory (1986-1988) and helped in the preparation of frog and later rat sarcolemma vesicles. Dr Tian Li Jun (1989) and Dr Douglas Bovell (1990) kindly helped to produce dispersed cardiac myocytes and skeletal muscle fibres. Conduct of the experiments and the analysis of the results was done by myself. None of the material has been previously presented for any other degree. Some of the results have been published during the period of this study, details of which are given below.

### Publications

BURTON, F.L., DÖRSTELMANN, U. & HUTTER, O.F. (1988). Single-channel activity in sarcolemmal vesicles from human and other mammalian muscles. *Muscle & Nerve* 11, 1029-1038.

BURTON, F.L. & HUTTER, O.F. (1989). Properties of 'inwardly rectifying' potassium channels from rat muscle in absence of 'intracellular'  $Mg^{2+}$ . *Journal of Physiology* 409, 51P.

BURTON, F.L. & HUTTER, O.F. (1988). The different actions of low intracellular pH and of formaldehyde on inwardly rectifying potassium channels from rat sarcolemmal vesicles. *Journal of Physiology* 410, 17P.

BURTON, F.L. & HUTTER, O.F. (1988). Sensitivity to flow of intrinsic gating in inwardly rectifying potassium channel from rat sarcolemmal vesicles. *Journal of Physiology* 410, 84P.

BURTON, F.L. & HUTTER, O.F. (1990). Sensitivity to flow of intrinsic gating in inwardly rectifying potassium channel from mammalian skeletal muscle. *Journal of Physiology* 424, 253-261.

BOVELL, D., BURTON, F.L., HUTTER, O.F. & TIAN, L.J. (1990). Effects of decreased internal pH on inwardly rectifying K channels in guinea pig ventricular cell membrane. *Journal of Physiology* 429, 111P.

## INTRODUCTION

It is sometimes supposed that knowledge of structure is prerequisite to successful analysis of function. But functional analysis can anticipate structure and often has done so. Thus long before the cell membrane was visualized by means of the electron microscope, its existence was established from permeability studies and its lipid bilayer structure anticipated from measurements of membrane capacitance. The existence of channels permitting the flow of ions across the membrane and of voltage-sensitive gates within such channels were also concepts first based on functional analysis, in particular on the great disparity between the magnitude of the ionic current which can cross the membrane and the much smaller charge displacement current within the membrane ascribable to the gating action which controls ionic flow. The direct study of single ion channels was opened up by the advent of the patch-clamp method fifteen years ago. This technique provided compelling evidence for the existence of a variety of membrane channels, and soon the powerful tools of molecular biology became engaged in the quest for their structure. As a result, we can now picture membrane channels as proteins with multiple transmembrane domains so arranged as to form a hydrophilic passage across the membrane. Recently, correlation between function and structure has become possible at the molecular level by combining site directed mutagenesis of channel proteins with analysis by the patch-clamp method of the functional changes so produced.

The work described in this thesis was begun in a laboratory with a long standing interest in the potassium and chloride channels responsible for the resting conductance of skeletal muscle. These channels had been studied by voltage clamping of the terminal portion

of a muscle fibre and by analysis of the noise content of the current flowing across an isolated segment of a muscle fibre, i.e. under conditions nowadays termed "macroscopic" because information on the properties of individual channels is deduced from the behaviour of many. Patch clamping had not been previously practised in this laboratory or elsewhere in this university. An important part of my work, therefore, was to set up this technique. This is reflected in Chapter 1 of this thesis which describes the patch clamp technique as now here established. Methods for computer analysis of patch clamp data also required adaptation and development as hardware became available. However, this task was considered too peripheral to the topic of this thesis to warrant detailed description.

One aim of the present work, consistent with the goal of the agencies which funded it, was to explore the properties of channels from fully developed mammalian muscle which had previously not been accessible to study. A promising approach to this end seemed the use of sarcolemmal vesicles, whose production in frog muscle had been described by other workers. After some necessary methodological adaptations, we established a reliable, simple technique for the production of sarcolemmal vesicles from mammalian muscle, including from biopsied human muscle. The novelty of this preparation warranted a survey of channels that could be readily studied in it. This survey is the substance of Chapter 2.

A feature of the work on mammalian vesicles was the extreme rarity with which Cl channels were found. This was puzzling inasmuch as sarcolemmal vesicles are composed of surface membrane which in skeletal muscle supposedly possesses a high Cl conductance. Fortunately, inwardly rectifying K channels could be found a little more frequently,

and, as these channels had at the time remained unexplored in skeletal muscle, a study of their properties was mounted. The results are described in Chapter 3. They highlight the involvement of  $Mg^{2+}$  ions in the origin of inward rectification and the existence also of an intrinsic voltage sensitive gate, as in cardiac muscle.

With the patch clamp technique, membrane patches may be detached from cells or vesicles so as to allow access to the inner surface of the membrane. The effect of changes in the composition of the 'intracellular' solution on channel activity may therefore be studied. For inwardly rectifying K channels, macroscopic experiments had shown them to be sensitive to changes in the intracellular, but not extracellular, pH. It seemed interesting to study this question also at the single channel level and a method was therefore set up for changing the composition of solution bathing the inner surface of a detached patch. This was done by exposing it to a stream of flowing solution of variable composition. In the course of these experiments, it was found that the kinetic properties of the inwardly rectifying K channel are influenced by flow itself. This entirely new phenomenon, the structural basis of which is as yet unknown, is described in Chapter 4. The flow phenomenon could be demonstrated that not only in patches detached from sarcolemmal vesicles but also in patches from single enzymatically dispersed muscle fibres and was not attributable to stretch of the membrane.

The effect of changing intracellular pH on the conductance and kinetic properties of single inwardly rectifying K channels from sarcolemmal vesicles under conditions of constant flow are reported and discussed in Chapter 5.

Chapter 6 is an extension of the work to the effects of flow and lowered 'intracellular' pH on inwardly rectifying K channels in patches isolated from enzymatically dispersed myocytes from guinea pig heart. Surprisingly, inwardly rectifying channels from that source were found to be insensitive to flow. The effects of changing intracellular pH also differed in detail.

Chapters 5 and 6 are presented in the manner of self-contained papers, so far published only in abstract form (Burton & Hutter, 1988; Bovell, Burton, Hutter & Tian, 1990). The original material in Chapters 2 to 4 has already been published (Burton, Dörstelmann & Hutter, 1988; Burton & Hutter, 1990).

**CHAPTER 1**

**Materials and Methods**

The patch clamp technique (Hamill *et al.*, 1981) involves the formation of a tight seal (of giga-ohm resistance) between the end of a glass micropipette and the cell membrane. The area within the rim of the electrode is thereby isolated electrically and currents flowing across the membrane patch can be measured. An essential condition for forming a gigaseal is that the pipette tip is smooth and the membrane "clean".

Three preparations amenable to patch clamping have been used: 1) sarcolemmal vesicles from frog and mammalian muscle, 2) dispersed mammalian skeletal muscle fibres and 3) guinea pig ventricular myocytes. The methods used to prepare these are described below. All tissues were from adult animals. This thesis is concerned with recorded currents in both "cell"-attached and inside-out patch configurations. The principal advantage of the latter configuration, obtained by simply withdrawing the pipette from the vesicle or cell, is that the solution at the cytoplasmic side of the membrane can be changed, allowing channels in the patch to be identified and their properties investigated. Sometimes the patch may be "silent", that is, it may contain no (active) channels; conversely, there may be more than one type of channel present, which restricts scope for analysis.

### Sarcolemmal vesicles

In fully developed skeletal muscle, the sarcolemma is covered by a coating of extracellular matrix. This prevents the formation of the electrically tight seal essential for patch clamping. One way in which this difficulty has been overcome is by the use of cultured myotubes or myoballs, which present a relatively clean sarcolemma (see for example

Hamill & Sakmann, 1981; Matsuda & Stanfield, 1989). Another approach, described by Standen *et al.* (1984) for frog skeletal muscle, is to make muscle swell and shed vesicles. This method was used at first with frog muscle; a simplified variant, described below, was applied with success to mammalian muscle. Moreover, it is possible to produce vesicles also from muscle fibres cut at both ends; so the method can be applied to fragments of human muscle such as are removed in surgery.

A small muscle or a bundle of muscle fibres about 1mm in diameter and 1-2cm long is excised from a freshly killed rat or mouse. The excised muscle is washed in 140mM KCl buffered to pH 7.8 with 5mM HEPES and fixed with fine pins through any already-injured cut ends in a Petri dish with a layer of Sylgard (Dow Corning) at the bottom. Fat, connective tissue and debris are removed. The solution is then changed to 140mM KCl plus collagenase (Sigma Type IA, 100 units/ml), and the covered dish is set onto a hot plate (34°C) for 20-30 minutes. That is usually long enough for some vesicles to be shed, but the majority of vesicles remain entrapped between the fibres. After transfer to the experimental solution, such vesicles are released by teasing the fibres apart with fine forceps. Vesicle size ranged from a few microns to over 100µm. All muscles tried so far have proved usable, but a muscle containing little connective tissue, e.g. semi-tendinosus, is preferred.

The samples of normal human muscle studied were parts of vastus lateralis or gluteus medius necessarily removed in the course of orthopaedic surgery. Dissected bundles were treated in the same way as described above. Spare material was kept frozen (-15°C) in buffered

KCl solution. When slowly thawed days later and treated with collagenase, it produced vesicles that were in appearance and function indistinguishable from vesicles produced by fresh muscle.

#### Dispersed muscle cells

Fibres of the mouse or rat flexor digitorum brevis (FDB) were enzymatically dissociated using a procedure similar to that described by Caldwell *et al.* (1986). Briefly, an animal was killed by stunning and cervical dislocation, FDB muscles were excised from one or both feet and pinned at one end of a strip of dental wax. The muscle was immersed in mammalian Ringer's (Table 1) to which was added bovine serum albumin (1mg/ml, Fraction V, Sigma) and collagenase (1mg/ml, Type I, Sigma). The solution was maintained at 36-37°C with a water bath and continuously bubbled with oxygen. Isolated fibres were obtained by trituration. This procedure yielded some fibres after only 15 minutes or so, but usually digestion was continued for 1 hour.

#### Myocardial cells

The procedure used is based on that described by Powell *et al.* (1980) and Isenberg and Klöckner (1982). A guinea pig was killed by a blow to the head, the heart removed quickly and mounted over the widened end of a cannula (Red Luer). The heart was perfused retrogradely through the aorta with a constant flow (cf. constant pressure of Powell *et al.*) of Tyrode's solution (Table 1). Flow rates were in the range 5-7ml/g body weight/min, a few drops per second. The temperature of the solution was kept at 37°C. After the coronary vessels were clear of blood, a mixture of collagenase (1mg/ml, Type 1, Worthington Biochemical Co., NJ,; or Type I, Sigma) and protease

**Table 1. Composition of solutions used in the preparation of dispersed skeletal and myocardial cells.**

|                                      | <b>Mammalian<br/>Ringer's</b> | <b>Tyrode's</b> | <b>KB<br/>Medium</b> |
|--------------------------------------|-------------------------------|-----------------|----------------------|
| <b>NaCl</b>                          | 140                           | 133.5           | -                    |
| <b>KCl</b>                           | 5                             | 4               | 120                  |
| <b>CaCl<sub>2</sub></b>              | 1.5                           | -               | -                    |
| <b>MgCl<sub>2</sub></b>              | 1                             | -               | -                    |
| <b>MgSO<sub>4</sub></b>              | -                             | 1.2             | 5                    |
| <b>NaH<sub>2</sub>PO<sub>4</sub></b> | -                             | 1.2             | -                    |
| <b>Glucose</b>                       | -                             | 11              | 10                   |
| <b>Succinic acid</b>                 | -                             | -               | 10                   |
| <b>Pyruvic acid</b>                  | -                             | -               | 5                    |
| <b>Taurine</b>                       | -                             | -               | 20                   |
| <b>Creatine phosphate</b>            | -                             | -               | 5                    |
| <b>K<sub>2</sub>ATP</b>              | -                             | -               | 1                    |
| <b>EGTA</b>                          | -                             | -               | 0.2                  |
| <b>HEPES</b>                         | 5                             | 10              | 10                   |
| <b>pH</b>                            | 7.4                           | 7.4             | 7.4                  |

(0.125mg/ml, Type XIV, Sigma) was added to the solution and perfusion continued for a further 2-5 minutes. The extent of digestion could be judged by gently squeezing the heart and observing the viscosity of the fluid dripping from the heart. The condition found to yield the largest numbers of healthy-looking cells was after the heart had stiffened and then become palpably soft again, when the draining perfusate usually became slightly more viscous. At this point the heart was flushed with enzyme-free Tyrode's for 30 seconds. It was then removed, still attached to the cannula, and small pieces of apical ventricular muscle cut into a vial containing Tyrode. The pieces were triturated gently with a wide-bored Pasteur pipette, and a few drops of suspension transferred to another vial containing Tyrode's or a KB medium (Table 1). This, or a further diluted suspension was added dropwise to the solution in the recording dish. The "stock" solution was stored in the fridge at 6°C for later use. Polyethylene vials and pipette were used throughout.

Cells which retained a rod shape (80-120 $\mu$ m long, 10-25 $\mu$ m wide) and with clear cross-striations were used in preference to ones which were contracted, rounded, speckled or vesiculating. Initially, 50 to 70% of myocytes were uncontracted, though the fraction dropped to well below 5% over a period of hours. Refrigeration delayed deterioration somewhat.

### Pipettes

Pipettes were pulled in advance of an experiment and kept clean under glass. They were fire-polished and filled immediately before use. Patch pipettes were pulled from hard borosilicate glass capillaries

(1.5mm o.d., 0.86mm i.d.) (GC150F, Clark Electromedical Instruments, Reading, UK) using a two stage electrode puller (Narashige, Tokyo). An ammeter was inserted into the heater circuit to allow the heater coil temperature to be set in the face of a varying mains voltage. Over several months the current needed to pull an electrode with the same tip diameter increased due to oxidisation of the Kanthal heater coil; this was replaced every nine months or so.

Pipettes were fire-polished by bringing them close to a V-shaped platinum wire heated to a dull red colour until the profile of the tip became just discernably softened; this took a few seconds. This procedure was viewed at 400x magnification through a 40x objective with a 1.5mm working distance (long enough to prevent the heat from the wire damaging the objective).

Pipettes were filled by dipping their tips into solution for a few seconds and then back-filling through a fine tube (Green Luer, 0.63mm o.d., Portex Ltd., Kent). To avoid flooding the holder when the pipette is inserted, pipettes were only half-filled. The fine fibre on the inner wall of the capillary made filling this way much easier. A single air bubble in narrow part of the filled pipette was dislodged with minimal tapping. All pipette-filling solutions were filtered through 0.22 $\mu$ m diameter pore filters (Millex-GS, Millipore (UK) Ltd., Middlesex). Care was taken to clean glassware and to prevent dust from settling on solutions. Use of old or "dirty" solutions reduced noticeably the success rate of patch formation. The resistance of pipettes filled with 140mM KCl was 8-16M $\Omega$ . Seal resistances were generally in the range 10-100G $\Omega$ .

Coating of pipettes with hydrophobic material such as Sylgard was found to be unnecessary. The extra noise introduced by the larger pipette-ground capacitance in uncoated electrodes was an insignificant proportion of total background noise. Moreover, the excessively curved meniscus as a coated pipette was dipped into the bath made it harder to manipulate the pipette in relation to the vesicle or cell.

### Dishes

Circular polystyrene dishes, 5cm in diameter (Sterilin, Middlesex, UK) with a layer of Sylgard at the bottom were used for all patch-clamp experiments. When using skeletal muscle vesicles (see above), the same dish could be used for both the preparation and recording, after the muscle bundle had been removed. The dish was placed in a circular recess of a flat Perspex block which could be moved in two dimensions with a normal mechanical stage. Using round dishes meant that most of the area at the bottom of the dish was accessible to the patch electrode, as the dish could be rotated freely.

### Microscope

Preparations were viewed and experiments done using a non-inverted microscope well suited to patch clamp work (Microtec M2, Micro Instruments Ltd., Oxford). Illumination came from a lamp unit outside the experimental cage through a flexible fibre-optic guide. Normal bright-field illumination was used, though visibility of very transparent objects such as vesicles could be improved by defocussing the condenser. Long working distance objectives (4x, 2.5cm wd; 20x, 1cm wd) allowed patch and solution-change pipettes to be manipulated within the field of view. Also, the entire objective, body tube and

eyepiece assembly could be raised away from the stage for free access to the recording dish. Finally, the binocular head contains inverting prisms, so that the sense of direction of pipette movement is preserved.

For gigaseal formation the patch pipette needs to be moved so that it is touching or pushing against the vesicle or cell. The pipette holder was mounted on a Huxley model micromanipulator with coarse and fine movements. The latter were modified by replacing the three manual micrometers with motorized drives (860-Series, Newport Ltd, Herts.) which were operated from outside the cage. The manipulator was fixed to a heavy base plate alongside the microscope, to minimize relative movement between pipette and dish contents. The base plate rested initially on an assortment of tyres and foam rubber slabs; these were replaced later by an air table (MICRO-g isolator, Technical Manufacturing Corp., Massachusetts).

### Electrodes

The pipette electrode consisted of a Teflon-coated 0.475mm diameter silver wire (AG-15T, Clark Electromedical Instruments, Reading, UK). One end of the wire was soldered into the probe's BNC connector. 4mm of Teflon was removed at the other end, and the remaining sheath sealed with epoxy. A blob of epoxy was applied to the tip of the wire, forming a short recessed region of bare silver which was chlorided. This arrangement reduced scratching which inevitably occurred when the pipette was inserted into the holder over the electrode. Even so, the electrode was re-chlorided regularly.

The bath electrode consisted of a Ag/AgCl plug immersed in 3ml KCl in a Perspex pot, connected to the bath solution through an agar bridge. To lessen junction potential changes which occur with solution changes involving (partial) replacement of, for example,  $K^+$  by a more or less mobile ion (e.g.  $TEA^+$ ), the reference half-cell and agar bridge contained a KCl solution more concentrated than that in the bath. A compromise value of 500mM was used; not so concentrated as to produce an excessive initial junction potential. Contamination of the bath by diffusion of KCl out of the agar bridge was kept low by making the aperture between bath solution and agar small.

#### Solution change

Detached membrane patches were exposed to solutions of differing composition initially by a multiple-barrel perfusion system similar to that described by Yellen (1982), and later by a single merged outflow tube like that used by Boll and Lux (1985). In both cases the solutions were driven from a set of 5ml glass syringes, using the same sort of motors used in the fine positioning of the patch electrode. Although the dead space of the second system is greater because the tip of the pipette is further from the solution outflow tubes, solution changes could be made more rapidly in practice as switching from one solution to another involved merely activating a different motor rather than moving the patch pipette or flow tubes. Once the tip of the patch pipette was in place, close to or inside the mouth of the single outlet, it was unnecessary to change its position for the duration of the experiment. Flow rates between 0.023ml/min (0.2cm/s) and 0.8ml/min (7cm/s) were used, giving dead times from less than a second to over 10 seconds. The efficacy of the system could be verified by exposing a

detached patch to solutions with different concentrations of KCl. Raising or lowering [KCl] produces a corresponding change in the current flowing through the leak conductance; such changes were swift in onset and reversible. All experiments were done at room temperature, usually between 18 and 23°C, but occasionally as high as 25°C.

### Electrical recording

Currents were measured with an EPC-7 patch clamp amplifier (List Electronic, West Germany) generally at a constant membrane potential set manually on the front panel. A voltage source driven by a Digitimer was used when voltage jumps were required. A chart recorder (Clevite Brush Mark 280; Multitrace, Electromed Ltd, Jersey; or PAR 1000, Reba Ltd., Nottingham) provided a permanent paper record of the experiment and acted as a backup for the tape recorder. Initially, current records from patch-clamp experiments were recorded on FM tape running at 15 inch/s (bandwidth DC-5kHz, <12 bit resolution). Later, the recording system was replaced with a more economical one consisting of a modified audio signal processor (Lamb, 1984) which uses domestic video tapes for storing signals. This system has a bandwidth of DC-20kHz with two analogue channels. One has 16 bit resolution and is used for storing pipette current. The other is further divided into a 12 bit channel, used for recording holding potential, and four 1 bit channels, one of which is used for a synchronisation pulse. Finally, there is a separate audio channel for commentary. The current signal from the patch-clamp amplifier is prefiltered at 10kHz with the EPC's internal low-pass filter before being recorded.

## Analysis

Current signals were replayed, further low-pass filtered and digitised as continuous records with an analogue-to-digital converter (AD11-K) or as a series of sweeps by a digital oscilloscope (Tektronics 7704A). Both sampling processes were under control of a PDP11/34 minicomputer. In the last year, this system was replaced by a PC/AT-type microcomputer with a laboratory interface card (DT2801A, Data Translation Ltd., Reading).

Analysis involving the measurement of open and closed times was done with the half-amplitude threshold technique (Colquhoun & Sigworth, 1983). Briefly, a cursor was set halfway between open and closed current levels determined from an amplitude histogram. Outward current above or below this threshold at the time of a sample is considered part of an open or closed state respectively. (When current is inward, the reverse applies.) The progress of transition detection is viewed on the screen. This is necessary because, in some recordings, baseline current may drift, but the cursor must remain midway between current levels. Although the program can compensate for slow drifts automatically, it can lose track of the baseline if it shifts suddenly. After the recording has been scanned in this way, all transitions are scrutinized in turn to exclude any dubious events, such as transients caused by minor gigaseal breakdown or mains spikes, from further analysis. A few isolated false events may have little effect on the results. However, the neglect of subconductance states, could severely distort the results, as the presence of noise fluctuations close to the threshold cursor would introduce many spurious short events. It is clearly unwise to trust the results of a completely automated analysis: one must look at the raw data.

Signals were filtered with an 8-pole Bessel filter (902LPF, Frequency Devices Inc., Massachusetts). The cutoff frequency ( $f_c$ ) set on the front panel is the frequency at which signal attenuation is -3db. When records were digitized for illustrative purposes,  $f_c$  was chosen to reduce noise to a minimum without obscuring the kinetic nature of the channel. For kinetic analysis, filter  $f_c$  was chosen more rigorously.  $f_c$  was adjusted so that noise peaks in the direction opposite to channel opening (or closing, if  $P_o$  was high) did not exceed 50% of single channel amplitude, thereby limiting the number of false events. It is not desirable to set the filter too low however, as this would have the effect of decreasing the fraction of true events detected, 1) by preventing the beneficial effect of noise on the fraction of detected events (McManus *et al.*, 1987) and, more importantly, 2) by increasing the minimum width of a rectangular pulse needed to give a half amplitude response ("dead time"). The filter's "optimal" setting is likely to vary from patch to patch with different noise levels, due to differences in seal resistance and pipette capacitance.

Measuring interval durations by sampling at a fixed rate gives rise to two kinds of errors: sampling promotion error and sampling detection error. In promotion error, the number of events included in the sampled duration is greater than expected on the basis of sampled duration because an interval with a measured duration of  $N$  sampling periods may have a true duration of between  $N-1$  and  $N+1$  sampling periods, and because durations are distributed exponentially (more short than long intervals). Sampling detection error is simply the missing of filtered events which, although exceeding the 50% threshold

level for detection, lie between sample points. The failure to detect short closed events has an effect on observed distributions of both closed and open intervals: the time constants are increased, and the relative magnitude of the exponential components may be increased or decreased. As more events are missed, the number of exponentials may change too. In practice, sampling errors of both kinds can be kept low by making the sampling interval at most one fifth of both the dead time and the fastest time constant in the data.

Histograms with constant bin width were fitted by least squares, in which the sum of squared differences between experimental and predicted distributions is minimized. The minimization engine was a modified Levenberg-Marquadt algorithm (Brown & Dennis, 1972). It is also desirable to avoid the error arising as a result of combining data into bins of a frequency histogram. If bin widths are less than 20% of the fastest time constant, this error becomes negligible. However, narrowing the bins eventually leads to an increasing proportion of bins with few (<5) counts, which would bias the fit; one assumption in non-linear regression is that errors are normally distributed. Therefore, it may be necessary to find a compromise between these two extremes, especially if the total number of events is small.

When precautions are taken in choosing  $f_c$  and sampling rate, and if channel kinetics are relatively slow and/or noise levels low, so that there are relatively few missed events, it is unnecessary to apply corrections of the type described by Roux & Sauvé (1985) or Blatz & Magleby (1986). The whole kinetic analysis process was tested using artificial signals generated with a hardware model with known rate

constants (Quantipore stochastic channel simulator, QS-100, Instrutech Corp.). This device is capable of producing voltage steps with pseudorandom dwell times whose statistics are determined by front-panel settings. Recordings from the same patch, at different potentials or in different ionic conditions, were analyzed in exactly the same way, with the same  $f_c$  and sampling rate.

Single channel current ( $i$ ) were measured in two ways. When openings or closing are very short ( $P_o$  close to 0 or 1), or when the length of recording is limited, it is necessary to measure individual unitary currents with cursors set by eye on open and closed levels. A number of such measurements would then be averaged. The size of other rare events, such as subconductance states, would need to be measured in this way too.

When the channel spends a significant fraction of time in both states, it is convenient to measure current from amplitude histograms. These are constructed by counting the number of times successive digitized samples fall within each of 256 bands spanning the current range. This count is expressed as a proportion of the total recording time. A channel fluctuating between two distinct levels will produce a histogram with two peaks. The distance between the peaks is the unitary current, and the width of the peaks gives an indication of the amount of noise in the recording after filtering. The relative areas under the peaks correspond to the proportion of time spent in each state. Two (or more) Gaussian curves can be fitted to the histogram to produce estimates of these quantities. The peaks may be made more distinct by decreasing  $f_c$  of the filter to a value lower than would be appropriate

for event detection. Such "over-filtering" of a process with relatively fast kinetics may appear as a skewed (non-Gaussian) distribution.

A number of measurements of single channel current at different holding potentials could be combined a current-voltage (IV) relation. Single channel chord conductance,  $\gamma$  was determined as  $\gamma = i/(V - V_r)$ , where  $i$  is the single channel current at holding potential  $V$ , and  $V_r$  is the reversal potential determined from the current-voltage plot.

Estimates of channel open probability ( $P_o$ ) were derived mostly from apparent open and closed times obtained as above, using the equation:

$$P_o = \hat{t}_o / (\hat{t}_o + \hat{t}_c)$$

where  $\hat{t}_o$  and  $\hat{t}_c$  are the mean values of all open and closed intervals respectively. This measure is relatively robust in the face of the sort of errors, described above, which affect time constant estimates.  $P_o$  may also be determined from the relative areas under the peaks of amplitude histograms. In the case of a single channel, this is equal to  $A_o / (A_o + A_c)$ , where  $A_o$  and  $A_c$  are the areas under the peaks corresponding to open and closed states. If the patch contains more than one channel,  $P_o$  is equal to

$$(\sum_{j=0}^N A_j \cdot j) / (A_{tot} \cdot N)$$

where  $A_j$  is the area under the peak corresponding to  $j$  channels open,  $A_{tot}$  is the total area under all the peaks, and  $N$  is the number of channels.

## **CHAPTER 2**

**Single channel activity in skeletal  
muscle vesicles: an overview.**

In this chapter, I will describe in turn the following channels seen in vesicles prepared from mammalian skeletal muscle: ATP-sensitive potassium channel, "delayed rectifier" potassium channel, Ca-activated potassium channel, a small conductance channel and a chloride channel. The inwardly rectifying potassium channel is considered in detail in later chapters. One type of chloride channel present in vesicles made from frog muscle will also be shown.

## METHODS

Patch pipettes usually contained 140 mM-KCl, 1 mM-CaCl<sub>2</sub> and 5 mM-PH buffer (HEPES or TrisOH). In some experiments, calcium was omitted from the pipette solution. The solution bathing the vesicle contained: 140 mM-KCl, 2 mM-MgCl<sub>2</sub>, 2 mM-K<sub>2</sub>ATP, 1 mM-EGTA and 5 mM-HEPES (or TrisOH). Both internal and external solutions had pH 7.8. In most experiments the patch was detached from the vesicle, so both inner and outer faces of the sarcolemma were then bathed in 140 mM KCl and  $E_K \approx E_{Cl} \approx 0$  mV. To separate  $E_K$  from  $E_{Cl}$ , in order to establish the ionic selectivity of a channel, the concentration of KCl at the inner surface of the membrane was raised or lowered. On occasion, K<sup>+</sup> at the inner and/or outer surface of the membrane was replaced by foreign cations. All experiments were done at room temperature, 19-23°C.

Vesicles could be obtained, using the method described in the previous chapter, on virtually all attempts: only if muscle is allowed to go into rigor does it fail to produce vesicles. The reliability of gigaseal formation was more variable, depending on the cleanliness of the preparation, for example the presence of connective tissue and other debris. Some patches were "silent" in that only a leak conductance of 10-100pS was present. This conductance was linear over a large (150-200mV) voltage range, though seal or membrane breakdown

artefacts appeared at extremes of polarisation. Other patches were noisy: this condition is characterised by a large (100-1000pS) conductance, often not linear (showing inward or outward rectification). This may have been due to the presence of large numbers of active channels, to a low seal resistance, or to a combination of the two. Of patches in which distinct channel activity was seen, most contained several channels, often of different types.

## RESULTS

### ATP-sensitive potassium channel

In most experiments, ATP-sensitive channels were kept closed, as in normal muscle, by the presence of ATP in the bath solution. However, when patches were detached into a bath solution from which ATP was omitted, they were the most frequently seen channels. In patches left attached to vesicles, rare, brief openings of this channel could be observed. Fig.2.1A-C shows inward current activity at -80mV recorded in the absence of ATP<sub>i</sub> and the cessation of activity when [ATP]<sub>i</sub> was raised to 2mM. Single channel conductance was 55-60pS at negative potentials. The current-voltage relationship was linear in the negative quadrant (Fig.2.1D). At potentials more positive to +40mV the channel shows slight inward rectification as has already been described for the ATP-sensitive channel in frog muscle (Spruce *et al.*, 1985, 1987).

### Delayed rectifier

In symmetrical 140mM KCl, when the membrane is in a depolarized state, delayed rectifier channels were inactivated. However, if the patch was held at a potential of -120mV, or more negative, for several

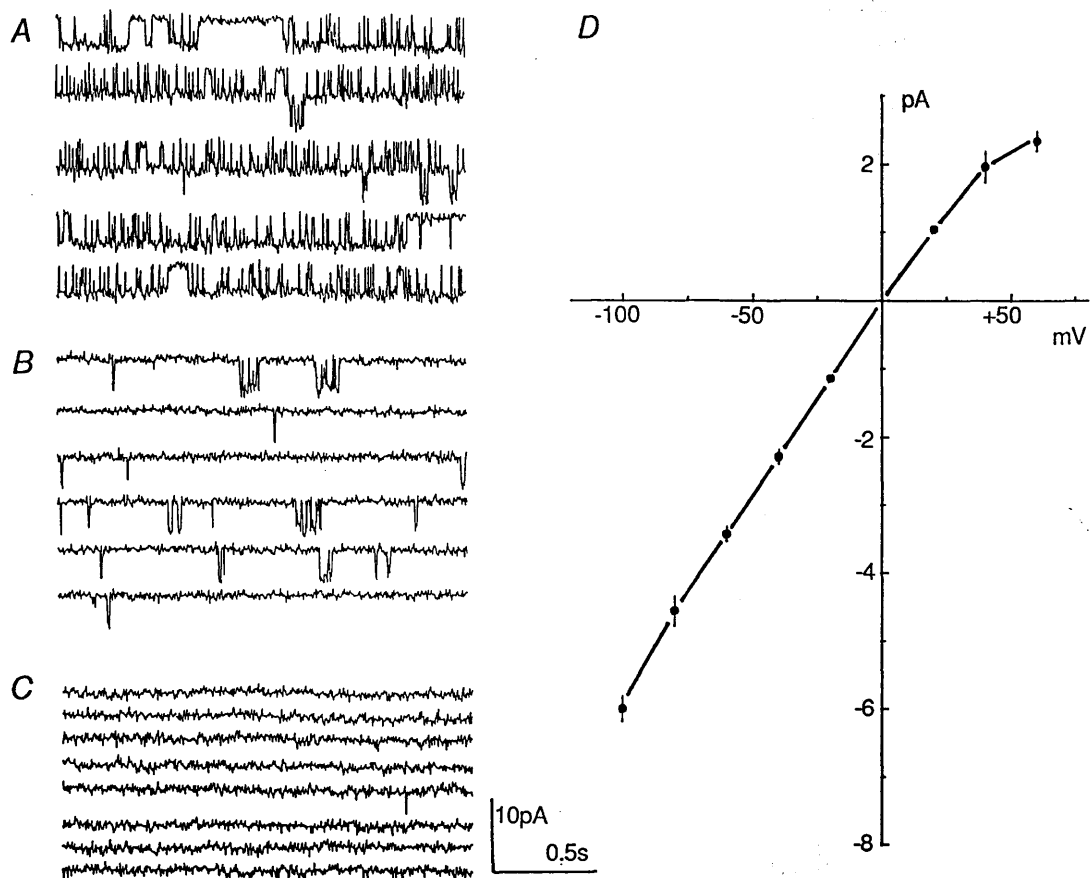


Figure 2.1. ATP-sensitive K channel. Inward current activity in inside-out patch from rat sarcolemmal vesicle at -80mV A, in the absence of internal ATP; B, cessation of activity as  $[ATP]_i$  rises to C, 2mM. Filter cutoff was 500Hz. D, current-voltage relation of ATP-sensitive channel.

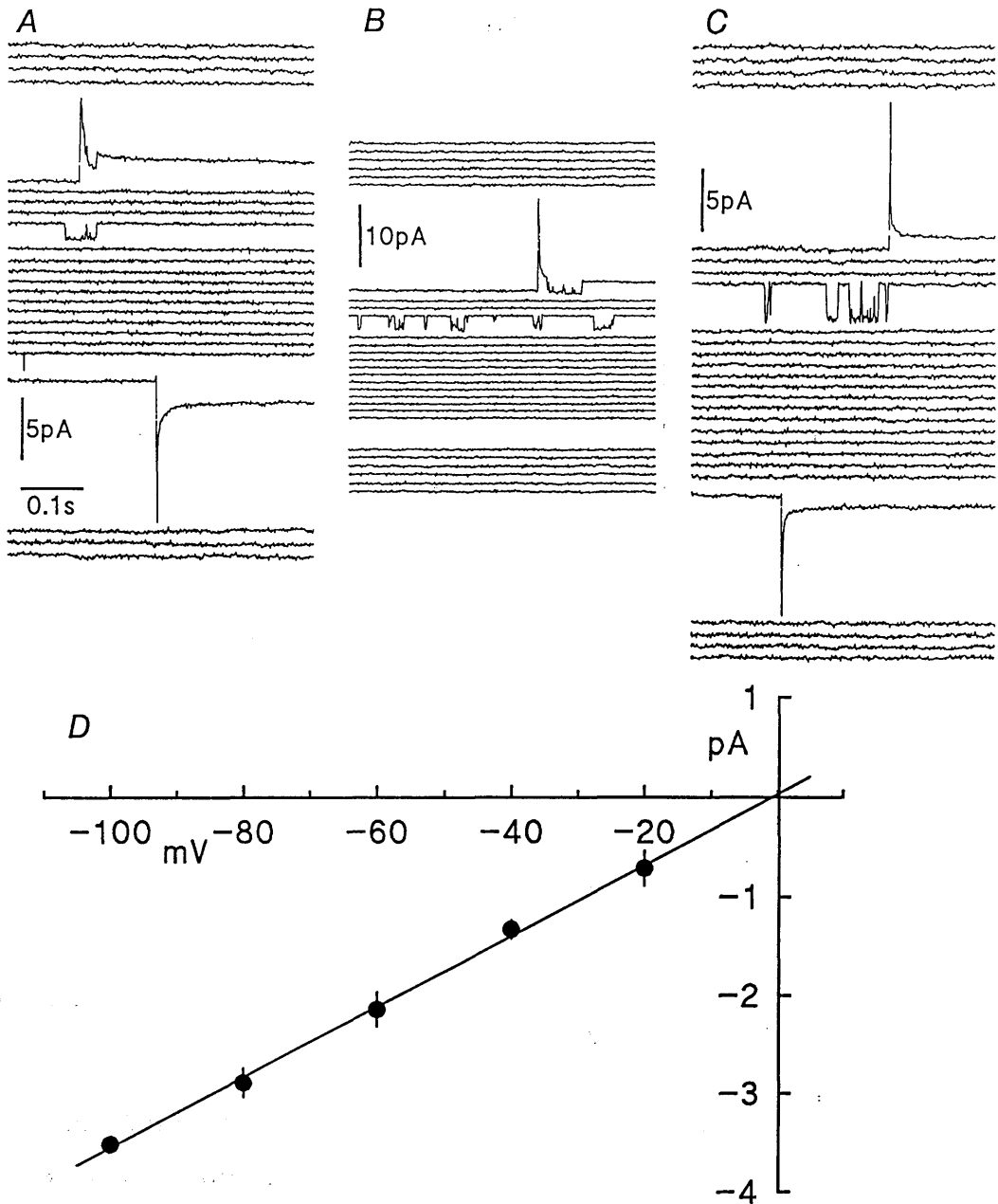


Figure 2.2. Transient opening of presumptive delayed rectifier in inside-out patch from rat sarcolemmal vesicle. Membrane potential was held at  $-120\text{mV}$  to re-prime for at least 30s before stepping to A  $-40\text{mV}$ , B  $-60\text{mV}$  and C  $-80\text{mV}$ . Continuous recording is plotted as successive sweeps, without subtraction of capacity current. Filter at 500Hz. D, current-voltage relation.

seconds, step depolarizations would frequently elicit a series of transient channel openings. Examples are shown in Fig.2.2A-C. When the potential was stepped from -120mV to -40mV and to -60mV, a channel opened during the capacity current transient and closed again within 50 ms or so. No early opening was seen after the step to -80mV. These findings are consistent with time constants of a few milliseconds for activation of the delayed rectifier in frog skeletal muscle, determined from macroscopic currents (Adrian *et al.*, 1970a) and from averaged single channel currents (Standen *et al.*, 1984). An additional feature of all three traces shown is the appearance, after a delay of more than a second, of channel openings of the same size as those occurring earlier. Such late openings were common in other experiments with a step protocol. They may represent spontaneous activity of the delayed rectifier channel, or activation of a different channel. This late activity may be related to the slow component of K<sup>+</sup> permeability described by Adrian *et al.* (1970b). The current-voltage relation for both early and late events (Fig.2.2D) is linear in the negative voltage quadrant, in which range conductance was 36pS, as compared to 30pS for frog muscle in symmetrical 120mM KCl (Standen *et al.*, 1984).

#### Ca-activated K channels

An easily identifiable channel, by virtue of its high ( $\approx 200$ pS) conductance and voltage dependent kinetics, was the calcium-dependent potassium channel (K<sub>Ca</sub>). It is activated by depolarization over a voltage range that lies further to the right the lower the internal free Ca<sup>2+</sup> concentration. Although in most experiments, stray Ca<sup>2+</sup> was buffered to negligible concentrations with 1mM EGTA, brief openings could be elicited in about 1/3 of all patches with strongly depolarizing potentials. Fig.2.3A shows typical K<sub>Ca</sub> activity at three holding

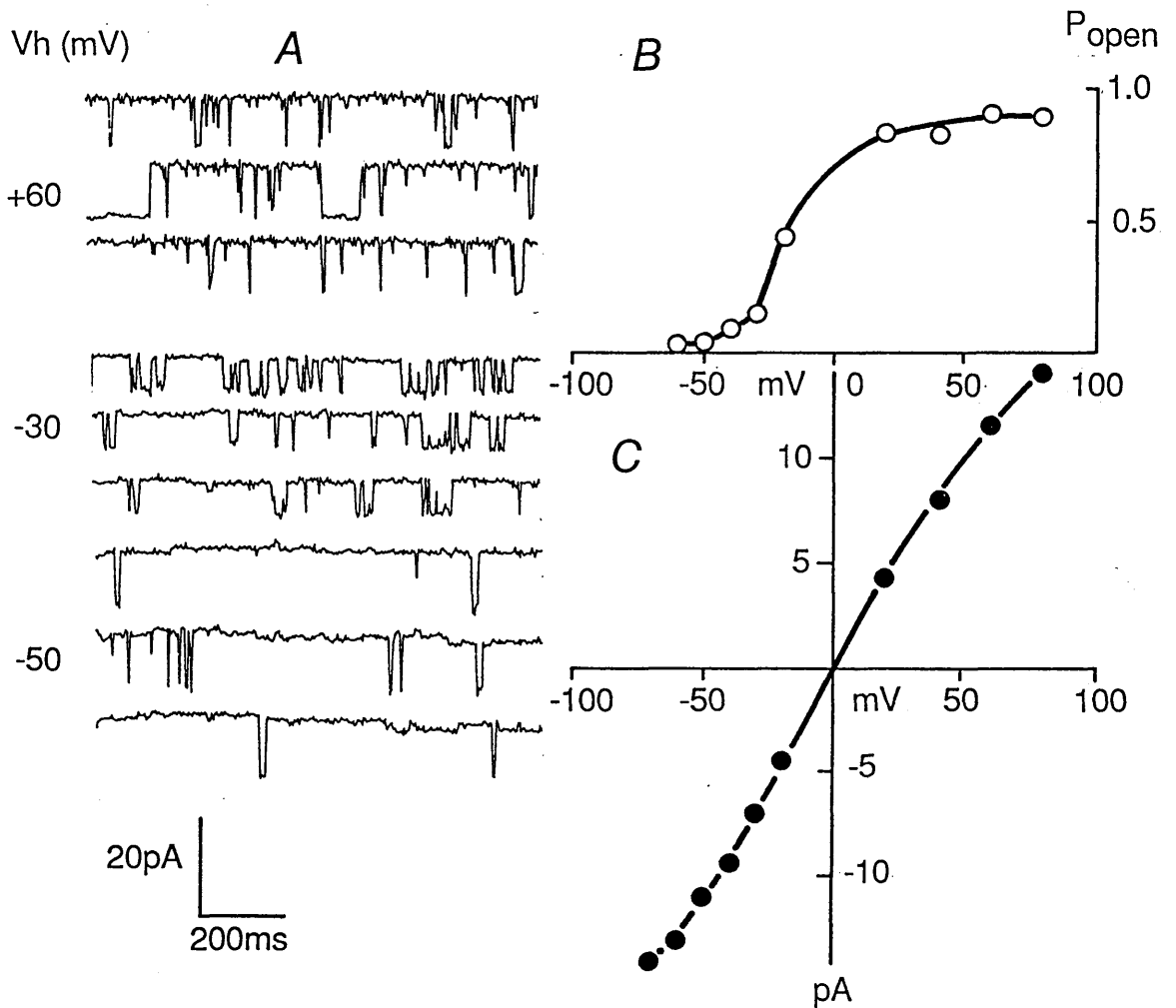


Figure 2.3. Calcium-activated K channel in inside-out patch of rat sarcolemma. Patch pipette contained no added  $\text{CaCl}_2$ .  $[\text{Ca}^{2+}]_i$  was buffered to  $30\mu\text{M}$ . A, single channel currents at three holding potentials; 1kHz filtering. B, Open probability-voltage relation. C, current-voltage relation.

potentials. In this experiment, the concentration of ionic calcium in the solution bathing the inner surface of the membrane was raised to  $30\mu\text{M}$ . At  $+60\text{mV}$  the channel passes outward current and is open most of the time; at  $-20\text{mV}$   $P_o$  is about 0.5 and bursts of openings are observable; at  $-50\text{mV}$  the channel is mainly closed. Fig.2.3B shows the activation curve for this channel determined from mean open and closed times. The current-voltage relation (Fig.2.3C) was linear in the middle range; at the extremes of the voltage range, the current-voltage relation became sub-linear, a feature observed by Yellen (1984) in  $K_{Ca}$  channels in bovine chromaffin cells. In order to determine the ionic selectivity of the Ca-activated channel, a current-voltage relationship was determined in symmetrical  $140\text{mM}$  KCl and after the concentration of KCl in the perfusion (intracellular) solution was lowered to  $70\text{mM}$  (Fig.2.4). The curve shifted to the right by  $18\text{mV}$  indicating that the channel is predominantly K selective.

The channel is blocked by foreign cations. When  $\text{K}^+$  in the pipette solution was replaced by  $135\text{mM}$   $\text{RbCl}_2 + 5\text{mM}$  CsCl, inward currents were abolished while outward currents were unaffected (Fig.2.5). This total rectification was reversed when  $\text{K}^+$  was replaced with the same mixture of foreign cations in the bath solution. When  $\text{K}^+$  was replaced bilaterally,  $K_{Ca}$  current was totally blocked.

$K_{Ca}$  channels exhibit complex kinetic behaviour. Fig.2.6 shows typical current fluctuations recorded at  $+60\text{mV}$  from an attached membrane patch containing a single  $K_{Ca}$  channel. Traces represent  $200\text{ms}$  sweeps taken at intervals over a period of about  $20\text{s}$ . Channel activity occurs in bursts separated by quiet periods. Bursts consist of successive apparent open and closed states. These apparent open states

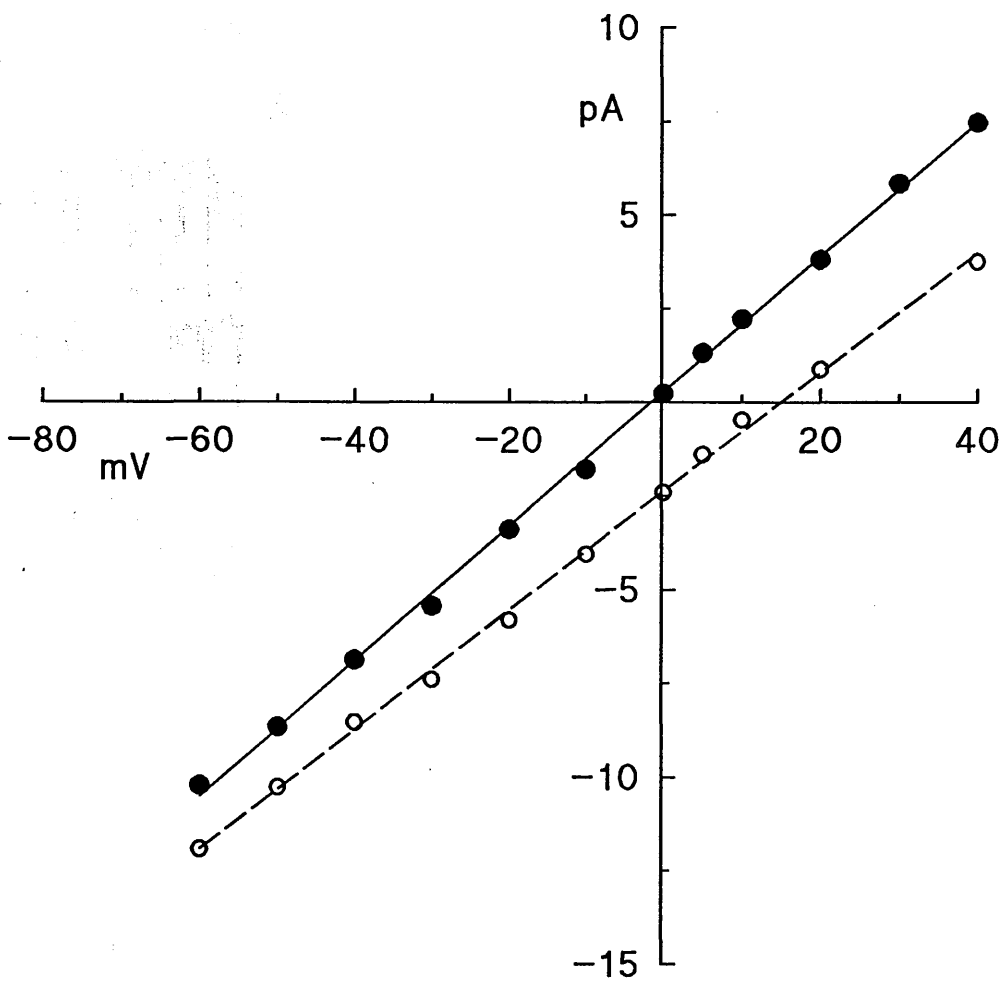


Figure 2.4. Current-voltage relation of  $K_{Ca}$  channel in inside-out patch detached from rat sarcolemmal vesicle. In symmetrical 140mM KCl (●, solid line), and after  $[KCl]_i$  was reduced to 70mM (○, dashed line).

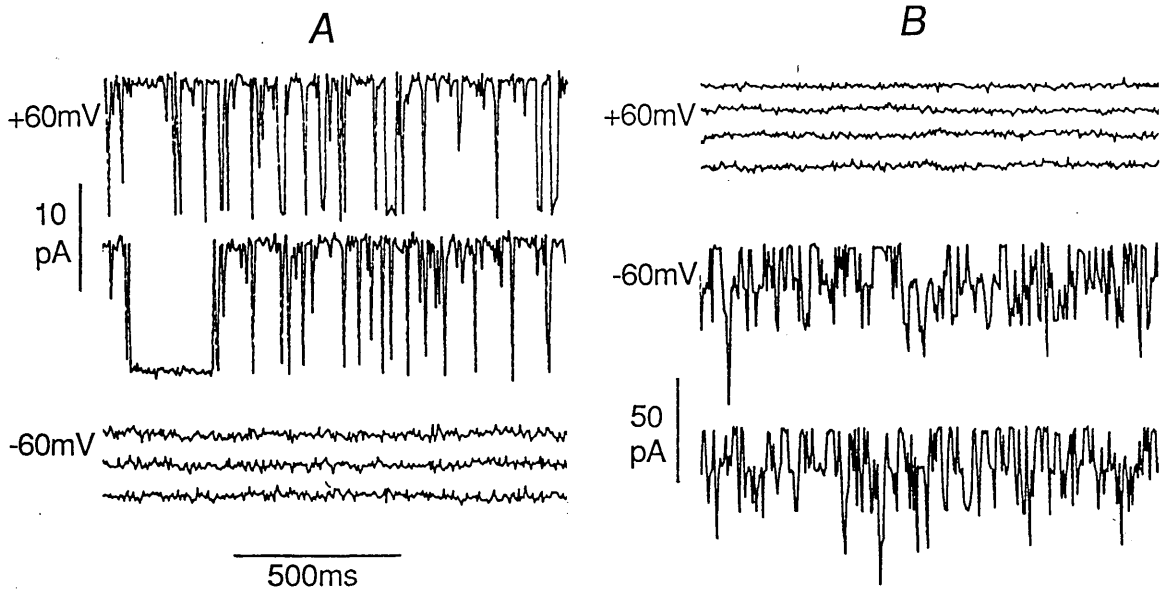


Figure 2.5. Rectification of Ca-activated K channel induced by blocking ions. Currents recorded from inside-out patches of rat sarcolemma. Membrane potential held at +60mV and -60mV; 2kHz filtering. A, pipette solution contained 135mM RbCl and 5mM CsCl; the bath solution contained 140mM KCl. Outward currents through a single  $K_{Ca}$  channel are present on depolarization, but inward currents are blocked on hyperpolarization. B, in another patch, the pipette and bath solutions were reversed. Inward currents through at least four active  $K_{Ca}$  channels when the membrane was hyperpolarized but outward currents were blocked when the membrane was depolarized.

are themselves interrupted by very short closures which appear as partial closures because of the limiting frequency response of the amplifier and low-pass filter, whose cutoff frequency was 2kHz in this case. For the same reason, some opening events are so short that they appear to be less than unit conductance. However, true substates, in which the current flowing through the channel is some fraction of the unitary current, were also observed. Three instances of substates appear in Fig.2.6.

The distributions of observed open and closed lifetimes were determined using the 50% threshold crossing method. All events were included in the analysis. Fig.2.7A&B show open and closed time histograms at +60mV. The channel mean open time was 8.1ms. The closed time distribution was best fitted with two exponentials;  $\tau_{c1} = 0.21\text{ms}$ ,  $\tau_{c2} = 1.3\text{ms}$ . Inter-burst closures were too few to contribute a significant third component. At -30mV (Fig.2.7C-E) mean open time was 3.4ms. At this potential three closed time components would be distinguished with  $\tau_{c1} = 0.27\text{ms}$ ,  $\tau_{c2} = 2.4\text{ms}$  and  $\tau_{c3} = 59\text{ms}$ .

Fig.2.6 shows another kinetic feature peculiar to the  $K_{Ca}$  channel, seen on several occasions, namely instability of channel kinetics. In the middle of the recording (shaded bar) the channel became relatively quiet, but not silent, for a couple of seconds. Most channel openings in this period are very short, and may correspond to the "short bursts" of Magleby & Pallotta (1983). It is as if  $[Ca]_i$  at the inner face of the membrane had been transiently lowered. The voltage dependence of  $K_{Ca}$  kinetics is summarized in Fig.2.8.

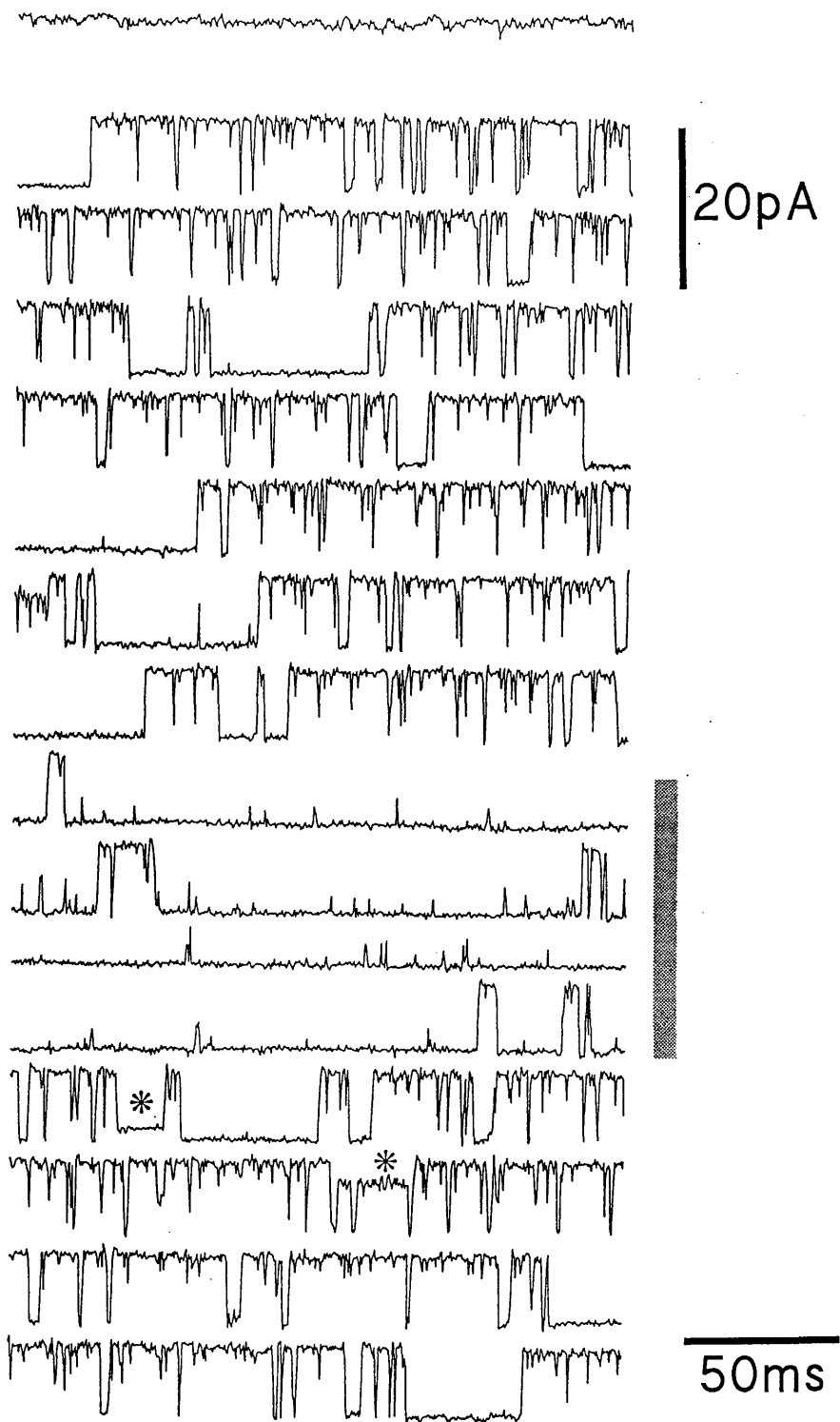


Figure 2.6.  $K_{Ca}$  channel activity showing substates and variable gating kinetics. Recording from vesicle-attached patch of rat sarcolemma at  $V_h +60mV$  (except for first trace at  $-80mV$ ). Successive 200ms sweeps were taken at 1s intervals. Substates are indicated by asterisks. Change in gating kinetics indicated by shaded bar.

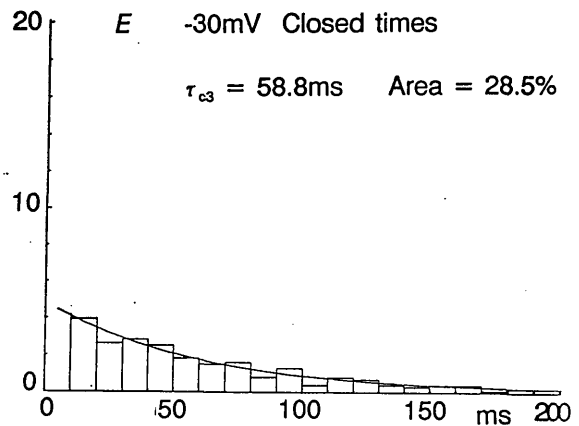
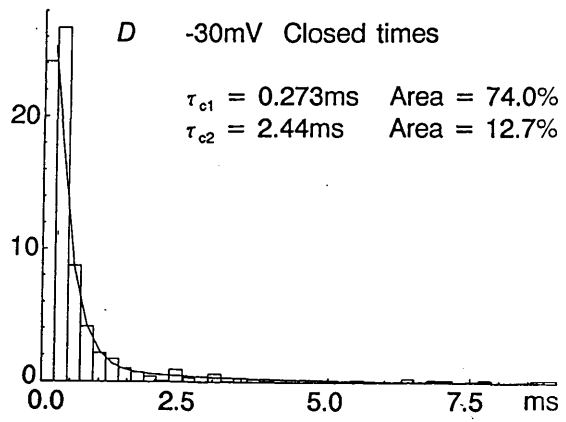
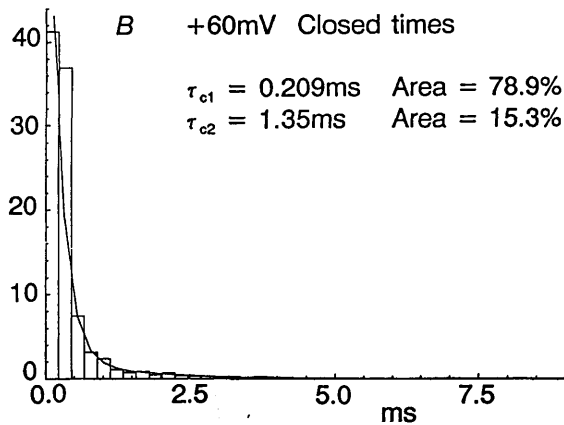
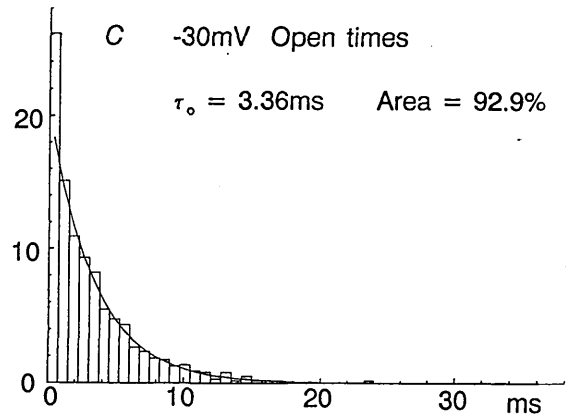
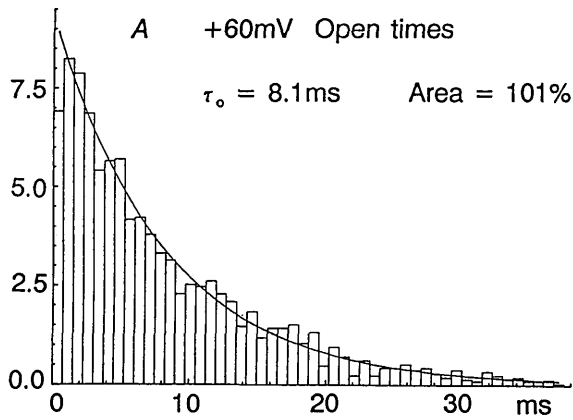


Figure 2.7. Distributions of open and closed times constructed from recordings of  $K_{Ca}$  channel activity in vesicle-attached patch (same patch as Fig.2.6). A, open time histogram at  $V_h +60\text{mV}$  with  $0.75\text{ms}$  bins (2110 events in 18s of recording). B, closed time histogram at  $V_h +60\text{mV}$  with  $0.166\text{ms}$  bins. C, open time histogram at  $V_h -30\text{mV}$  with  $0.75\text{ms}$  bins (985 events in 20s of recording). D, closed time histogram at  $-30\text{mV}$  with  $0.166\text{ms}$  bins. E, closed time histogram at  $-30\text{mV}$  with  $10\text{ms}$  bins. Ordinates of each plot are percentage of events. Parameters of fitted exponentials are given with each plot. Sampling rate  $10\text{kHz}$ , filter  $2\text{kHz}$ .

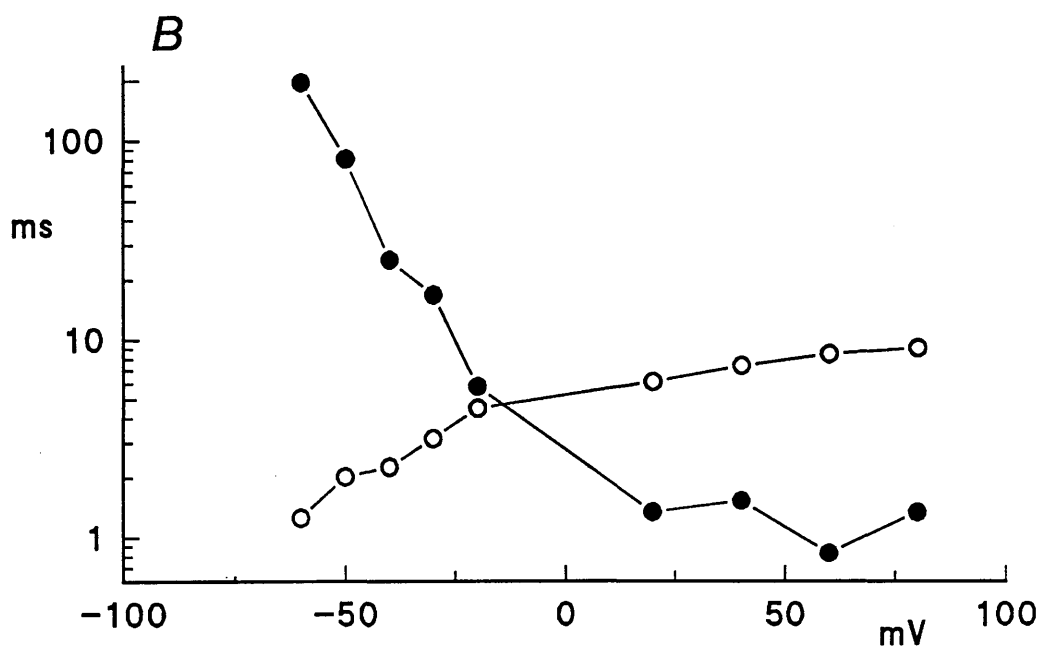
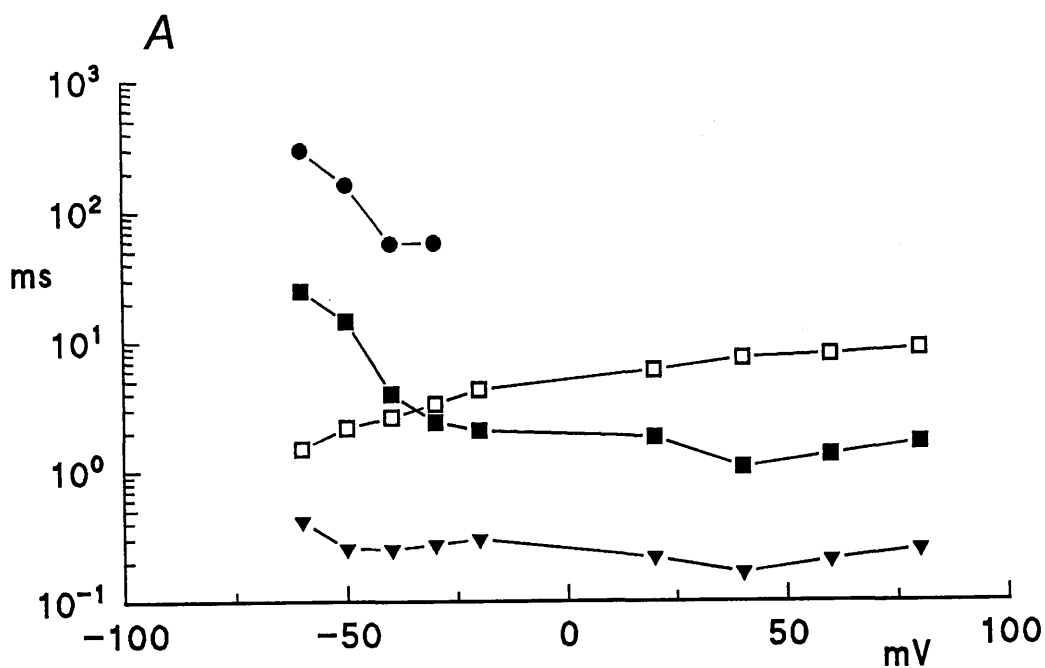


Figure 2.8. Voltage dependence of  $K_{Ca}$  channel kinetics. A, open and closed time constants at different holding potentials were determined as in Fig.2.7. Open time constant:  $\square \tau_o$ . Closed time constants:  $\blacktriangledown \tau_{c1}$ ,  $\blacksquare \tau_{c2}$  and  $\bullet \tau_{c3}$ . The longest time constant  $\tau_{c3}$  was detectable only at  $V_h \leq -30\text{mV}$ . B, mean open (O) and mean closed ( $\bullet$ ) times at the same holding potentials.

### Small conductance channel

Fig.2.9A shows a channel with a conductance of 5-6pS with unknown selectivity that appeared in a few patches. In this experiment, at +40mV, the small channel was the sole current carrying component. At -40mV, small channel currents are superimposed on current through an inward rectifier. The current voltage relation of this channel is shown in Fig.2.9B. Matsuda and Stanfield (1989) have infrequently seen a channel in rat and mouse myotubes with conductance about 9pS, which is similar to the channel we observed in kinetic appearance, but which rectifies inwardly, at least in cell-attached patches.

### Chloride channel

Only one type of channel was identified as predominantly selective for chloride ions on the basis of a shift of its reversal potential to the right, when the concentration of KCl at the inner surface of the membrane was raised threefold (Fig.2.10). In this experiment, the clamped patch of membrane contained more than one channel. This is evident from the two current levels observable at +40mV. At negative potentials, the channel opens in bursts separated by silent periods. The current-voltage relation of this Cl channel showed outward rectification, the chord conductance being 15pS at -60mV and 50pS at +60mV in 140mM KCl. Fig.2.11 shows chart records of chloride channel activity in another patch. It is evident that at positive potentials the channel undergoes inactivation, and the effect seems to be faster at +60mV than at +40mV. Again, bursts are seen at negative potentials.

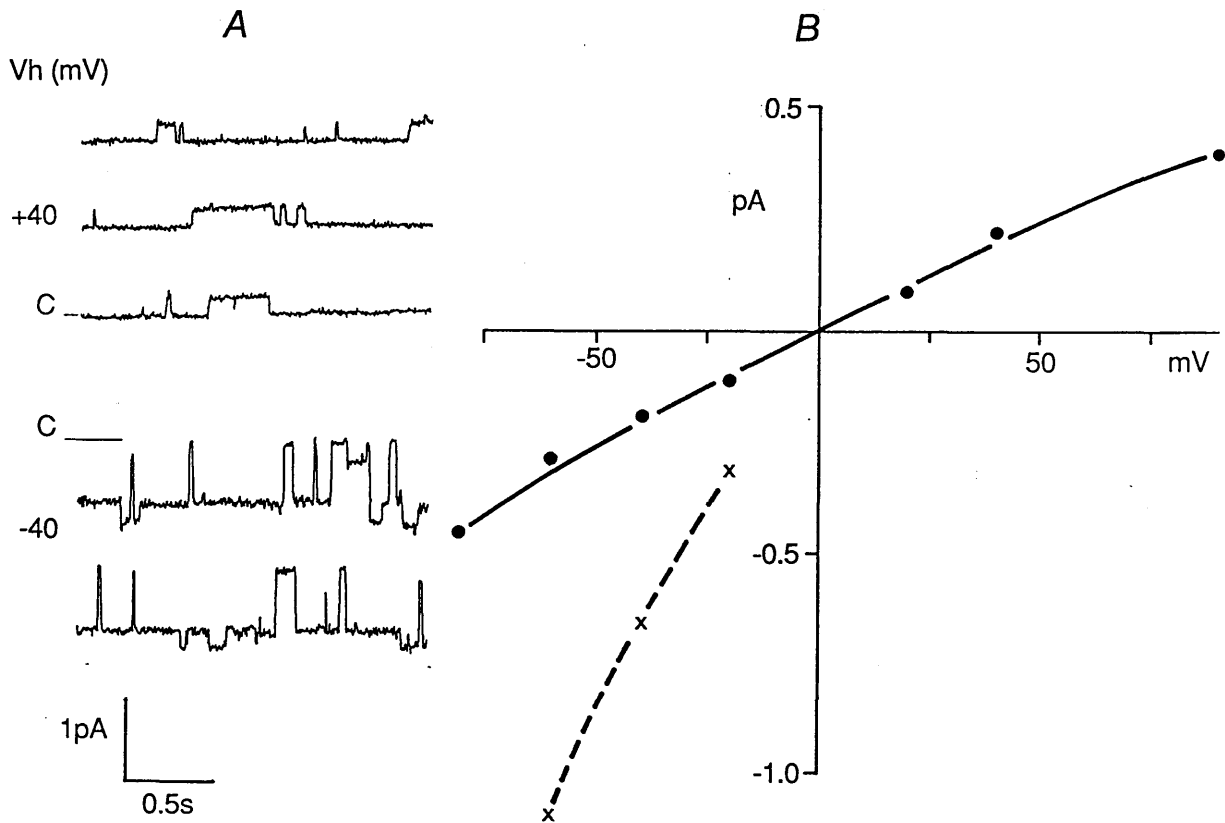


Figure 2.9. Small conductance channel of unknown selectivity in inside-out patch from rat sarcolemmal vesicle. A, at +40mV only small channel activity is seen. At -40mV small channel currents are superimposed on current through an inward rectifier. Current level at which no channels are open is indicated with letter C. B, current-voltage relation for small channel (●, solid line) and for inward rectifier (x, dashed line).

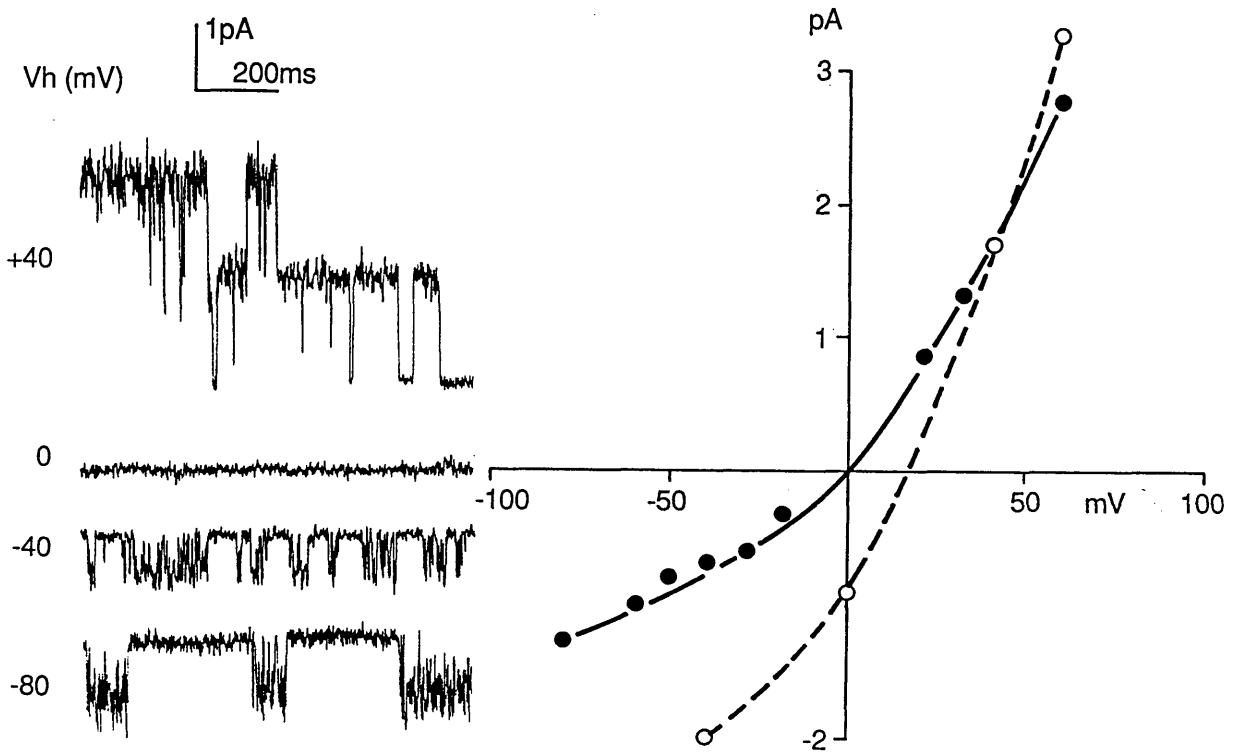


Figure 2.10. Chloride channel activity in inside-out patch of human sarcolemma. A, single channel currents at different potentials. B, current-voltage relation in symmetrical 140mM KCl (●, solid line) and after the concentration of KCl bathing the inner surface of the membrane was raised to 420mM (○, dashed line).

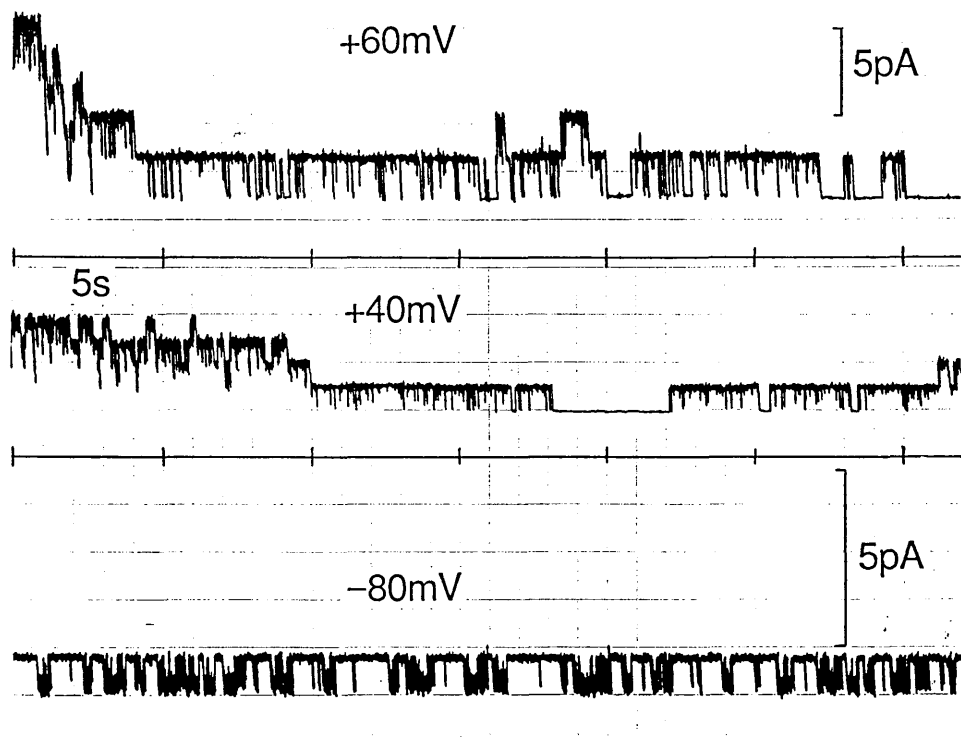


Figure 2.11. Chart recordings of chloride channel activity in the same patch as Fig.2.10 at three holding potentials. Patch contained at least five channels. Channels undergo partial inactivation at positive potentials.

### Chloride channels in frog muscle

There was one type of chloride channel which was never seen in mammalian skeletal muscle, but which was abundant in frog skeletal muscle and had a very large conductance (250-300pS). It appeared frequently, after patches were detached from vesicles. The channel was identified as being chloride selective by the shift to the right of the current voltage relation when  $[Cl]_i$  was raised. Similar channels have been reported in inside-out patches from frog toe muscle in symmetrical 110mM NaCl (Woll *et al.*, 1986, 1987).

Fig.2.12A shows unitary currents recorded when the potential across an inside-out vesicle membrane patch was stepped away from the holding potential of 0mV to +40mV and -40mV three times. In this experiment, both patch and perfusion pipettes contained 115mM RbCl, 5mM CsCl, 2mM MgCl<sub>2</sub>, 2mM Na<sub>2</sub>ATP, 1mM EGTA and 5mM Tris-maleate;  $pH_i = pH_o = 7.2$ .  $5 \times 10^{-7}$  TTX was added to the pipette solution. This patch contained at least six active channels, as is evident from the number of channel closing steps on depolarization. Channel gating was voltage dependent and graded. When the potential was stepped for 1.4s, inactivation of the channels is clearly visible on depolarization, while on hyperpolarization, the channels remained largely open. Inactivation became faster when the magnitude of the voltage steps in either direction was increased. Fig.2.12B shows the linear single channel IV relation; conductance was 275pS. Strong positive potentials (>+80mV) applied to the patch for several seconds would often cause activity of these channels to appear suddenly in previously silent patches. This curious "induction" of channel activity was also observed by Woll *et al.* (1987) in frog skeletal muscle.

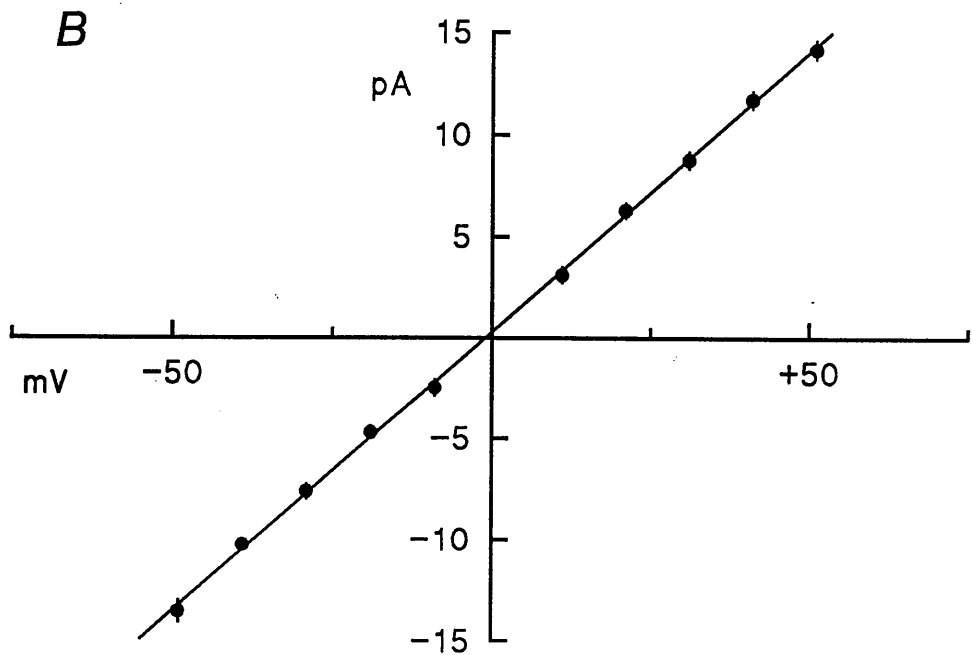
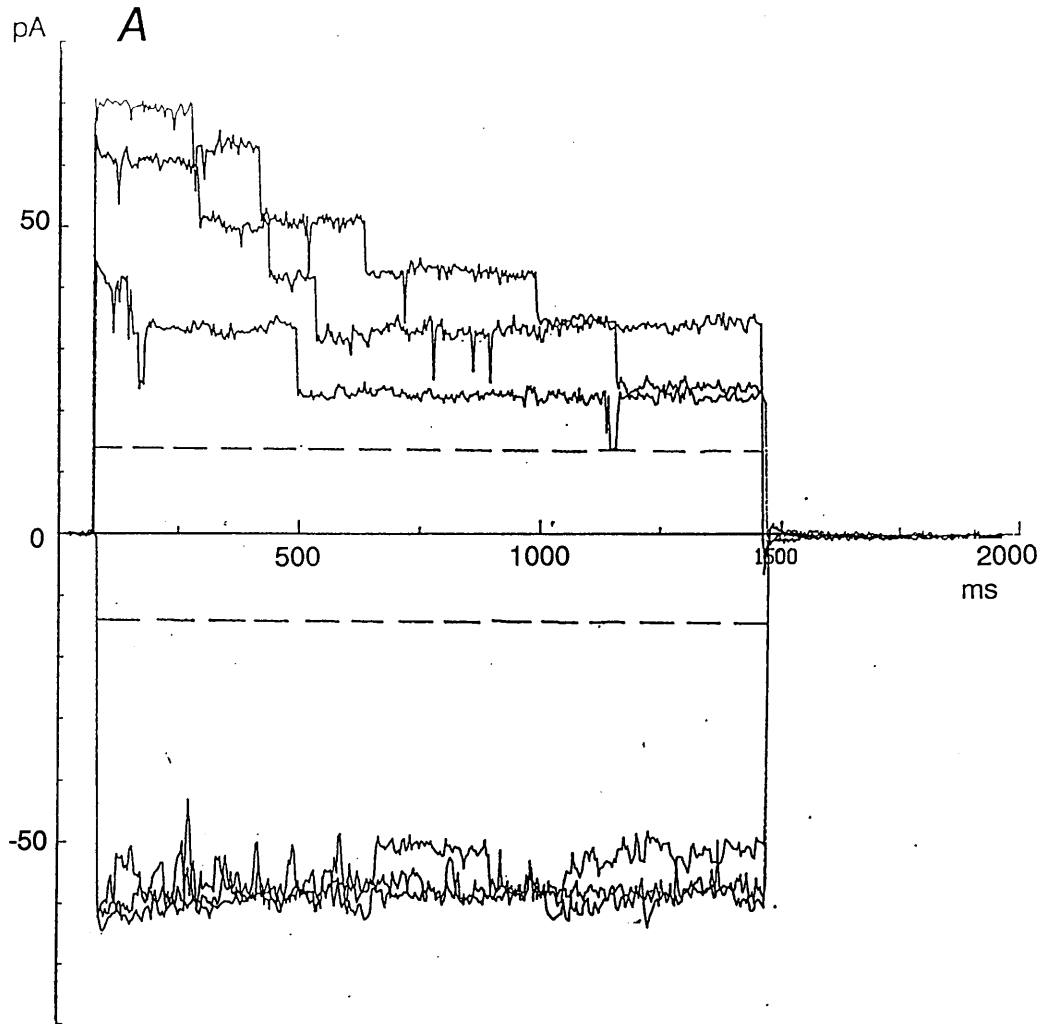


Figure 2.12. Giant chloride channel activity in an inside-out patch detached from frog sarcolemmal vesicle.  $V_h$  was held at 0mV and stepped to  $\pm 40$ mV. A, at +40mV channel activity undergoes inactivation. At -40mV little inactivation is evident. Dashed line indicates leak current. B, current-voltage relation.

Channels with similar characteristics have been reported in a wide range of other tissues which include rat cultured muscle (Blatz & Magleby, 1983), Schwann cells (Gray *et al.*, 1984), renal-derived epithelial cells (Nelson *et al.*, 1984), macrophages (Schwarze & Kolb, 1984) and rat cultured cardiac cells (Coulombe *et al.*, 1987).7)..

### CHAPTER 3

**Properties of inwardly rectifying K channels:  
role of intracellular Mg and of intrinsic gating.**

## INTRODUCTION

Inwardly rectifying properties of the resting  $K^+$  conductance were first described by Katz (1949) in skeletal muscle fibres. Membrane conductance when the membrane is negative to the potassium equilibrium potential ( $E_K$ ) greatly exceeds that at potentials more positive to  $E_K$ . Rectifying properties of macroscopic  $K^+$  currents have also been studied in heart (Hall, Hutter & Noble, 1963; Beeler & Reuter, 1970; Rougier, Vassort & Stämpfli, 1968), in neurones (Kandel & Tauc, 1966) and in egg cells (Hagiwara & Takahashi, 1974).

More recently, following refinement of patch-clamp techniques, much work has been done on inwardly rectifying K channels in cardiac tissues to establish the contribution of these channels to the "background" current ( $I_{K1}$ ) and to determine the mechanism of rectification itself. However, there have been relatively few patch-clamp studies of the inwardly rectifying conductance in skeletal muscle. This conductance is important by virtue of its magnitude; about one third of the resting conductance of skeletal muscle is due to the K inward rectifier, the remainder being a Cl conductance (Hutter & Noble, 1960).

In this chapter, some of the characteristic properties of inwardly rectifying K channels will be described.

## METHODS

Vesicles prepared from skeletal muscle, or isolated cardiac myocytes were bathed in solution which contained (unless otherwise stated) 140 mM-KCl, 1 mM-EGTA, 5 mM-HEPES (pH 7.4 or 7.8). 2 or 5 mM- $K_2$ ATP was added to silence ATP-sensitive channels.  $MgCl_2$  was varied to

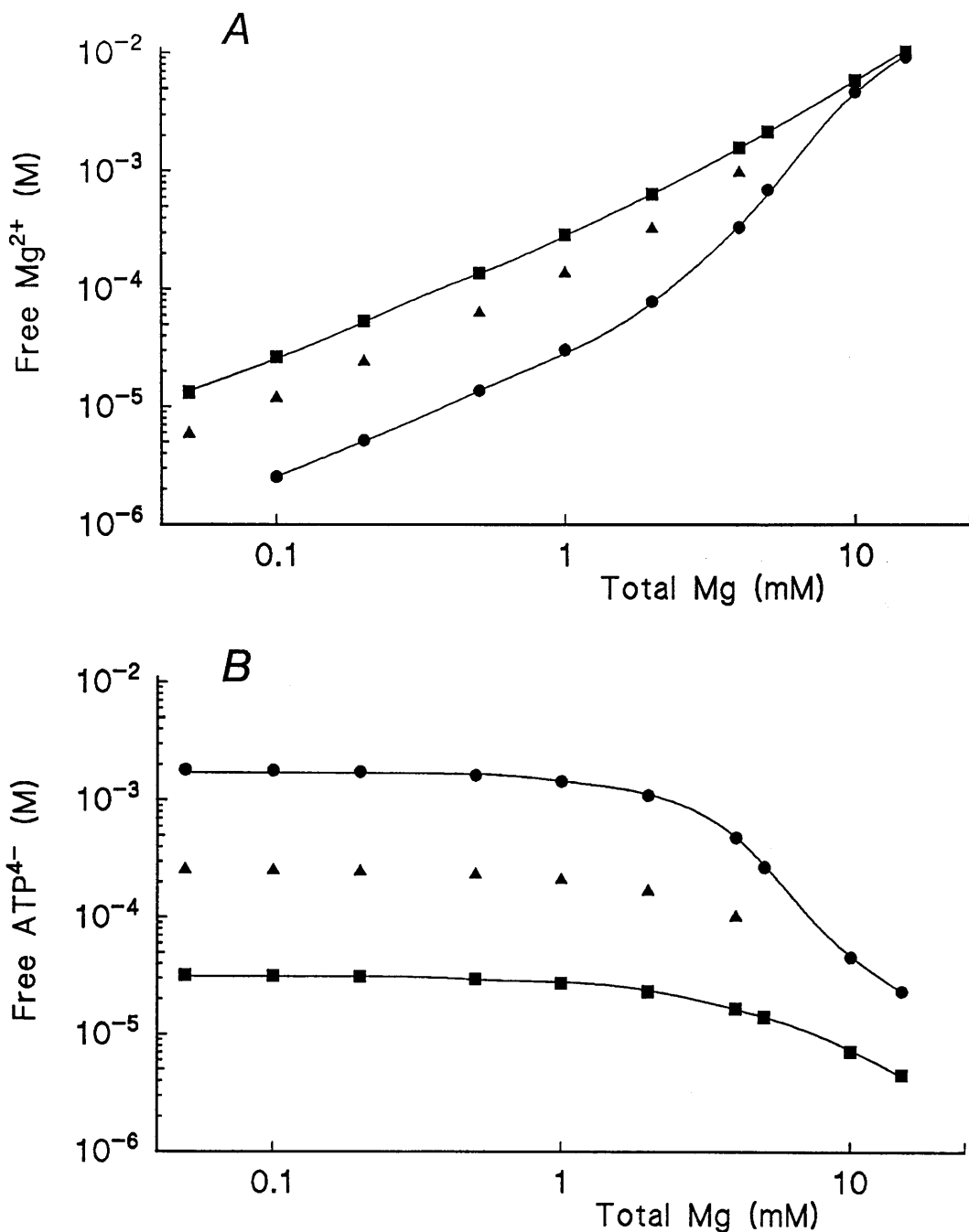


Figure 3.1. Effect of pH on magnesium buffering in standard high K solution. Free  $Mg^{2+}$  concentration was calculated for a given concentration of  $MgCl_2$  added to a solution containing 140mM KCl, 5mM  $K_2ATP$ , 1mM EGTA and 5mM HEPES at a set  $pH_a$ . Binding constants at 20°C (given below) were taken from Smith & Martell (1974) and corrected for ionic strength effects. A, free  $[Mg^{2+}]$  for a range of  $[MgCl_2]$  and at  $pH_a$  7.4 (●), 6.0 (▲) and 5.0 (■). B, free  $[ATP^{4-}]$  for the same  $[MgCl_2]$  and  $pH_a$ .

|           | ATP   |      |      |      | EGTA   |       |       |       | HEPES |      |
|-----------|-------|------|------|------|--------|-------|-------|-------|-------|------|
| $H^+$     | 6.95  | 4.05 | 1.00 | 1.00 | 9.625  | 9.000 | 2.813 | 2.117 | 7.55  | 1.00 |
| $Ca^{2+}$ | 3.982 | 1.80 |      |      | 11.188 | 5.509 |       |       |       |      |
| $Mg^{2+}$ | 4.324 | 2.74 |      |      | 5.30   | 3.47  |       |       |       |      |
| $K^+$     | 0.903 | -0.3 |      |      |        |       |       |       |       |      |

Values for ion/ligand affinities are  $\log K_{1..n}$ .

alter the free  $Mg^{2+}$  concentration.  $Mg^{2+}$  is mainly buffered by ATP and very little by EGTA or HEPES. The relationship between  $[Mg^{2+}]_{free}$  and total added  $MgCl_2$  at different pH was determined using the computer program REACT described in Smith (1983) and is plotted in Fig.3.1. The pipette solution mostly contained 140 mM-KCl and 5 mM-HEPES (pH 7.4 or 7.8). In some experiments, 1 mM- $CaCl_2$  was added to the pipette.

## **RESULTS**

Typical recordings from an inwardly rectifying channel in a vesicle-attached patch of human sarcolemma are shown in Fig.3.2A. In this experiment, a single ATP-sensitive channel was also active, but opened infrequently; the brief event at +5mV is such an opening. This experiment shows the easily recognized feature of the inwardly rectifying channel, namely the absence of detectable current activity at positive holding potentials, when the driving force on internal cations is outwards. At negative potentials, by contrast, the channel was mostly open and closes at random intervals. Both the size and frequency of the transitions between open and closed states depend on the patch membrane potential. As the holding potential approached 0mV inward current steps became undetectable in the background noise. Here the potential is close to  $E_K$ , assuming an intravesicular  $K^+$  concentration similar to that inside the pipette, i.e. 140 mM. The current-voltage relation is shown in Fig.3.2C. That of the ATP-sensitive channel is plotted for comparison.

Another feature seen in this experiment was the presence of rapid flickering in steady-state currents at potentials closer to  $E_K$ . These rapid transitions became less frequent at more negative potentials. Of interest also is the finding that channel open probability is limited at the more negative potentials, i.e. it does not reach unity

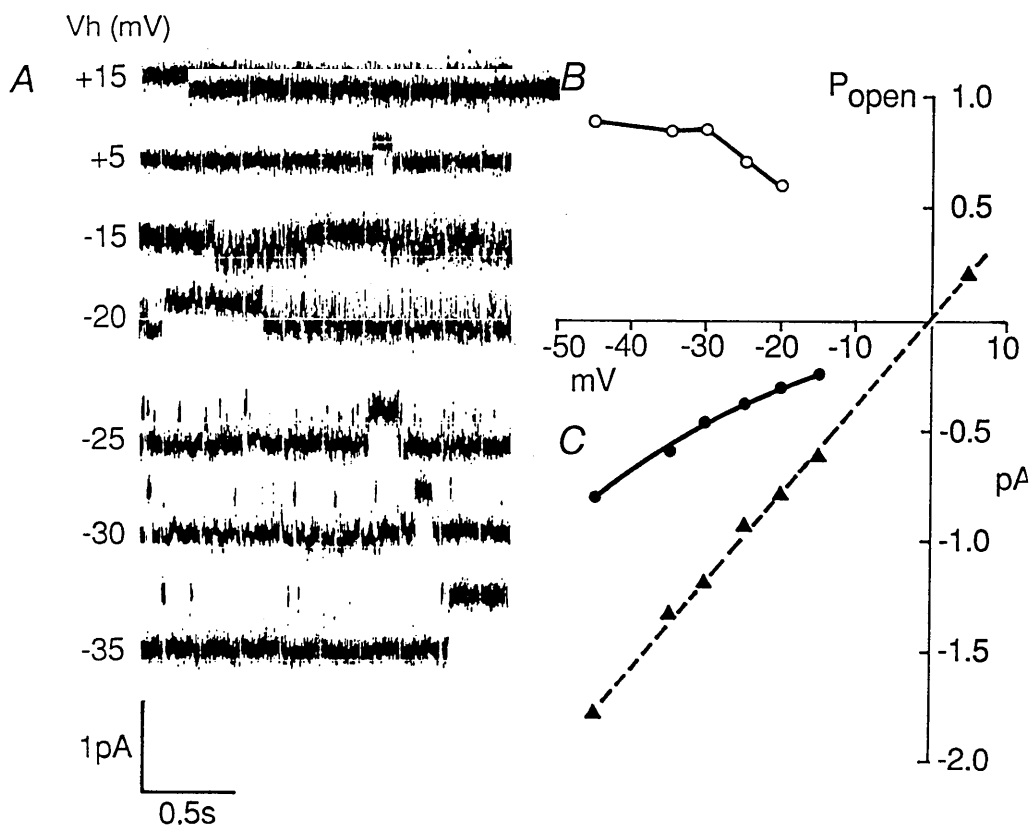


Figure 3.2. Inwardly rectifying K channel and ATP-sensitive K channel in vesicle-attached patch of human sarcolemma; 21°C. *A*, inward rectifier currents at different holding potentials. The brief current event at +5mV is an opening of the ATP-sensitive channel; 500Hz filtering. *B*, open probability-voltage relation of the inwardly rectifying K channel. *C*, current-voltage relation of the inwardly rectifying K channel (●, solid line) and ATP-sensitive K channel (▲, dashed line).

(Fig.3.2B). This raises the question of whether the activation of the inwardly rectifying channel is as complete at -40mV as has been supposed (Ohmori *et al.*, 1981; Leech & Stanfield, 1981) and opens the possibility that the channel contains an intrinsic inactivating mechanism as does its counterpart in cardiac muscle (e.g. Sakmann & Trube, 1984b).

#### Ion selectivity and conductance of the open channel

Fig.3.3A shows recordings from an inwardly-rectifying channel in a detached inside-out patch of rat sarcolemma. The single-channel current voltage relationship is given in Fig.3.3B and the corresponding conductance-voltage relation in Fig.3.4. In order to verify the ionic selectivity of the channel, its activity was recorded also after  $[K^+]_i$  was raised to 424mM. This produced a shift in the current-voltage relationship to the left as would be expected for a predominantly  $K^+$ -selective channel. To determine the single channel conductance-voltage relation at raised  $[K^+]_i$  requires knowledge of the new value of  $E_K$ . Allowing for differences in the activity coefficient, but supposing  $[K^+]_o$ , i.e. the concentration of  $K^+$  at the tip of the patch clamp electrode, to have remained constant, yields  $E_K = -24mV$ . Inspection of the current-voltage relation in 424mM  $[K^+]_i$ , however, indicates that  $E_K$  is likely to have a less negative value. This could happen if water flowed from the electrode tip to the more concentrated bath solution. Supposing the true value of  $E_K$  to be -20mV (implying that  $[K^+]_o$  had risen from 140 to 175mM), the single-channel conductance at weakly negative potentials would be noticeably higher, but at more strongly negative potentials the difference would become negligible. This is in accordance with the behaviour of the inwardly rectifying conductance as established by macroscopic voltage-clamp experiments on egg cells

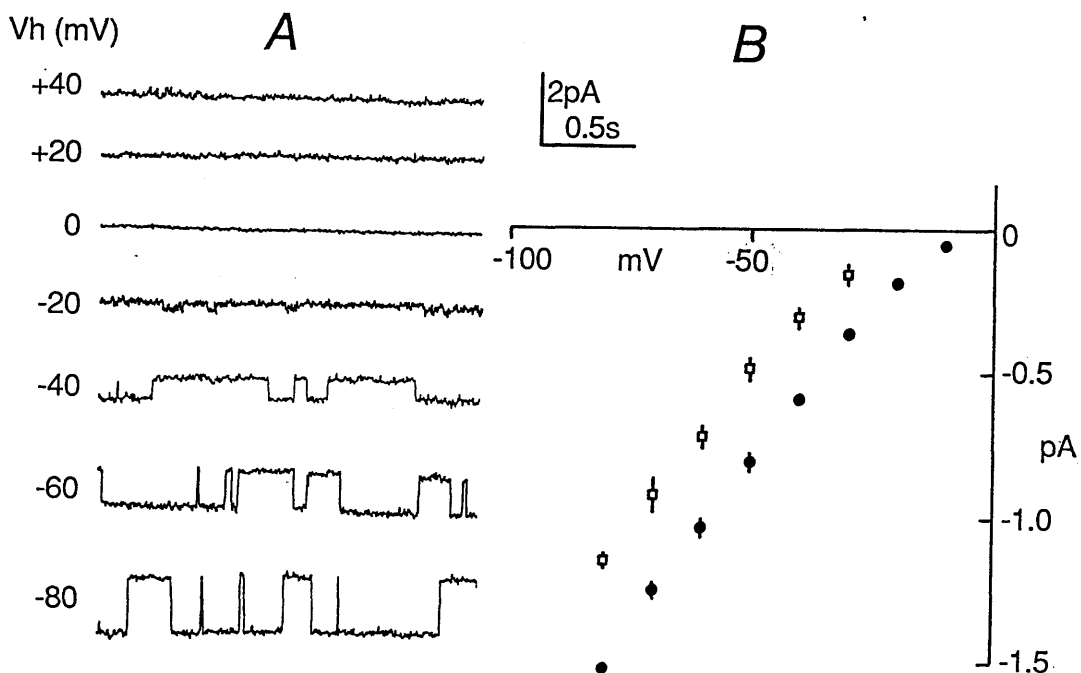


Figure 3.3. Inwardly rectifying K channel in an inside-out patch of rat sarcolemma; 22°C. A, single-channel currents at different holding potentials. Bath solution contained (mM) 140 KCl, 2 MgCl<sub>2</sub>, 2 K<sub>2</sub>ATP, 1 EGTA, 5 HEPES, pH 7.8. Patch pipette contained (mM) 140 KCl, 1 CaCl<sub>2</sub>, 5 HEPES, pH 7.8. Inward currents are downward; 500Hz filter. B, current-voltage relation when [K<sup>+</sup>]<sub>i</sub> = 144 mM (●) and after [K<sup>+</sup>]<sub>i</sub> was raised to 424 mM (□). Bars indicate SD of measurements where this is larger than the symbols.

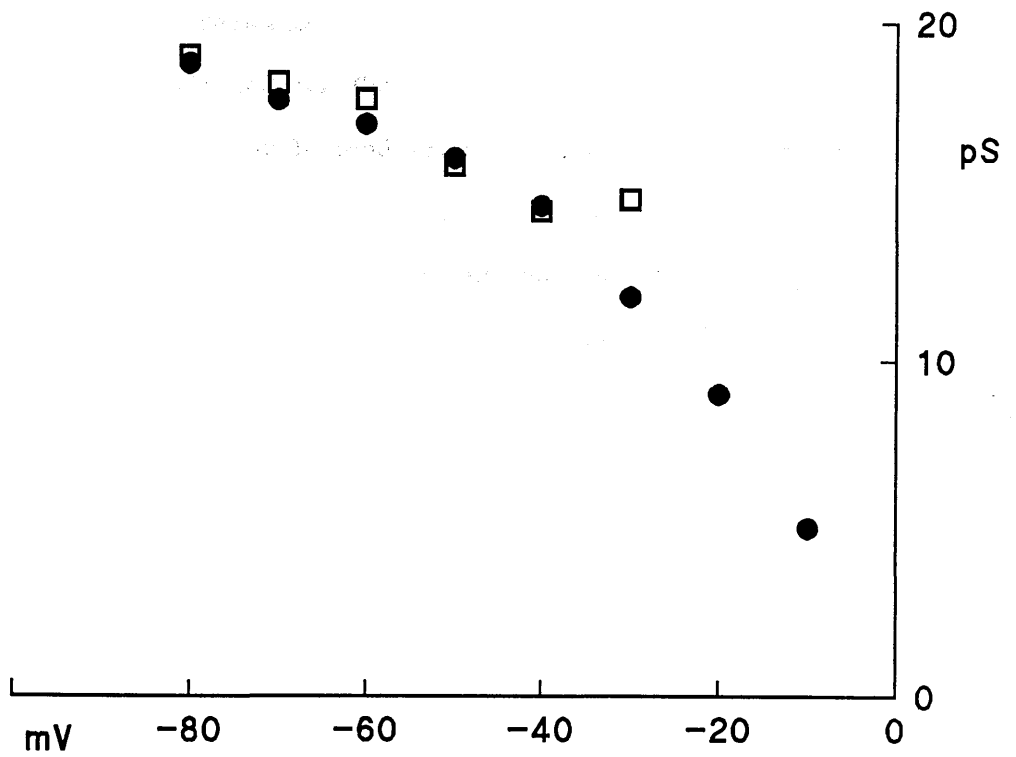


Figure 3.4. Conductance-voltage relation for inwardly rectifying K channel of Fig.3.3. Chord conductance was calculated assuming  $V_K = 0$  mV when  $[K^+]_i = 144$  mM (●), and  $V_K = -20$ mV when  $[K^+]_i = 424$  mM (□).

(Hagiwara & Yoshii, 1979) and muscle fibres (Hestrin, 1981; Leech & Stanfield, 1981).

#### Block by foreign cations

Rubidium and caesium ions are known to block the inwardly rectifying K conductance (Adrian, 1964; Hagiwara *et al.*, 1976) and have been used in the past to establish favourable conditions for the study of the chloride conductance (Hutter & Warner, 1972). With this aim in mind, vesicles were released into a solution in which 140mM KCl was replaced by 135mM RbCl and 5mM CsCl. Inwardly rectifying channels were encountered also under such conditions. Their conductance to inward current was of the same order of magnitude as when  $K^+$  carried the current, but channel openings occurred much more seldomly, and the openings were briefer. In the experiment shown in Fig.3.5A-C, the pipette concentrations of Rb and Cs were three times those in the bath solution. The extrapolated reversal potential was about +25mV. Open probability was as low as 0.005 at -40mV, but with strong hyperpolarization  $P_o$  increased markedly. This is akin to the relief by hyperpolarization of block by external  $Rb^+$  (and  $Cs^+$ ) of the inward rectifier in frog muscle described by Standen and Stanfield (1980).

#### Mechanism of inward rectification

For cardiac muscle it has been shown that inward rectification arises from a block of K channels by  $Mg^{2+}$  (Matsuda *et al.*, 1987; Vandenberg, 1987). When  $[Mg^{2+}]_i$  is reduced to or below micromolar concentrations, the channel conductance is ohmic. That this also holds true for skeletal muscle is shown below.

Fig.3.6A shows recordings made from a patch in the cell-attached configuration. As the contents of the vesicle were derived from the

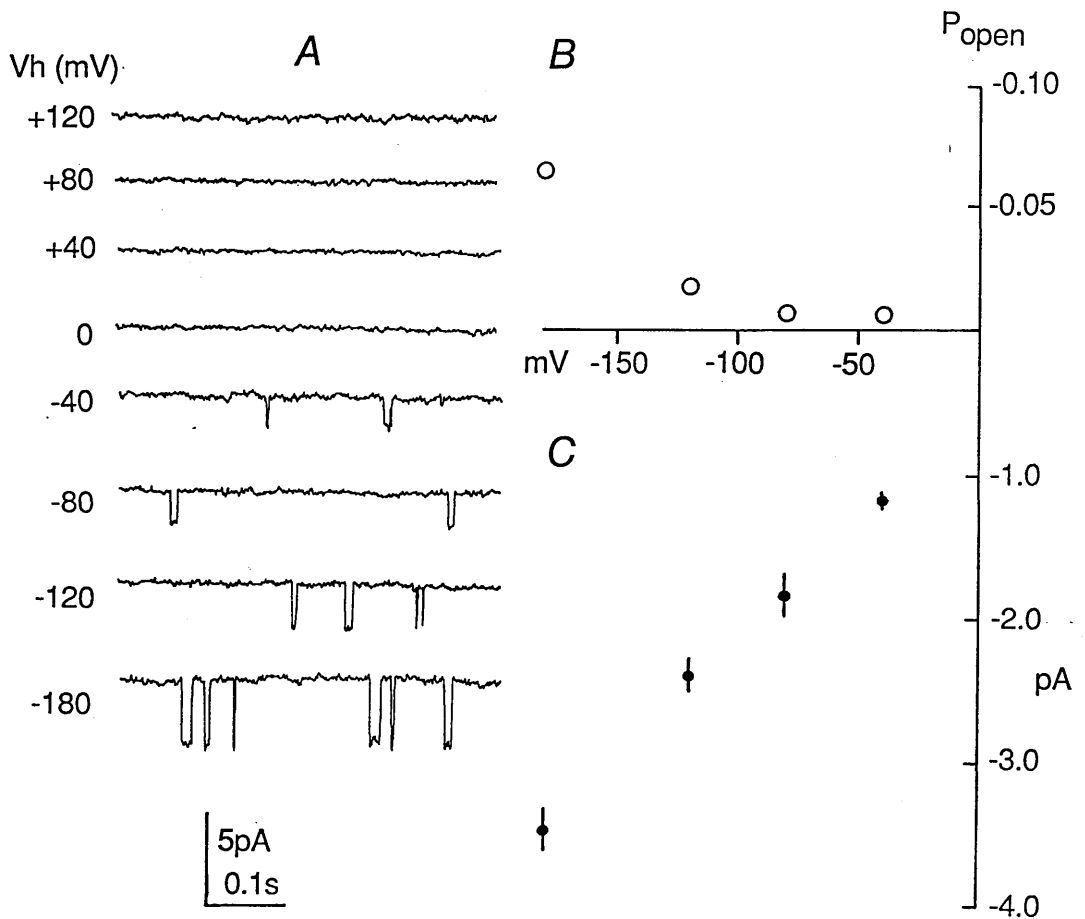


Figure 3.5. Foreign cations reduce open probability of inwardly rectifying K channel. Inside-out patch of rat sarcolemma. Pipette solution contained (mM) 405 RbCl, 15 CsCl, 1 CaCl<sub>2</sub>, 5 TRIS/RbOH, pH 7.8. Bath solution contained (mM) 135 RbCl, 5 CsCl, 2 MgATP, 1 EGTA, 5 TRIS/RbOH, pH 7.8; 22°C. A, single channel currents at different potentials; 1kHz filtering. B, open probability-voltage relation. C, current-voltage relation.

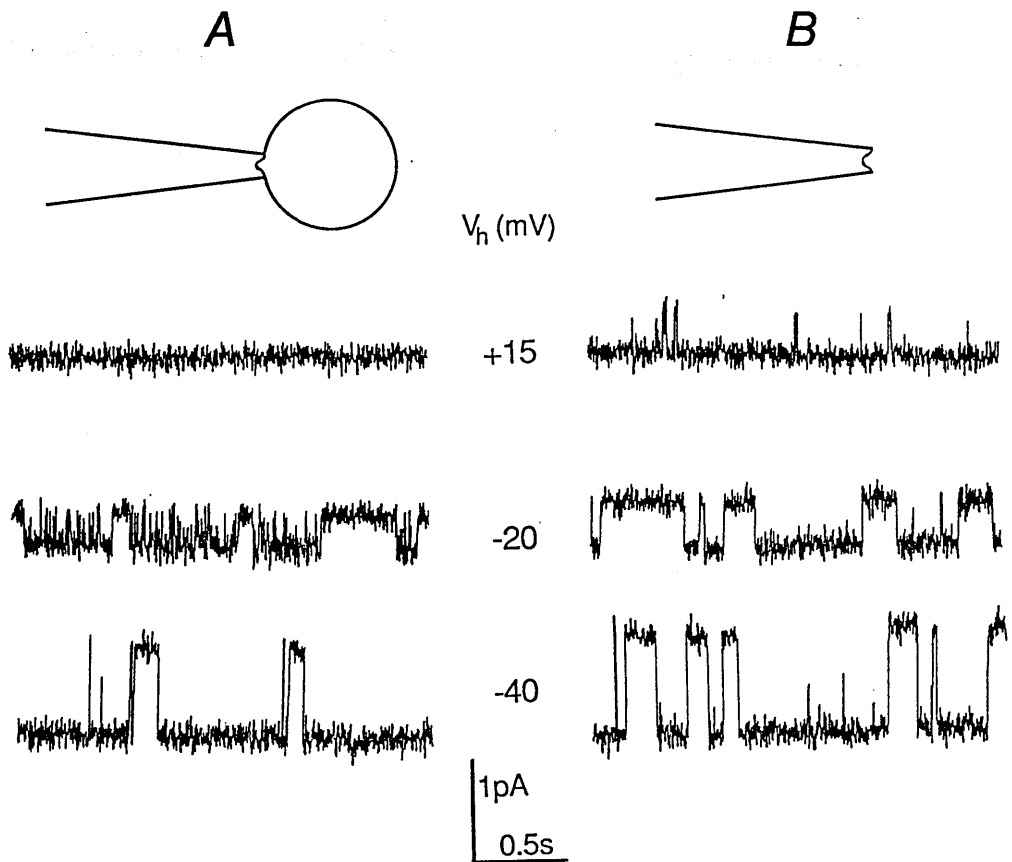


Figure 3.6. Effect of lowering internal  $Mg^{2+}$  concentration on inwardly rectifying K channel. A, currents recorded in vesicle-attached patch of rat sarcolemma; 22°C. B, currents recorded in same patch after detachment into 140mM KCl solution containing 2.5 $\mu$ M  $Mg^{2+}$ . Records filtered at 500Hz.

cytosol,  $Mg^{2+}$  ions were present at the inner surface of the membrane. At  $-40mV$  the channel passed about  $1pA$  of inward current and was open for most of the time. By contrast, at  $+15mV$  (and also at more positive potentials) no outward current events were observed. At potentials just negative to  $E_K$ , as we saw earlier, the open state is interrupted by brief closures. This suggests that when the inside potential is only slightly negative some positively charged particle momentarily enters into the channel to produce a flickery block. At positive potentials we may suppose the blocking ion resides in the channel more permanently and so block is more complete.

That intracellular  $Mg^{2+}$  responsible may be concluded from comparing the traces obtained in the cell-attached situation with the traces (Fig.3.6B), obtained after detachment of the patch into a low  $Mg^{2+}$  solution. The flickery block at  $-20mV$  then disappears. Moreover, at  $+15mV$ , the channel can now pass current also in the outward direction.

Fig.3.7A,B gives a more comprehensive picture of the behaviour of an originally inwardly rectifying channel after detachment of the patch into  $Mg^{2+}$ -free solution. Before detachment, this channel passed no outward current. At positive potentials, outward current events are present. Their magnitude is proportional to the driving force (Fig.3.7B). In fact, in the absence of magnesium, the channel behaves as an ohmic conductance over the whole voltage range. The single channel conductance was  $24pS$  at  $23^{\circ}C$ . In these conditions, it becomes possible to study the intrinsic gating mechanism of the channel.

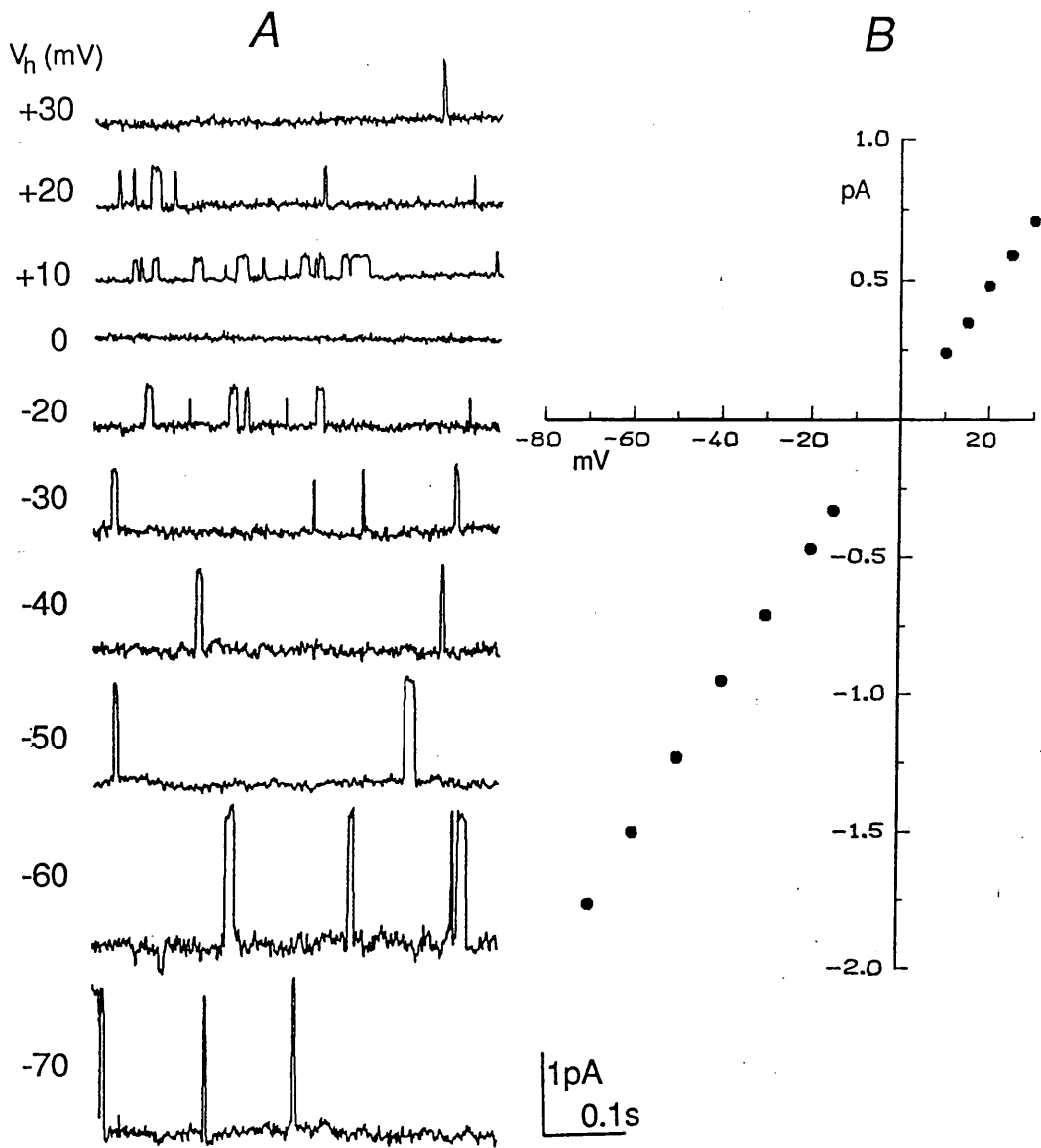


Figure 3.7. Inwardly rectifying K channel in inside-out patch of rat sarcolemmal vesicle excised into  $Mg^{2+}$ -free symmetrical 140mM KCl solution. In the attached state, the single channel in this patch displayed inward rectification. A, kinetic behaviour of the channel at negative and positive holding potentials. Inward current downwards. At negative potentials the channel is mostly open; at positive potentials mostly closed. B, current-voltage relation; single channel conductance was 24pS ( $25^{\circ}C$ ) over the whole potential range.

### Kinetics in the absence of $Mg^{2+}$ : intrinsic gating

Histograms of open and closed times were constructed from recordings filtered at 500Hz and digitized at 5kHz. Infrequently, the channel entered a prolonged closed state, but such rare long (>1s) closures were not included in the analysis. In fact, at negative potentials, only two long closed periods (4.4s) occurred during a total of 340s of analyzed recording.

Histograms at +20mV and -60mV are shown in Fig.3.8. Each could be fitted with a single exponential, suggesting that the gating mechanism has just one open and one closed state. At +20mV, the mean open time is short and the closed time long (4.5ms and 227ms respectively). At -60mV the reverse holds true, with the mean open time increased to 237ms and the closed time reduced to 6.2ms.

That there may in fact be yet another shorter lived closed state, not quantified in the above analysis, was suggested by the excess of detected events in the first bin of the closed-time histograms. This is reflected also by the low figures for the percentage area of the histogram under the fitted exponentials (Fig 3.8B,D). Therefore, an extended period at -60mV (150s, including the original 110s) was analyzed with  $f_c$  at 1kHz (sampling rate 10kHz) (Fig.3.9A,B). When a histogram of closed times with bins of width 0.95ms was plotted, the presence of a faster component with time constant 0.84ms became apparent. This component accounted for 22% of the area under the fitted curve. The slower component had a time constant of 6.3ms, almost the same as  $\tau_c$  found with  $f_c=500$ Hz and accounted for the remaining 78% of the area. Analysis of the other potentials in this experiment could not be done in the same way since the noise at 1kHz was too large in relation to the single channel current: the proportion of spurious

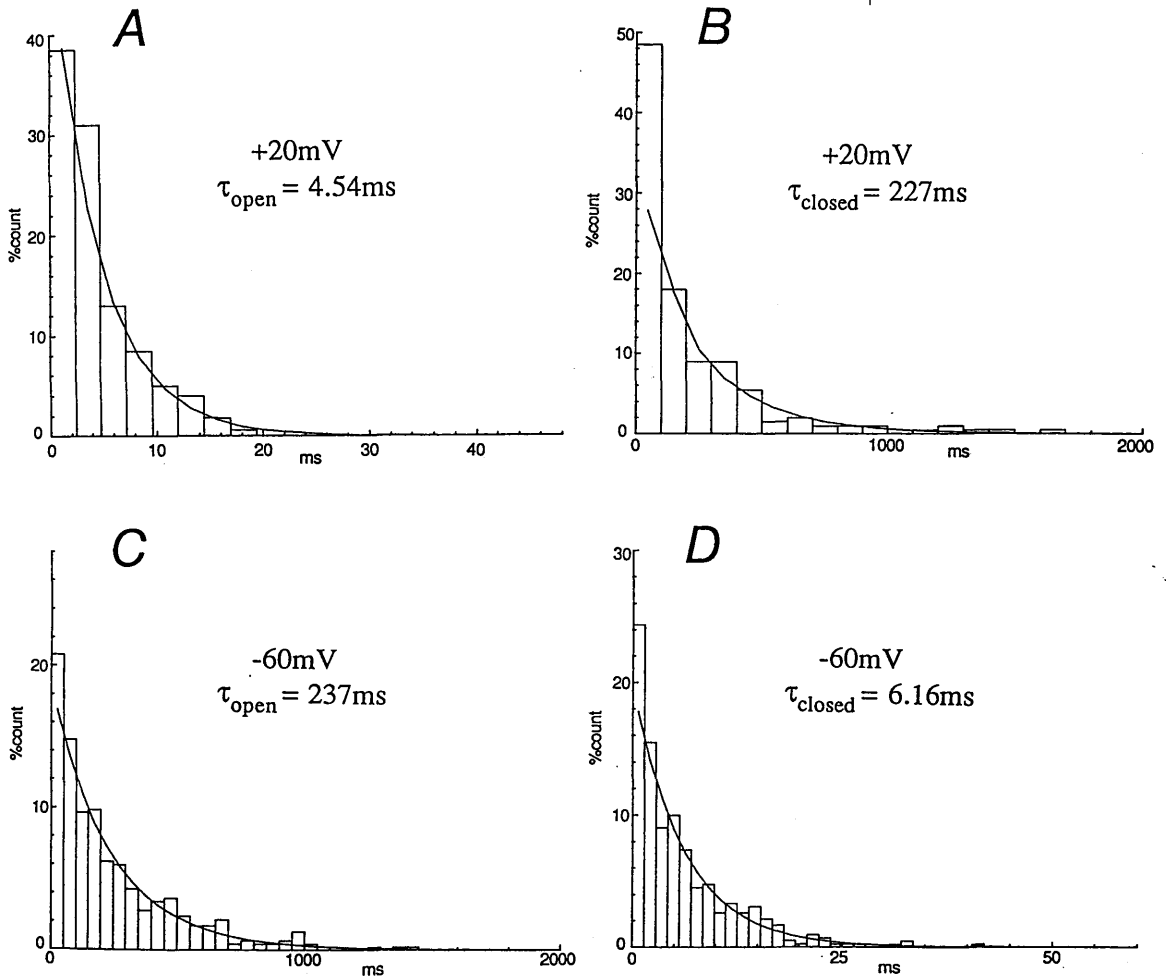


Figure 3.8. Distributions of open and closed times constructed from recordings of  $K_{\text{inw}}$  channel activity in inside-out patch of rat sarcolemma (same patch as Fig.3.7). Dwell time histograms are plotted with fitted single exponential line. Time constants are given with each plot; percentage areas under exponentials follow. A, open time histogram at +20mV (200 events in 45s recording) (95.2%). B, closed time histogram at +20mV (76.2%). C, open time histogram at -60mV (420 events in 110s) (94.7%). D, closed time histogram at -60mV (87.6%). Sampling rate 5kHz; filter 500Hz.

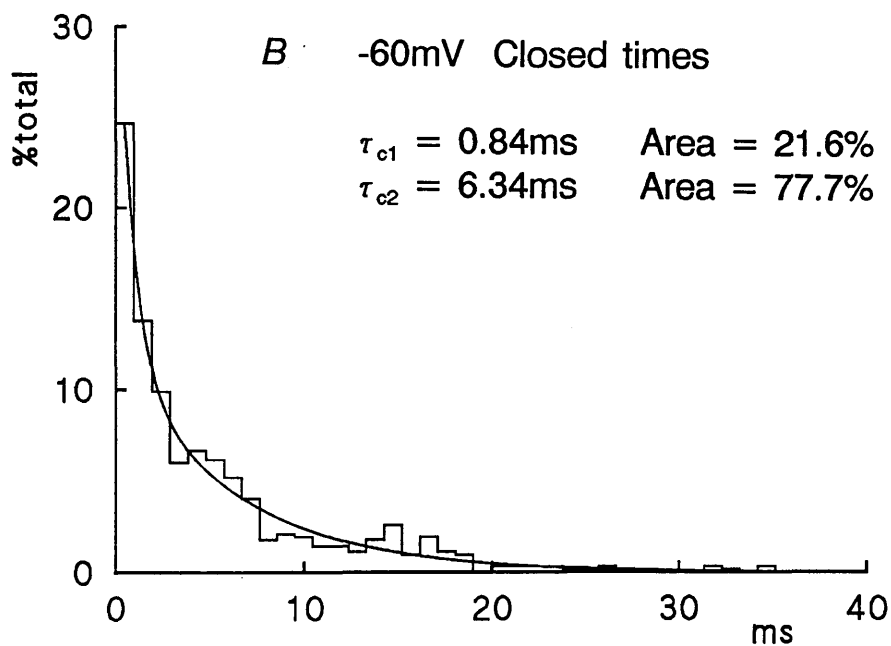
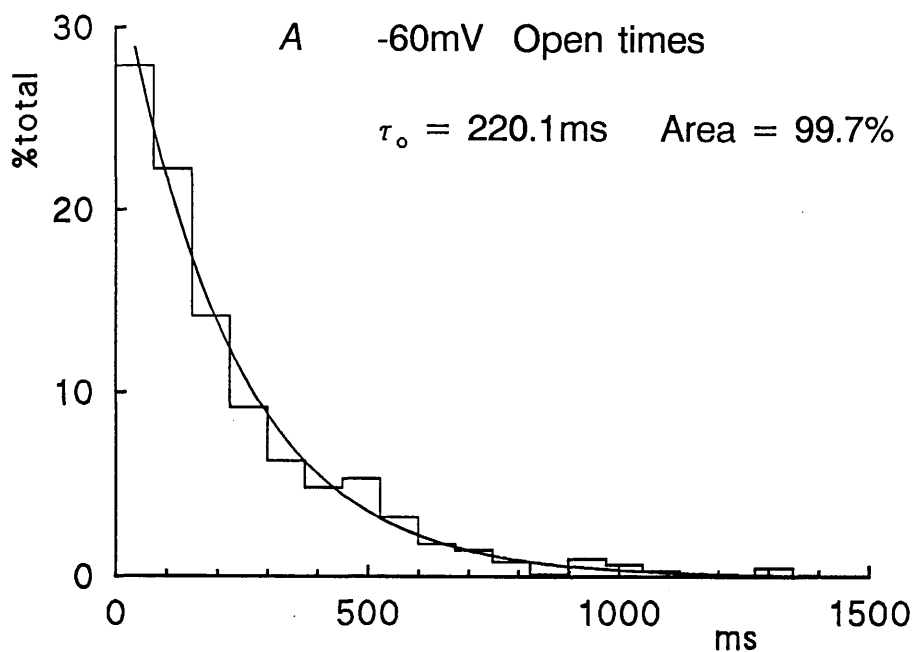


Figure 3.9. Distributions of open and closed times for same  $K_{inw}$  channel as in Fig.3.8 from 150s recording at  $V_h$  -60mV. A, open time histogram, fitted with single exponential (620 events, bin width 74.87ms). B, closed time histogram, fitted with sum of two exponentials (bin width 0.95ms). Sampling rate 10kHz; filter 1kHz.

short events due to threshold crossing by noise peaks would be too large. In any case, records at other potentials may have been too short (50-60s) for reliable estimation of the shorter closed time constant. The following description, therefore, is based on a simplified view of the channel kinetics.

Fig.3.10 shows the rate constants for all the voltages explored. The opening rate constants,  $\alpha$ , can be fitted with a sigmoid curve. The closing rate constants,  $\beta$ , have a finite low value at negative potentials and then rise exponentially on depolarization. In Fig.3.11  $P_o$  determined from the mean open and closed times is plotted as the ordinate against membrane potential. The data can be fitted with a Boltzmann function. The fact that  $P_o$  never reaches quite unity is reflected in a numerator which is less than one. This is because  $\beta$ , the closing rate constant, had a finite value even at extreme negative potentials. The midpoint of the curve is +4.8mV, and the slope factor is 4.13. This slope factor may be compared to a value of 5.38 calculated from the rate constants reported by Kurachi (1985) for the inward rectifier in guinea-pig ventricular cells. He also found that the steady-state kinetics behaved according to a simple two-state model at potentials more positive to  $E_K+55mV$ , equivalent to about -20mV at  $[K^+]_o=150mM$ ).

Matsuda & Stanfield (1989) studied the kinetics of an inwardly rectifying channels in cell-attached patches on a cultured [rat or mouse] muscle cell. Their pipettes contained 150mM KCl. Recordings were filtered at 1kHz and sampled at 4kHz. They too found that the distribution of open times was well fitted by a single exponential. The mean value of  $\hat{t}_o$  for 3 experiments was 257ms, comparable with our value of 237ms at -60mV. However, their closed times apparently contained

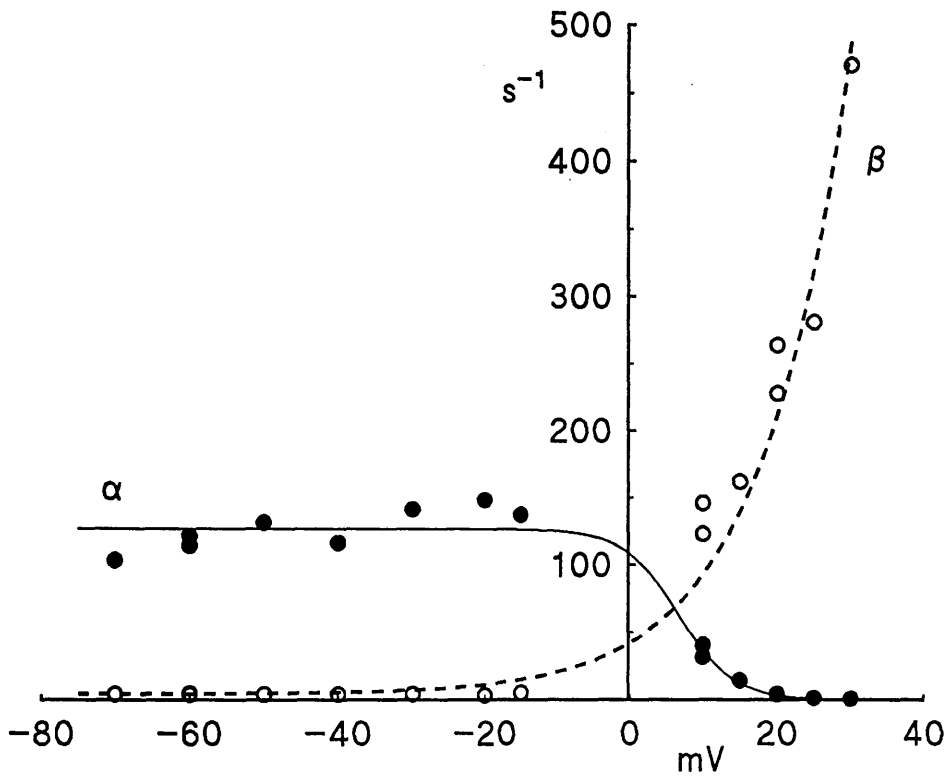


Figure 3.10. Rate constants at different holding potentials for  $K_{inw}$  channel. Same experiment as Fig.3.7. Rate constants are reciprocal of time constants of single exponentials determined from kinetic analysis as in Fig.3.8. A, opening rate constants (●) and fitted sigmoid relation  $126/[1+\exp((V_h-6.67)/3.77)]$  (solid line). B, closing rate constants (○) and fitted exponential relation  $3.72*\exp(V_h+1.65)+4.48$  (dashed line).

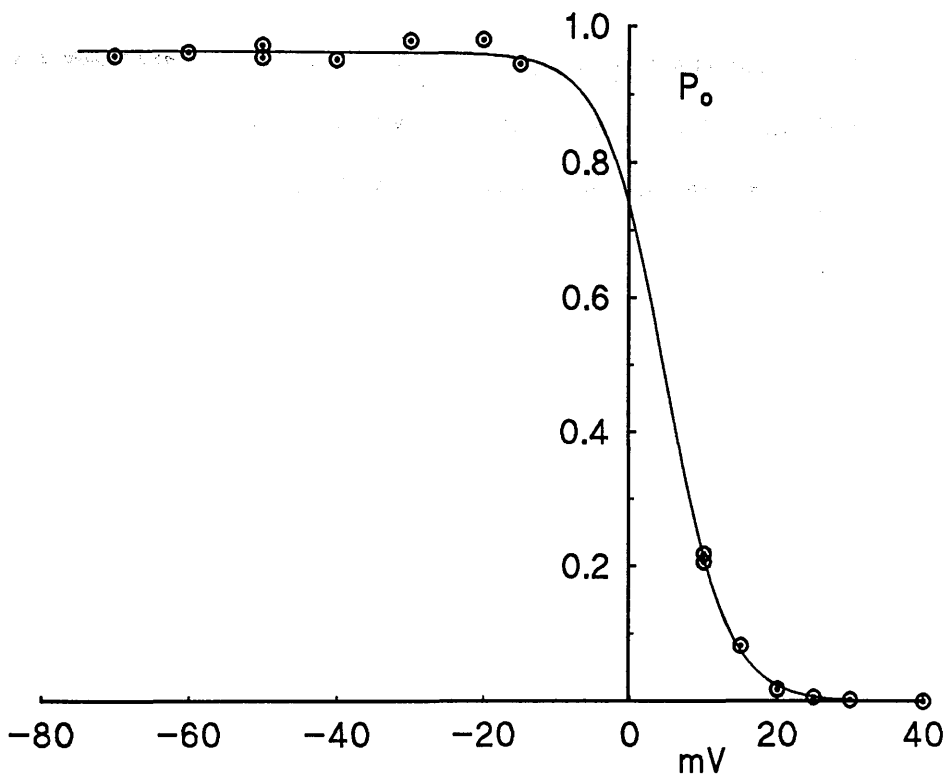


Figure 3.11. Open probability-voltage relation for  $K_{inw}$  channel. Same experiment as Fig.3.7.  $P_o$  points were calculated from individual mean open and closed times, and fitted with the Boltzmann relation  $0.96/(1+\exp((V_h-4.8)/4.13))$ .

three exponential components (ignoring a small component of closed times longer than 1s, as we did) with time constants 0.57ms, 18.8ms and 90.6ms (compared to 0.84ms & 6.3ms of the present experiment). Whether a third, slower component would be revealed under the conditions of the present experiments by analysis of longer recordings, or whether there is really a difference in the kinetics of the channel, remains to be explored.

To summarize, the inward rectification in skeletal muscle arises from two sources: a) blockade by  $Mg^{2+}$  with very fast kinetics, and b) a gating mechanism which is highly voltage dependent and which closes on depolarization.

## CHAPTER 4

**Sensitivity of skeletal muscle inwardly**

**rectifying K channels to flow.**

## SUMMARY

1. Current through inwardly rectifying  $K^+$  channels was measured in inside-out patches from rat and human sarcolemmal vesicles and from dispersed rat flexor digitorum brevis muscle fibres. The patches were positioned so as to face the aperture of a large-diameter pipette from which solution of the same composition as the bath solution could be ejected. The solution within the patch pipette and the bath solution contained principally 140 mM-KCl.

2. The kinetic behaviour of the inwardly rectifying channel was found to vary according to whether the patch was in static or flowing solution. At negative holding potentials, when the channel is open most of the time in static solution, flow produced a reversible and repeatable decrease in open probability.

3. In  $Mg^{2+}$ -free solution the inwardly rectifying channel allows outward current to pass at positive holding potentials. This allows the kinetic behaviour of the channel in static and flowing solution to be compared over a wider voltage range.

4. In both static and flowing solution, the open probability-voltage relation is sigmoidal and can be fitted by a Boltzmann curve. As a result of flow, the maximum open probability at negative potentials is decreased and the mid-point of the relation is shifted to the right by more than 20mV.

5. No evidence could be found for the existence of a local concentration gradient sensitive to flow. Application of suction to the patch pipette showed the inwardly rectifying channels not to be sensitive to membrane stretch. The possibility is contemplated that

shear stress upon the inner face of the patch modulates the kinetic behaviour of the channel.

6. In contrast to the inwardly rectifying  $K^+$  channel, neither the  $Ca^{2+}$ -activated  $K^+$  channel nor the ATP-regulated  $K^+$  channel are sensitive to flow.

## INTRODUCTION

One way to study the effects on channels of changes in intracellular composition is by detaching inside-out patches from cells, and then changing the bulk solution surrounding the tip of the pipette. Where very rapid (millisecond) changes are not required, it is common to place the pipette tip in the outflow of a much larger perfusion pipette. Solution changes may then be performed by moving the patch pipette into a different perfusion stream or, as we have done, by switching the solution flowing to a single outlet. In experiments designed to study the effects of chemical agents on the intrinsic gating mechanism described in the last chapter inside-out patches containing inwardly rectifying  $K^+$  channels were thus exposed to a stream of solution of variable composition. In control experiments, when the patch was superfused with a solution of the same composition as the bath solution, the open probability of the inwardly rectifying  $K^+$  channels changed, while single channel conductance remained constant. In this chapter, I will describe this effect on gating in detail.

## Methods

Vesicles from rat and human skeletal muscle and dispersed fibres from rat skeletal muscle were prepared by treatment with 140mM KCl containing collagenase as described in Chapter 1. Except where otherwise stated, patch electrodes were filled with (mM): KCl, 140;

HEPES, 5; pH 7.6. Gigaseals were readily obtained with shed vesicles or dispersed fibres, and patches were detached by raising the patch electrode towards the top of the bath. The composition of the bath solution was (mM): KCl, 140; MgCl<sub>2</sub>, 0.5; K<sub>2</sub>ATP, 5; EGTA, 1; HEPES, 5; pH 7.6. Free Mg<sup>2+</sup> in this solution was calculated to be 12μM. In some experiments MgCl<sub>2</sub> was omitted from the bath solution.

In the relatively few cases where patches contained active inwardly rectifying channels, the 'intracellular' face of a detached membrane patch was manoeuvred so as to face a stream of the same composition as the bath solution emanating from a pipette with a tip diameter of about 0.5mm. Initially experiments were done with linear flow speeds of 5-7cm/s at the mouth of the flow pipette. Later flow rates down to 0.5cm/s were used as the stability of the current records tended to be better without any obvious decrease in the magnitude of the flow effect. For exploration of a quantitative relation between flow rate and effect, rates below the lowest so far used are therefore likely to be necessary.

In some experiments patch pipette pressure was altered by injecting or withdrawing air with a water manometer (±30cmH<sub>2</sub>O) or a 20ml syringe (for pressure/suction exceeding 30cmH<sub>2</sub>O). A calibrated integrated circuit sensor (LX06001G, 0±1psig, Sensym Ltd.) was then used to monitor the pressure within the patch pipette system.

## RESULTS

An example of how flow influences the behaviour of an inwardly rectifying K<sup>+</sup> channel is shown in Fig.4.1A. Throughout the experiment, the patch was in symmetrical 140 mM-KCl solution and the potential was held at -40mV, so that inward current flowed when the channel was open.

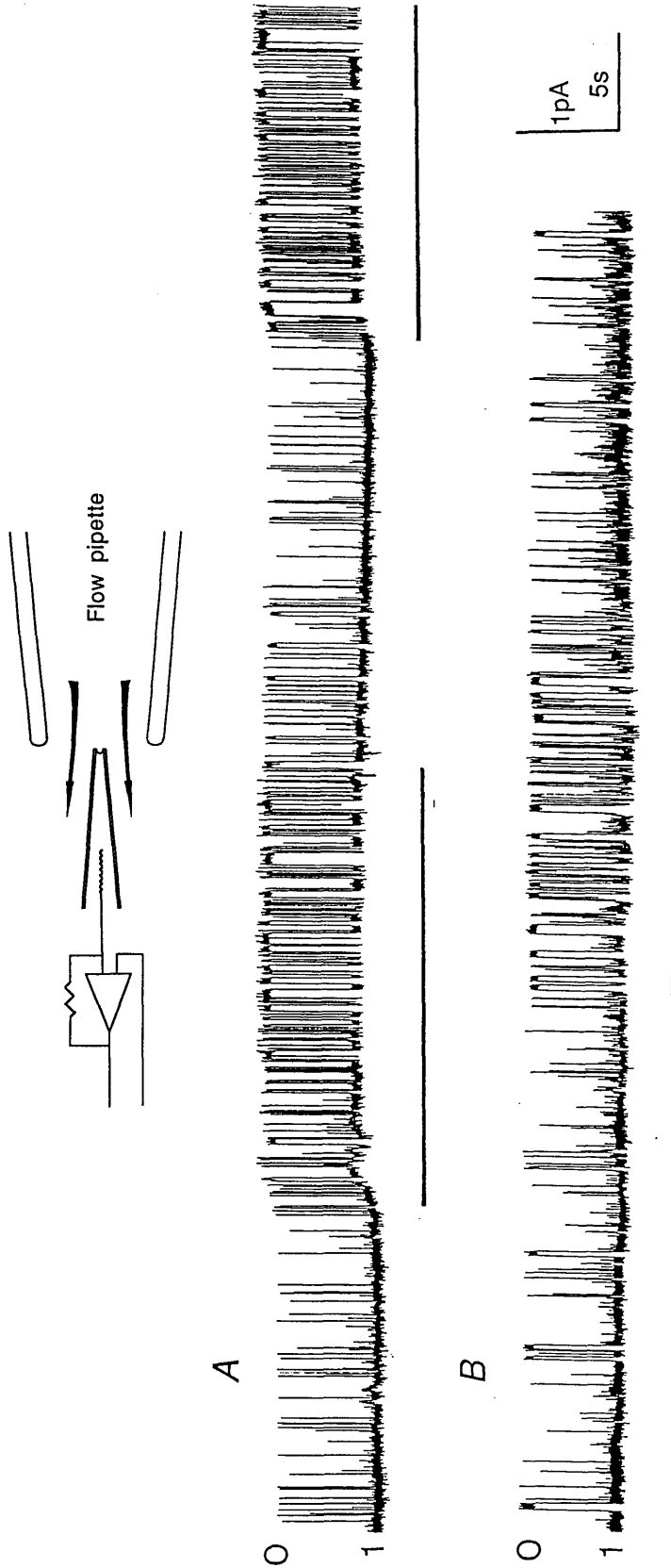


Figure 4.1. Effect of flow on kinetic behaviour of single  $K_{inw}$  channels. Above, schematic diagram showing relative positions of patch and flow pipettes (not to scale). Below are single-channel currents from inside-out patches held at  $-40\text{mV}$  in symmetrical  $140\text{ mM-KCl}$ . O indicates closed state; inward current downwards. Records low-pass filtered at  $200\text{ Hz}$ . A, patch detached from rat sarcolemmal vesicle. B, patch detached from dispersed rat muscle fibre. Duration of superfusion periods indicated by bars.

At the beginning of the trace, no flow emanated from the perfusion pipette and the channel was open most of the time, with a conductance of 23pS (22°C). On initiation of flow, the baseline shifted slightly probably owing to an incidental change in the leak conductance, and the channel open probability fell as a result both of a reduction in mean open time and an increase in mean closed time (Table 2A). Interruption of flow promptly led to a return to the initial high open probability state, and on resumption of flow the open probability once more fell promptly.

An effect of flow could be demonstrated almost always when a successfully detached patch containing an inward rectifier was positioned so as to face the stream. Removal of the pipette from the stream had the same effect as cessation of flow. Occasionally I found no response to flow or that the effect was erratic. In all such cases I found that debris had accumulated around the tip of the patch pipette, which would presumably have the effect of shielding the surface of the patch from flowing solution.

In experiments on dispersed rat skeletal muscle fibres, patches containing inwardly rectifying  $K^+$  channels were occasionally found. When such patches were excised and exposed to flow, the channels responded in an identical manner to those from sarcolemmal vesicles (Fig.4.1B, Table 2B).

Since the gating behaviour of some channels is known to respond to stretch deformation of the membrane (Guhuray & Sachs, 1984), the possibility that the present phenomenon was another instance of stretch sensitivity of a channel was considered. To test this hypothesis, suction was applied to patch pipettes while recording from an inwardly

Table 2. Kinetics of inwardly rectifying K<sup>+</sup> channel in static and flowing solution.

|   | Flow | Duration<br>(s) | Mean open<br>time (ms) | Mean closed<br>time (ms) | P <sub>o</sub> |
|---|------|-----------------|------------------------|--------------------------|----------------|
| A | Off  | 30              | 308                    | 7.2                      | 0.98           |
|   | On   | 20              | 115                    | 74                       | 0.61           |
|   | Off  | 15              | 305                    | 18                       | 0.94           |
|   | On   | 30              | 104                    | 71                       | 0.59           |
| B | Off  | 30              | 281                    | 26                       | 0.92           |
|   | On   | 15              | 82                     | 41                       | 0.67           |
|   | Off  | 15              | 251                    | 19                       | 0.93           |

Same channels as shown in Fig.4.1. Current records were low-pass filtered at 500 Hz and digitized at 5 kHz. Dwell times were measured by threshold crossing, with the threshold set half-way between open and shut levels. Open probability (P<sub>o</sub>) was calculated as the ratio of mean open time to the sum of mean open and mean closed times.

rectifying channel. In contrast to flow, progressively stronger suction produced no change in open probability (Fig.4.2). The same held true for experiments in which the pressure within the pipette was lowered in a stepwise fashion.

To rule out the possibility that flow acts by stirring up a local concentration, patch pipettes as well as perfusion pipettes were filled with the bath solution so that the minor components (i.e.  $Mg^{2+}$ , ATP, EGTA) as well as KCl and buffer were symmetrically distributed. Under such conditions also, the flow effect made its appearance. Even so, it is possible that there may still have been some unrecognized contaminant present in the bath. Therefore, an experiment was done in which the patch and flow pipettes were filled using bath solution in which vesicles had been sitting for 15 minutes or so. Yet again, flow had its effect on  $P_o$ . Bar supposing that the membrane patch produces a substance that is washed away by flow, or consumes a substance that is delivered by flow, it is difficult to escape the conclusion that the phenomenon is due not to a change in the chemical environment of the channel but rather to the physical flow itself.

#### Experiments in $Mg^{2+}$ -free solutions

In the experiments of Fig.4.1, the bath and superfusion solution both contained  $12\mu M Mg^{2+}$ . In such an environment, a progressively more intense flickery block is liable to appear at potentials less negative than  $-40mV$  (Kurachi, 1985; Chapter 3 this thesis) and at positive potentials the channel will pass no outward current owing to complete block by  $Mg^{2+}$ . In order to examine what might be the effect of flow over a wider range of membrane potential, we excised patches into  $Mg^{2+}$ -free bath solution and also omitted  $Mg^{2+}$  from the superfusion solution.

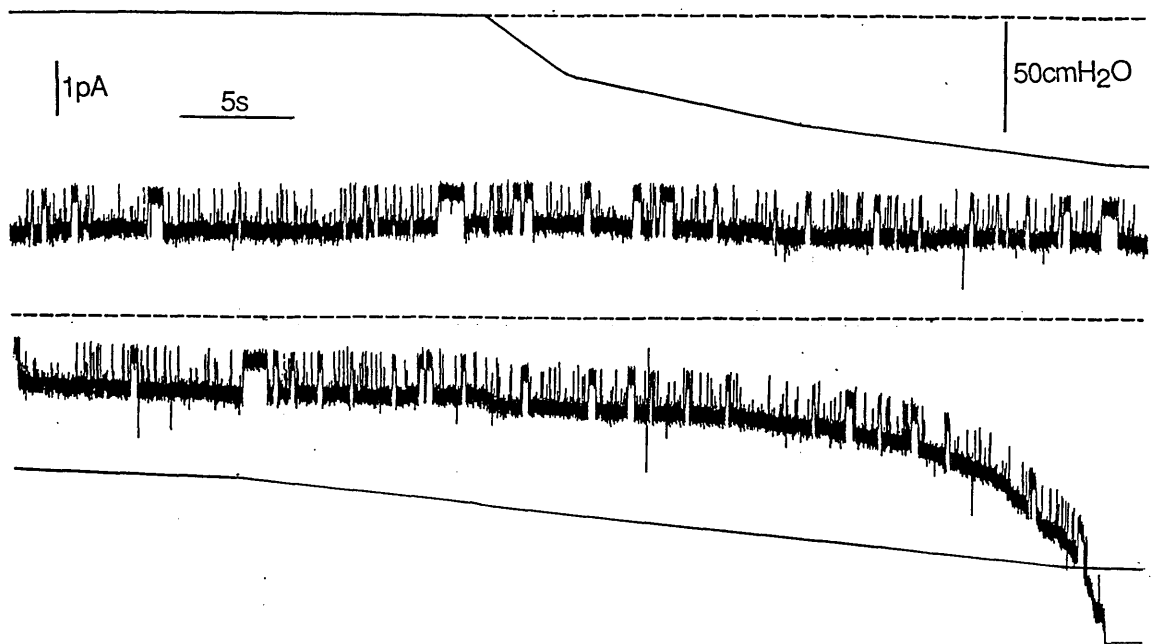


Figure 4.2. Insensitivity of inwardly rectifying  $K^+$  channel to stretch deformation of membrane produced by suction. Patch detached from human sarcolemmal vesicle voltage clamped to  $-40\text{mV}$  in symmetrical  $140\text{ mM KCl}$ . Continuous current and pressure records split into upper and lower sections. Negative pressure in patch pipette shown by continuous line. Dashed line represents zero pressure difference. Current record low-pass filtered at  $500\text{ Hz}$ . For clarity, the lower portion of the current record has been shifted upwards relative to the corresponding pressure trace. When negative pressure was increased beyond about  $80\text{ cmH}_2\text{O}$  leak current increased; at  $110\text{ cmH}_2\text{O}$  the patch broke down. Neither single-channel current, nor channel kinetics were altered in the course of this procedure.

When the effect of flow was tested at positive potentials in the absence of  $Mg^{2+}$ , the response was surprising: on initiation of flow the open probability *increased* (Fig.4.3A). This reversal of the effect was unconnected with the removal of  $Mg^{2+}$ , as shown by the finding that when the same patch was clamped at -20mV the usual decrease in open probability occurred on initiation of flow (Fig.4.3B). As a corollary, intrinsic gating displayed little voltage sensitivity when the clamp potential was varied between -60 and +20mV whilst flow was maintained. However, when more positive potentials were explored, the open probability reached only low levels in the presence of flow (Fig.4.4). The overall effects of flow therefore are (i) a decrease in the maximum open probability at negative potentials, and (ii) a shift to the right by more than 20mV in the midpoint of the sigmoidal open probability-voltage relation.

#### Selectivity of the flow effect

In some experiments on sarcolemmal vesicles ATP was omitted from the bath and perfusion solutions, so as to allow the 70pS  $K^+$  channels modulated by ATP to make their appearance (Noma, 1983; Spruce, Standen & Stanfield, 1987). No effect of flow on such channels was ever found. Similarly, the 200pS calcium-activated  $K^+$  channels proved insensitive to flow. By contrast to the inwardly rectifying  $K^+$  channel from sarcolemmal vesicles or dispersed skeletal muscle fibres, inwardly rectifying channels in patches detached from guinea-pig ventricular myocytes were unresponsive to flow (Fig. 6.4).

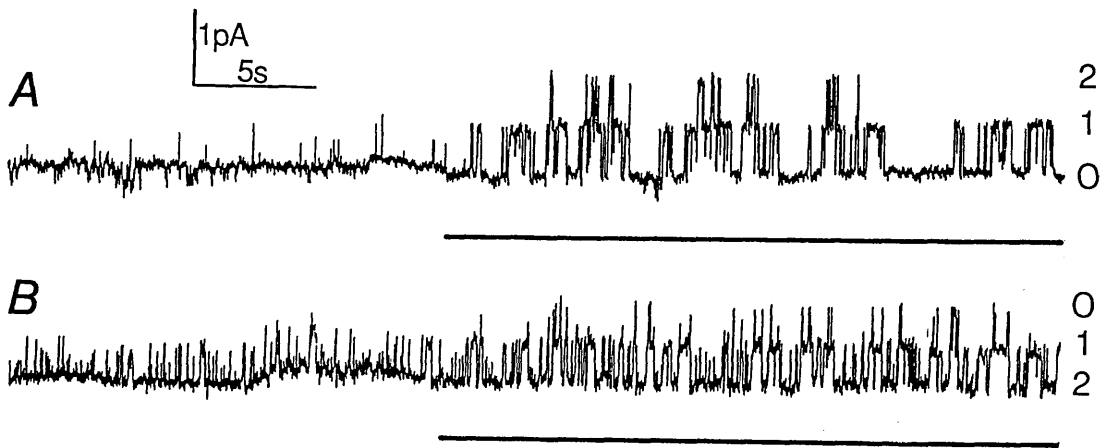


Figure 4.3. Single-channel currents recorded from a patch of rat sarcolemmal vesicle membrane containing two inwardly rectifying  $K^+$  channels in symmetrical  $Mg^{2+}$ -free 140 mM-KCl solution. 0, 1 and 2 indicate number of channels open. A, holding potential +30 mV; B, holding potential at -20mV. Bars indicate when solution was flowing over patch.

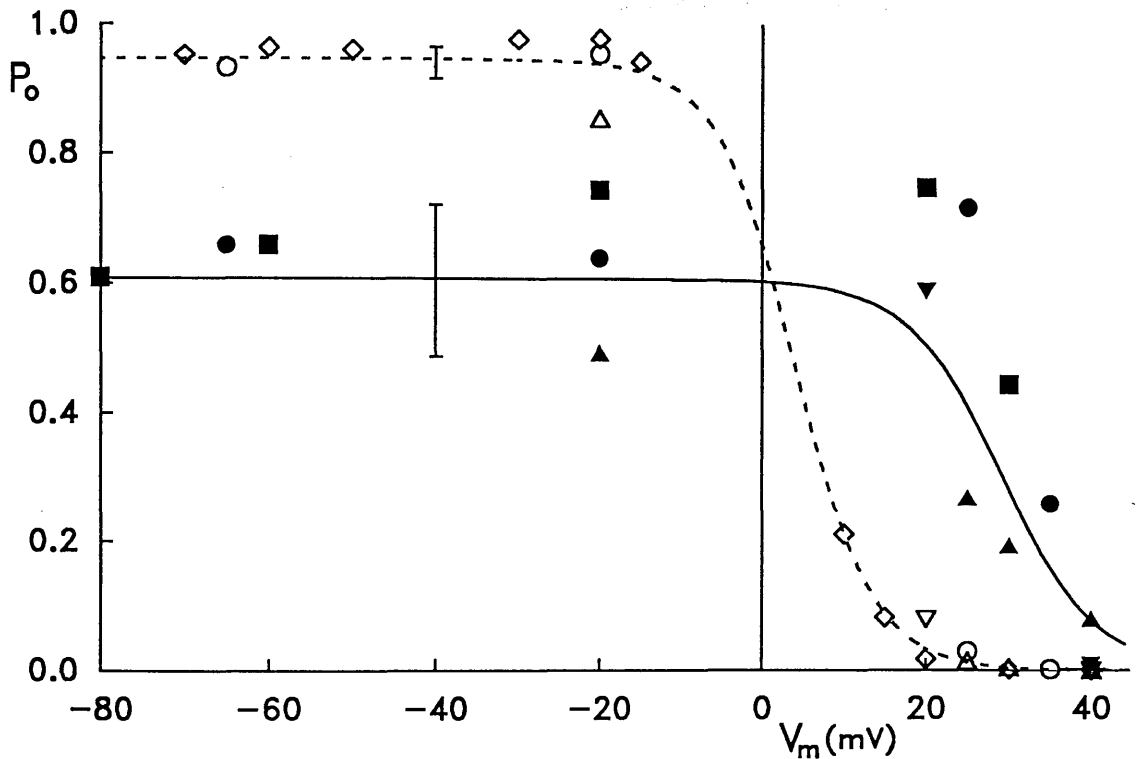


Figure 4.4. Dependence of open probability ( $P_o$ ) on membrane potential ( $V_m$ ) in static and flowing solution. Open symbols for patches in static solution. Filled corresponding symbols from same patches in flowing solution. At -40 mV, mean open probability was  $0.94 \pm 0.024$  (S.D.,  $n=15$ ) in static solution and  $0.60 \pm 0.11$  (S.D.,  $n=11$ ) in flowing solution.  $\diamond$ , data from Fig.3.7. Dashed curve gives open probability in static solution fitted by Boltzmann relation,  $P_o = 0.95 / (1 + \exp((V_m - 4.0) / 4.8))$ . Continuous curve gives corresponding open probability in flowing solution,  $P_o = 0.606 / (1 + \exp((V_m - 29.1) / 5.6))$ .

## DISCUSSION

The changes in open probability of inwardly rectifying channels from sarcolemmal vesicles, or from dispersed skeletal muscle fibres, produced by flow were regular in appearance, of striking magnitude and readily reversible. The effect was also specific inasmuch as it was not demonstrable in all types of  $K^+$  channels that are present in similar patches, nor in inwardly rectifying channels from dispersed ventricular myocytes. This phenomenon cannot therefore be dismissed as due to some general abnormality associated with the production of sarcolemmal vesicles or of dispersed cells. At the very least, it is a systematic idiosyncrasy which needs to be understood if only because it is likely to enter as a variable in experiments designed to study the effects of chemical composition on the kinetic properties of the inwardly rectifying channel in skeletal muscle.

### Chemical mechanisms

In searching for mechanisms that might explain the effects of flow, the stirring effect of flow provides an obvious starting point. Here we have ruled out the pre-existence of a local concentration gradient at the inner face of the patch, such as might conceivably arise if the composition of the solution within the patch pipette differs from that of the bath and superfusion solutions. The idea that electric current flow through the permselective channel leads to local accumulation or depletion of ions with the patch in static but not in flowing solution can also be dismissed: apart from such a transport number effect being unlikely in view of the high  $[K^+]$  employed in the present experiments, flow was found to increase  $P_o$  even at potentials so positive that the channel carries negligible current in static solution. To entertain a chemical hypothesis it therefore becomes necessary to suppose that a substance is released from the inner

surface of the membrane, or is produced at that site through the action of a membrane-bound enzyme. If so, the repeatability of the effect in the same patch and the rapid return upon cessation of flow to the  $P_o$  appropriate to the static state would require the store of substance to be substantial, or the substrate to be plentiful and the rate of production or consumption to be rapid. In the present experiments, the only likely substrate was ATP. Supposing ATP is hydrolysed at the inner surface of the membrane at a sufficient rate, its local concentration may be lower in static than in flowing solution. A consequent increase in local negativity on initiation of flow might then cause a shift of the activation curve of the inwardly rectifying channel to the right, as found experimentally. However, this hypothesis seems less attractive when it is recalled that the ATP-sensitive  $K^+$  channel is uninfluenced by flow.

#### Physical mechanisms

Initially, the notion that the inwardly rectifying channel in skeletal muscle belongs to the growing group of stretch-sensitive channels (see e.g. review by Morris, 1990) seemed attractive. In all such channels, changes in membrane tension produce changes in channel gating and hence  $P_o$  (while channel conductance remains constant). However, with the flow rates used in the present experiments, the reversal in momentum yields only low distending forces. For example, given a circular patch of diameter  $2\mu\text{m}$  in a stream of solution flowing at 5 cm/s, the force exerted on the patch would amount to only  $1.5 \times 10^{-11}$  N, equivalent to 50 dyn/cm<sup>2</sup> or 0.05cmH<sub>2</sub>O, a very low pressure indeed: smaller patches and/or lower flow rates yield even smaller estimates. Besides, we were unable to elicit changes in  $P_o$  by applying suction of several cm of H<sub>2</sub>O to the patch pipette.

There remains a possibility that flow influences the gating of inwardly rectifying  $K^+$  channels by deforming the membrane or molecular appendages left attached to its inner surface (Jung, Song & Sachs, 1987). In this connection, recent findings by Olesen, Clapham & Davies (1988) on vascular epithelial cells are noteworthy. When such cells are subjected to shear stress by flow of solution over their surface, they become hyperpolarized and this effect is attributable to activation of a  $K^+$  conductance which rectifies inwardly like that in skeletal and cardiac muscle. Olesen *et al.* (1988) searched for flow-sensitive  $K^+$  channels in numerous outside-out patches from vascular epithelium, to no avail. As possible explanations they advanced a low channel density, or that the membrane area of a detached patch is too small to allow deformation of the membrane by flow. The present finding belie the second interpretation and they raise the possibility that membrane deformation produced by shear applied to the surface of the sessile cell exerts its effect through transmission to molecules at the inner surface of the membrane which are normally connected to the cytoskeleton. In muscle fibres it is conceivable that mobile intracellular structures may generate shear stresses at the inner surface of the membrane through cytoskeletal molecules anchored there. In this regard, it would be interesting to see whether exposure of the intracellular face of the membrane patch to non-specific protease activity (which exists in the collagenase currently used to prepare vesicles) has any affect on the flow phenomenon. The abolition of the flow effect by such treatment, without other changes in channel behaviour, would suggest the involvement of other, possibly cytoskeletal, proteins.

It would be useful to know the relationship between the rate of solution flow and the reduction in  $P_o$ . In these experiments, the effect

is apparently already saturated at a flow rate of 0.2 cm/s, the lower limit of the present perfusion system. Clearly, lower flow rates need to be investigated.

Recently, Kirber and others (1989, 1990) reported that K<sup>+</sup>-selective channels in smooth muscle cells were activated, i.e. P<sub>o</sub> was increased, by flow from 1 μm pressure ejection pipette at the extracellular face of outside-out patches. The effect of flow required external Ca<sup>2+</sup> to be present in micromolar concentrations. Further, the response to flow was enhanced when [Ca<sup>2+</sup>]<sub>o</sub> was raised. Whether the flow effect in skeletal muscle is also modulated by some Ca<sup>2+</sup> would be interesting to investigate, but would require the large Ca-activated K<sup>+</sup> channel first to be blocked by e.g. charybdotoxin (Miller, 1985).

ions. Further, the response to flow was enhanced when [Ca<sup>2+</sup>]<sub>o</sub> was raised. Whether the flow effect in skeletal muscle is also modulated by Ca<sup>2+</sup> would be interesting to investigate, but would require the large Ca-activated K<sup>+</sup> channel first to be blocked by e.g. charybdotoxin (Miller, 1985).

## CHAPTER 5

**Effect of lowering intracellular pH on inwardly  
rectifying K channels in skeletal muscle.**

## SUMMARY

1. The sensitivity of inwardly rectifying  $K^+$  channels to changes in  $pH_i$  was studied in inside-out patches from rat sarcolemmal vesicles under conditions of constant flow.

2. When  $pH_i$  was lowered from 7.4 to 6.9, 6.5 or 6.0, the channel continued to show transitions between open and short closed states, but this activity became interrupted by long lasting closures, the more so the lower  $pH_i$ . On exposure to  $pH_i$  5.0, the channel soon closed down until  $pH_i$  was returned to 7.4.

3. During the periods of channel activity at  $pH_i$  below 7.4, the open probability decreased in graded fashion the lower  $pH_i$ . Both a decrease in mean open time and an increase in mean closed time contributed to this reduction in open probability.

4. The reduction in open probability during the periods of channel activity was not obviously voltage dependent and cannot therefore be attributed to a shift in the open probability-voltage relation.

5. The current through a single inwardly rectifying channel decreased with lowered  $pH_i$ . At  $pH_i$  6.9 or 6.0, the single channel current was on average respectively 0.94 or 0.88 that at  $pH_i$  7.4. Closure of channels at lower  $pH_i$  limited the range over which this effect could be studied. The reduction in single channel conductance was not obviously voltage dependent.

6. The decrease in open probability due to the changed kinetics whilst the channel remains active, and to the entry of the channel into a prolonged closed state, was combined with the decrease in single channel current to yield the expected reduction in macroscopic current when  $\text{pH}_i$  falls. This relation is compared with that reported in the literature.

7. When  $\text{pH}_i$  is lowered the leak current decreased to a similar extent as the single channel current. The effect of low  $\text{pH}_i$  on leak current, and on the kinetic and conductive properties of the inwardly rectifying channel were readily reversed on restoring  $\text{pH}_i$ .

## INTRODUCTION

In 1978, Hagiwara, Miyazaki, Moody and Patlak described a block of the macroscopic inwardly rectifying potassium current ( $I_K$ ) in starfish egg membrane on lowering the pH of the external solution ( $\text{pH}_o$ ). In the range  $\text{pH}_o$  7.0-6.0, there was little decrease in membrane current, but beyond  $\text{pH}_o$  6.0 the ratio  $I_{K,\text{pH}6.0}/I_{K,\text{pH}7.0}$  fell sharply, and at  $\text{pH}_o$  5.0, most of  $I_K$  was abolished. However, it later became clear that their use of the permeant buffer acetate in the bathing solution had led to a secondary internal acidification, and that this had contributed substantially to the observed effect. With impermeant biphthalate as the buffer, they saw only a relatively weak block by external  $\text{H}^+$  ( $I_{K,\text{pH}5.0}/I_{K,\text{pH}7.0} = 0.88-1.0$ ).

Using acetate buffer, but also measuring intracellular pH with a microelectrode, Moody & Hagiwara (1982) showed a block of the inward current with lowered intracellular pH ( $\text{pH}_i$ ) which was essentially complete by  $\text{pH}_i$  5.6. The steep titration curve for  $\text{pH}_i$  was interpreted by assuming that 3 protons bind to a site to block the channel with a

pK of 6.26. This block showed no voltage dependence, and  $H^+$  did not affect the kinetics of the current. The interpretation of the results in starfish oocytes is complicated, however, by the fact that intracellular sodium rose on acidification, and that an increase in  $[Na]_i$  enhanced  $I_K$  (Hagiwara & Yoshii, 1979).

In experiments on frog skeletal muscle, Blatz (1984) using cut fibres with the vaseline gap voltage clamp technique showed that  $I_K$  was blocked by internal but not by external acidification (except for a small irreversible block at  $pH_o$  5.0). The inside of the fibre was made more acid in two ways: 1) by lowering the pH of an external acetate buffer, and 2) by allowing biphthalate buffer to diffuse into the myoplasm through the cut ends of the fibre. The dependence of inward rectifier conductance (at -48mV) on internal pH was again well described by a model assuming three blocking sites and a pK of 6.1. There was no shift in the voltage dependence of inward rectification with reduced  $pH_i$ . Although there is no mention of the fact, Blatz' experiments showed there are no obvious changes in the K current kinetics with  $pH_i$ .

The methods used in the experiments just described do not allow composition of the internal solution to be changed easily or quickly. An advantage of using the patch clamp method is the control over  $pH_i$  it affords. On the other hand, it requires that one finds relatively rare patches containing inwardly rectifying K channels (Matsuda & Stanfield, 1989) and that patches are successfully detached. These put limits on what can be done. Nevertheless, it proved possible to reveal the general character of the phenomenon at the single channel level.

## METHODS

Single inwardly rectifying  $K^+$  channels from rat sarcolemmal vesicles was examined by detaching patches into solution containing (mM) 140 KCl, 5  $K_2$ ATP, 1 EGTA, and 0.5  $MgCl_2$  buffered to pH 7.4 with 5 mM-HEPES/KOH. The pipettes were filled with 140 mM-KCl buffered as above. With 0.5 mM added  $MgCl_2$ , the free  $[Mg^{2+}]$  was  $14\mu M$  at pH 7.4. Under these conditions the channel passed only inward currents, and was open most of the time. The presence of  $Mg^{2+}$  was useful to identify the channel as the inwardly rectifying  $K^+$  channel. A value of 7.4 was chosen as the standard  $pH_i$  so that pH was the same on both sides of the membrane. This is a couple of points beyond the upper end of the pH range occurring *in vivo*. Patches were placed in the mouth of a perfusion pipette from which flowed solution with the same composition as the bath and whose pH could be changed. Added Mg was adjusted to keep free  $[Mg^{2+}]$  constant at  $14\mu M$  with changes in pH. Holding potential was generally -40mV or -60mV. In some experiments, when positive potentials were to be explored, Mg was omitted from the perfusion solution.

## RESULTS

The most striking effect of a decrease in intracellular pH is on channel kinetics so as to decrease channel open probability. In addition small but consistent decreases in single channel currents and in leak currents are observable. The more  $pH_i$  was lowered the more pronounced are these three effects. All these changes are readily reversible.

In the experiments of Fig.5.1A,B  $pH_i$  was lowered from 7.4 to 6.0. This caused the channels to spend more time in the closed state but they continued to undergo frequent transitions. By contrast, when  $pH_i$

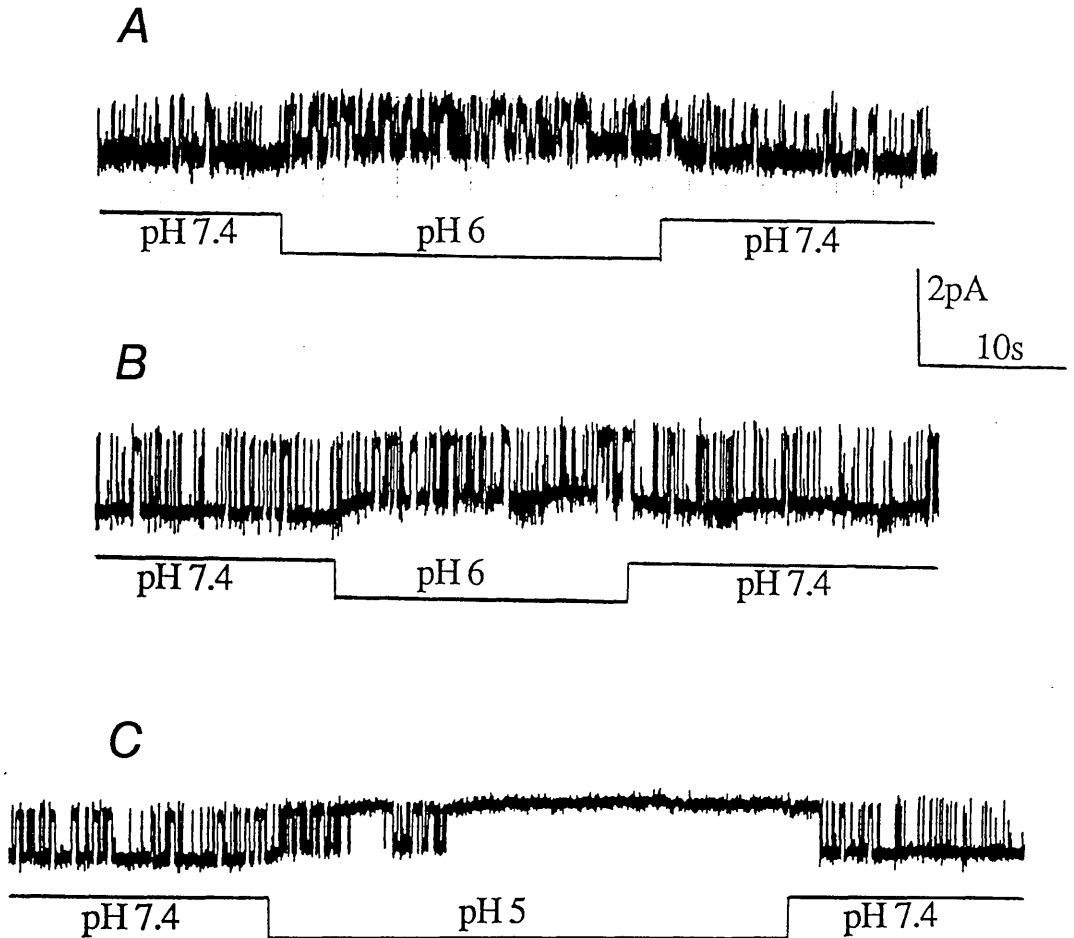


Figure 5.1. Effects of lowering  $pH_i$  on skeletal muscle  $K_{inw}$  channels. Three inside-out patches detached from rat sarcolemmal vesicles. Chart recordings of channel activity at a holding potential of A,C -40mV and B -60mV. When  $pH_i$  was lowered from 7.4 to 6.0 (A,B) as indicated, open probability and single channel current decreased; when  $pH_i$  was lowered from 7.4 to 5.0 (C) channel activity was abolished.

was lowered to 5.0 (Fig.5.1C) the channel soon entered into a long closed state and, after a transient burst, remained closed until  $\text{pH}_i$  was raised again. A decrease in single channel current is detectable both in Fig.5.1A and Fig.5.1B, but more easily in the second case because the currents there are larger owing to the more negative holding potential. At pH 5.0, the decrease in single channel current is clearly seen even at a moderately negative holding potential. The upward shift in the top of the traces is indicative of a decrease in leak current.

From those experiments in which traces of adequate stability were recorded, an estimate of channel open probability ( $P_o$ ) including both long and short closed periods could be obtained. The reduction in overall  $P_o$  on acidification, for several pH values is plotted in Fig.5.2, as a first approximation of the likely contribution of the change in kinetics to the reduction in macroscopic conductance. It can be seen that  $P_o$  falls with progressively lower  $\text{pH}_i$ ; at pH 6.9 open probability has decreased to about 80% of its value at pH 7.4. There is a considerable scatter of points at 6.0 owing to the fact that at this pH a significant proportion of the analyzed periods contained long closures. The curve drawn through the data points is a Boltzmann with a slope factor of 1 and midpoint at pH 6.6.

#### Effect on channel kinetics

Analysis of the kinetic properties of the inwardly rectifying channel at pH 7.4 has led to the conclusion that there exists one open and at least two closed states (Chapter 3; Matsuda & Stanfield, 1989). Most of the time, transitions are between short open and closed states. But occasionally sojourns in a distinctly longer closed state occur.

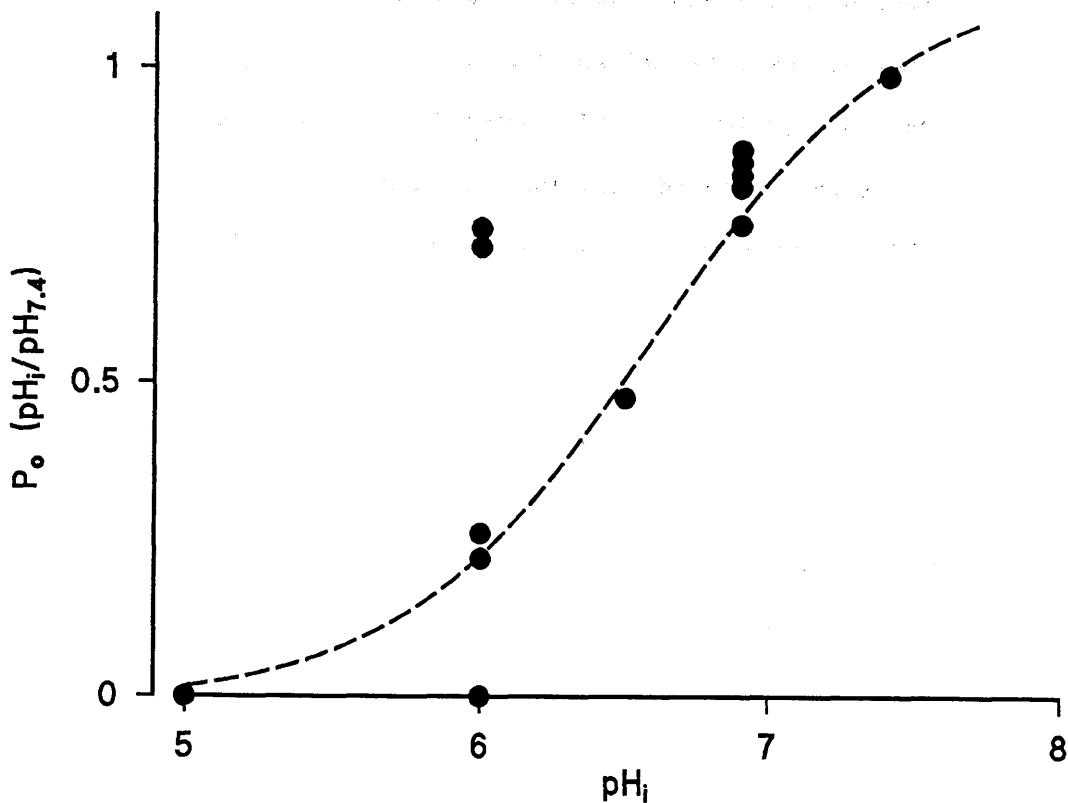


Figure 5.2. Overall open probability of  $K_{inw}$  channel at different  $pH_i$ . Open probability was determined from total open and closed times including periods of long lasting closure. Curve has equation  $1.17/[1+\exp(-2.3 \cdot (pH_i - 6.6))]$ .

In the present experiments, entry into a long closed state occurred more frequently at lower  $\text{pH}_i$ . In more than half of the changes from 7.4 to 6.0, the channel closed completely either for several seconds or did not reopen until after  $\text{pH}_i$  was restored to 7.4. When  $\text{pH}_i$  was lowered to 5.0, the channel closed down within a second or two in almost all cases. The durations of the long closed periods are such that it is impracticable to obtain reliable dwell-time estimates; for that, recordings of tens of minutes would be required, longer than the typical lifetime of a patch. However, it is valid to ask what effects lowering pH has on the transitions between the set of relatively short states which predominate in the kinetics at neutral pH. To this end, an analysis with the half-amplitude threshold crossing technique (see Chapter 1) was carried out in which long ( $>1\text{s}$ ) closed states were excluded. The values of mean open time ( $\hat{t}_o$ ), mean *short* closed time ( $\hat{t}'_c$ ) and the open probability during bursts, given by  $P'_o = \hat{t}_o / (\hat{t}_o + \hat{t}'_c)$ , are given in Table 3. It can be seen that, in all cases,  $\hat{t}_o$  decreased when pH was lowered. The mean ratio of  $\hat{t}_o$  pH6.0/pH7.4 was 0.5, and of  $\hat{t}_o$  pH5.0/pH7.4 0.2. Mostly  $\hat{t}'_c$  increased on acidification, but in two cases it decreased slightly. Despite the greater variability in the ratios of  $\hat{t}'_c$  estimates compared with those of  $\hat{t}_o$ , the resulting  $P'_o$  was consistently reduced in acid. The mean ratio  $P'_o$  pH6.0/pH7.4 was 0.65, and pH5.0/pH7.4 was 0.46.

In experiments in which  $\text{pH}_i$  was lowered to 6.9, long closed periods were not observed, so that a straightforward analysis could be carried out.  $\text{Mg}^{2+}$  was omitted from the internal solution, allowing depolarizing potentials to be studied. In one experiment, the patch contained two channels, so dwell times could not be measured. However, estimates of  $P_o$  were obtained, at holding potentials -65mV and -20mV, by constructing amplitude histograms and determining the relative areas

Table 3. Kinetics of inwardly rectifying K<sup>+</sup> channel at pH<sub>i</sub> 7.4/5.0 and pH<sub>i</sub> 7.4/6.0.

| V <sub>h</sub><br>(mV) | pH <sub>i</sub> | t <sub>o</sub><br>(ms) | t <sub>c</sub><br>(ms) | P <sub>o</sub> | τ<br>(ms) |
|------------------------|-----------------|------------------------|------------------------|----------------|-----------|
| -40                    | 7.4             | 271                    | 57                     | 0.82           | 47        |
|                        | 5.0             | 56                     | 94                     | 0.37           | 35        |
| -40                    | 7.4             | 186                    | 66                     | 0.73           | 49        |
|                        | 5.0             | 37                     | 65                     | 0.35           | 24        |
| -40                    | 7.4             | 129                    | 35                     | 0.79           | 27        |
|                        | 6.0             | 77                     | 146                    | 0.35           | 12        |
| -40                    | 7.4             | 193                    | 70                     | 0.73           | 51        |
|                        | 6.0             | 84                     | 74                     | 0.53           | 39        |
| -40                    | 7.4             | 176                    | 74                     | 0.70           | 52        |
|                        | 6.0             | 50                     | 109                    | 0.31           | 34        |
| -40                    | 7.4             | 99                     | 46                     | 0.68           | 31        |
|                        | 6.0             | 53                     | 124                    | 0.30           | 37        |
| -60                    | 7.4             | 193                    | 37                     | 0.84           | 31        |
|                        | 6.0             | 105                    | 61                     | 0.63           | 38        |
| -60                    | 7.4             | 213                    | 36                     | 0.85           | 31        |
|                        | 6.0             | 143                    | 29                     | 0.83           | 24        |

under the peaks. Amplitude histograms at -65mV are shown in Fig.5.3A,B. At pH 7.4 (Fig.5.3A) both channels are open 62% of the time, one channel 33.2% and neither channel 4.4%. According to the binomial theorem, the probability that  $x$  channels are open ( $P_x$ ) in a patch containing  $N$  channels varies with the probability of one channel being open ( $P_o$ ), according to the relation

$$P_x = N!/[x!(N-x)!] \cdot P_o^x \cdot (1-P_o)^{(N-x)}.$$

Comparing  $P_0$ ,  $P_1$  and  $P_2$ , determined from the areas under the peaks, with values predicted by the above equation yields  $P_o = 0.8$ . When  $pH_i$  is lowered to 6.9 (Fig.5.3B), the amplitude histogram changes to reflect the fact that both channels spend less time in the open state, and  $P_o$  is reduced from 0.8 to 0.61. The reduction of  $P_o$  over a range of voltages is shown in Fig.5.4; the reduction varied between 10 and 25%. These data do not indicate a strong voltage dependence of the effect of pH on  $P_o$ .

#### Effect on single channel current and leak current

The reduction in  $i$  developed hand in hand with the reduction in leak current, within a few seconds of switching the perfusing solution. It is probable that the time course of these changes reflects mainly the effective change in the acidity of the solution bathing the patch, as determined by the dead space of the perfusion system. Once reduced,  $i$  remained constant. Recovery of  $i$  on return to  $pH_i$  7.4 was equally rapid. In Fig.5.1C  $i$  was fully restored when channel activity resumed, presumably because the residence in the long closed state outlasted the return to pH 7.4.

In Fig.5.5A,B amplitude histograms constructed from the experiment of Fig.5.1B are shown. The top histogram corresponds

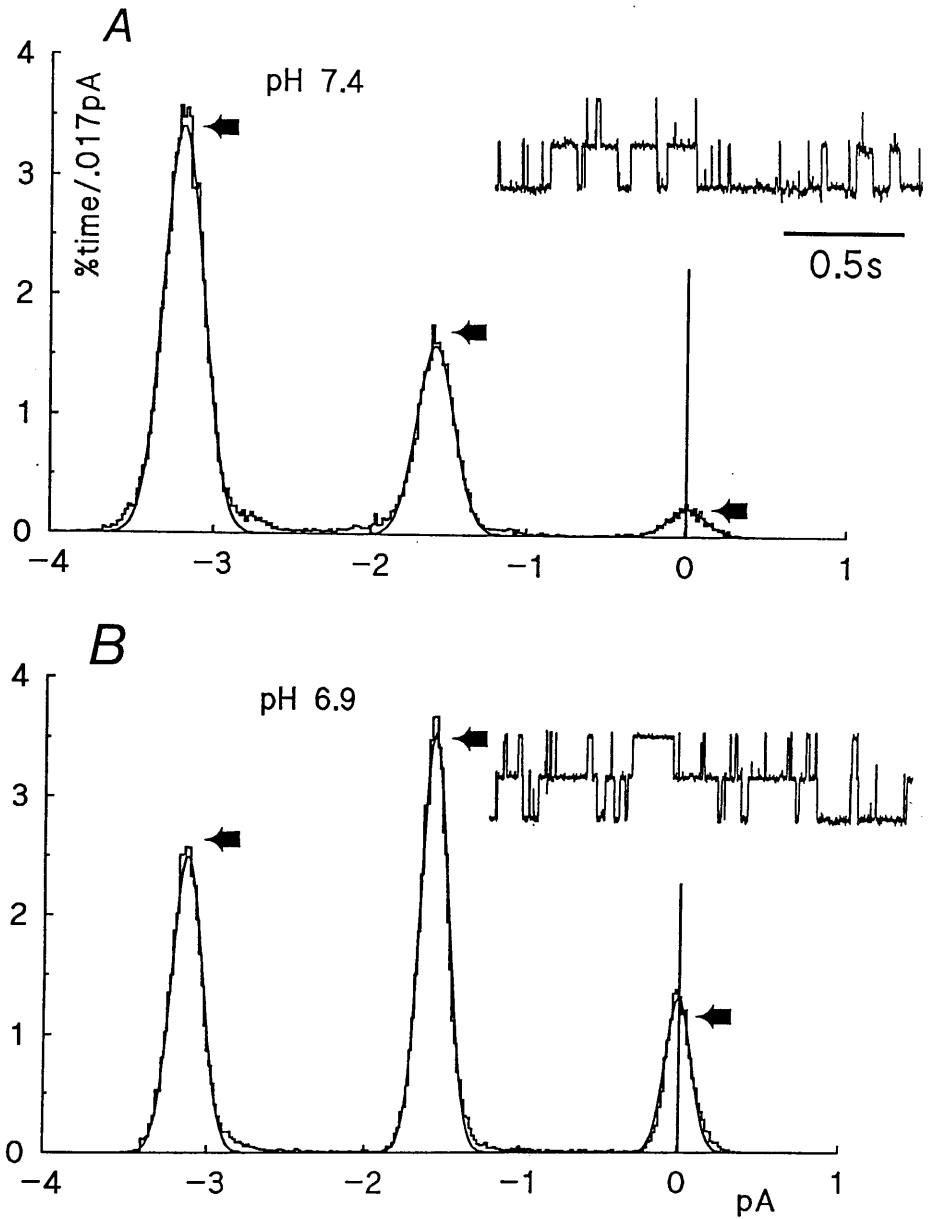


Figure 5.3. Amplitude histograms of  $K_{inw}$  currents at  $pH_i$  7.4 and 6.9. Histograms were constructed from 25s periods of continuous recording; sampling rate 2kHz, filter 300Hz. Insets show short sections of recording. Gaussian curves were fitted to peaks corresponding to (left-right) 2, 1 and 0 open channels. Arrows indicate the height of peaks predicted from the binomial theorem assuming two channels were active throughout the recording with open probabilities of A 0.8 at  $pH_i$  7.4, and B 0.61 at  $pH_i$  6.9.

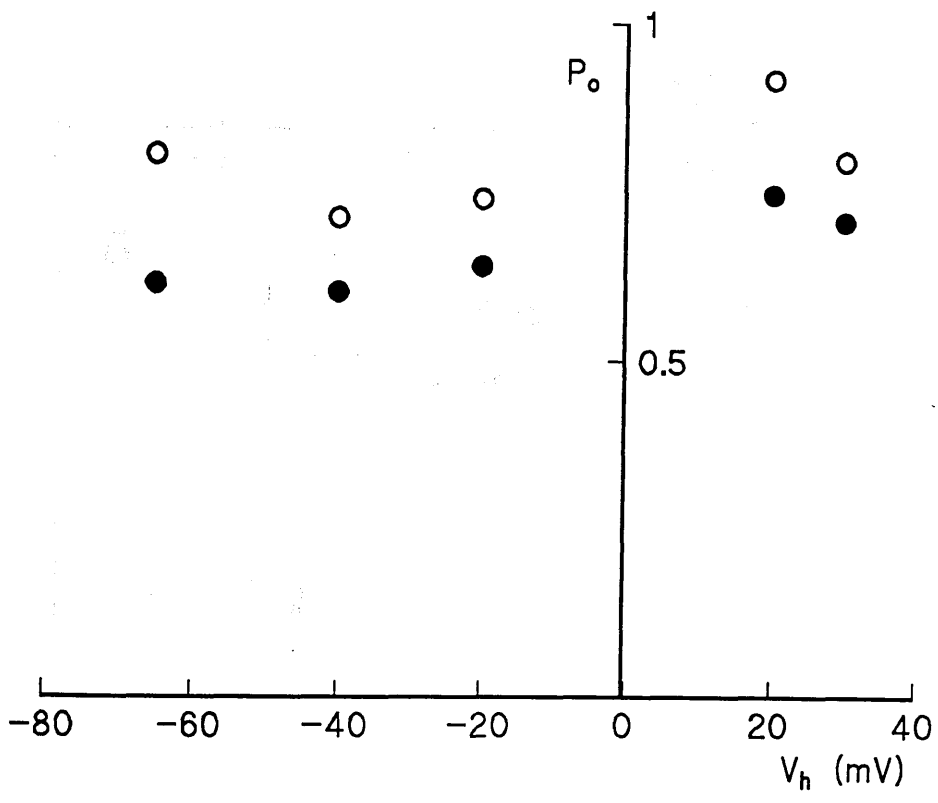


Figure 5.4. Reduction in open probability of  $K_{inw}$  channels with mild internal acidification. Results from two patches. Open probability was determined as in Fig.5.3 (-65mV, -20mV) or from measurements of open and closed times, at  $pH_i$  7.4 (○) and  $pH_i$  6.9 (●).

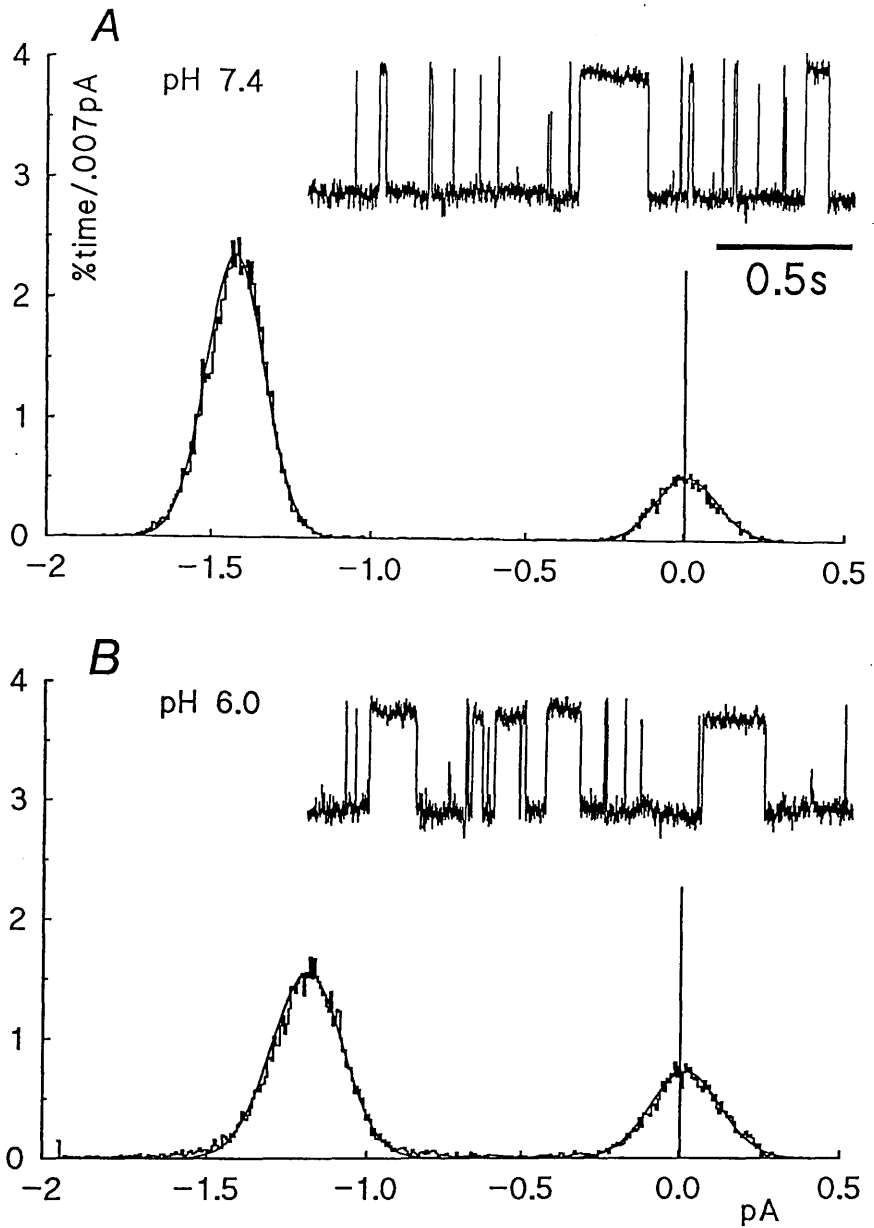


Figure 5.5. Amplitude histograms of  $K_{inw}$  channel currents at A  $pH_i$  7.4, and B  $pH_i$  6.0. 10s of recording; sampling rate 2kHz, filter 300Hz. Insets show short sections of recording. Gaussian curves were fitted to open and closed current levels.

to a 10s period recorded at pH 7.4 immediately before the first solution change. Open and closed current levels are at 0 and -1.42pA respectively. The bottom histogram was taken from another 10s period, after  $\text{pH}_i$  was changed to 6.0. The open peak has shifted to the right indicating a reduction of  $i$  to -1.2pA. (Note also the redistribution of areas under the peaks, due to the reduction in  $P_o$ .) In this experiment, the long lasting closed state did not appear while  $\text{pH}_i$  was reduced, and we can be reasonably confident that current measurements taken from the middle of this period represent a true steady-state value of  $i$  in pH 6.0.

Estimates of the decrease in  $i$  from a number of experiments are plotted against pH in Fig.5.6. The points at pH 5.0 are from the two experiments (including that of Fig.5.1C) where channel activity continued long enough after the solution change for a reliable estimate of  $i$  to be obtained. In general, single channel currents were reduced to a greater degree in more strongly acid  $\text{pH}_i$ . A curve through the points was fitted by eye, ignoring the singular point at pH 6.5. When the same data are plotted against voltage, no obvious voltage dependence of the decrease in  $i$  was detectable (Fig.5.7).

A significant leak current was present in all patches. The magnitude of this current varied from patch to patch, from 0.6 to 3 times the single inward rectifier current at pH 7.4. It also decreased when  $\text{pH}_i$  was lowered. Fig.5.8 shows a record from a silent patch held at -40mV in which  $\text{pH}_i$  was changed from 7.4 to 5.0 and back. Here the reduction in leak current is clearly visible. The time course of the effect is somewhat slower than in

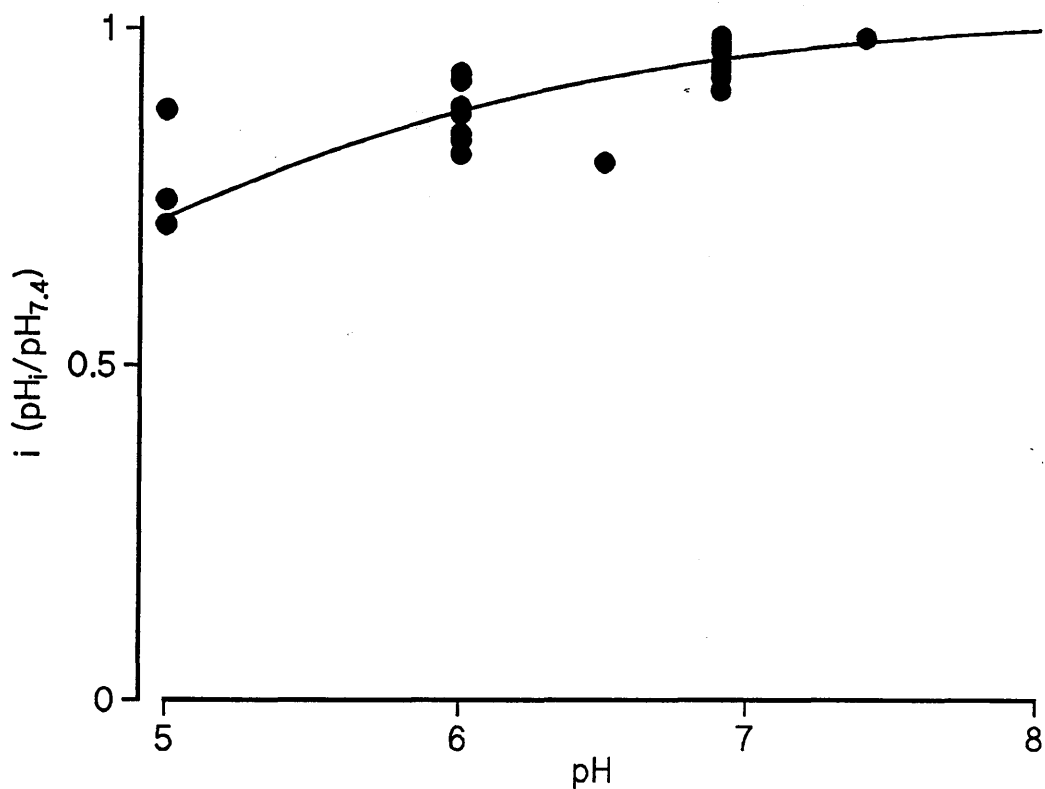


Figure 5.6. Reduction in single  $K_{inw}$  channel current at different  $pH_i$ . The ratios of unitary currents measured before and after  $pH_i$  was lowered from 7.4 were plotted. Curve has equation  $1.045/[1+\exp(-0.9 \cdot (pH-4.1))]$ .

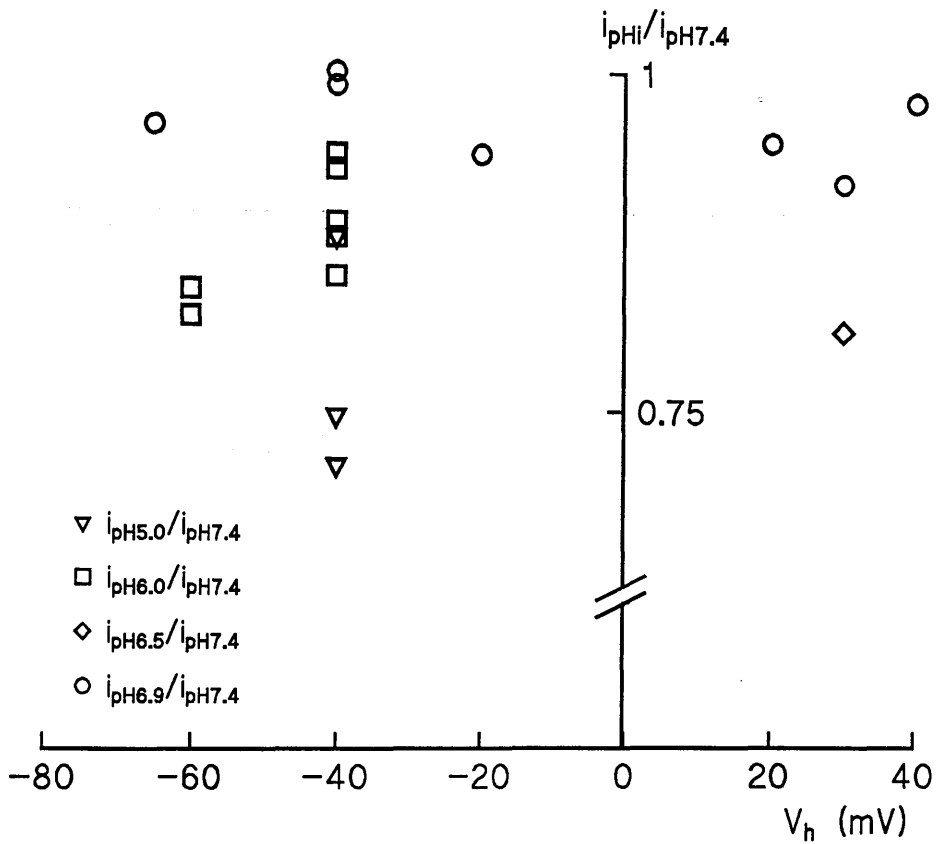


Figure 5.7. Reduction in single  $K_{inw}$  channel current at different holding potentials. Data from same experiments as shown in Fig.5.6.

Figure 5.8. Reduction of leak current on lowering  $pH_i$ .

Inside-out patch detached from rat sarcolemmal vesicle containing no active channels was exposed to solutions with

pH 7.4 and 5.0 at  $V_h$

-40mV. Dashed line indicates zero current level.

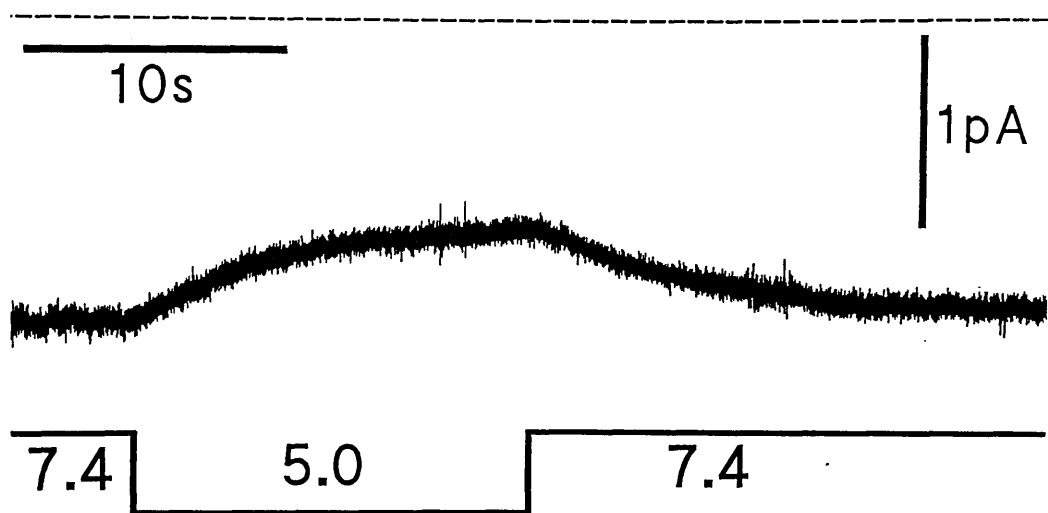


Figure 5.8. Reduction of leak current on lowering  $pH_i$ . Inside-out patch detached from rat sarcolemmal vesicle containing no active channels was exposed to solutions with pH 7.4 and 5.0 at  $V_h$  -40mV. Dashed line indicates zero current level.

experiments of Fig.5.1, due to a lower flow rate of the perfusion system. In those experiments involving changes of  $\text{pH}_i$  from 7.4 to 5.0, the mean reduction in leak current was to  $0.74 \pm 0.08$  ( $n=11$ ), which is comparable to the decrease in single channel current.

## DISCUSSION

### Comparison between the effects of internal acidification as measured in single channel and in 'intact' cell experiments

In macroscopic experiments the current recorded will be given by  $N \cdot i \cdot P_o$ , where  $N$  is the number of channels in the preparation,  $i$  is the single channel current and  $P_o$  the mean open probability. To establish a basis for comparison with macroscopic results, the  $P_o$ -pH relationship from Fig.5.2 and the  $i$ -pH relationship from Fig.5.6 were therefore combined (Fig.5.9). Since the effect of  $\text{pH}_i$  on  $i$  is relatively small, the resulting relationship is only slightly steeper than the simple titration curve in Fig.5.2. By way of comparison, Fig.5.9 reproduces the result obtained by Blatz (1984) on segments of frog muscle fibres. It can be seen that although the  $\text{pK}$  of the two curves is similar the macroscopic relationship is much steeper.

As no ready explanation can be offered for this major disparity, the differences in the experimental conditions will be enumerated and each evaluated as a possible cause. First (i), Blatz's (1984) experiments were done on frog muscle whereas the present experiments were done on mammalian muscle. As the  $\text{pH}_i$  sensitivity of the inward rectifier is well preserved between echinoderm egg cells (Moody & Hagiwara, 1982) and frog muscle, it seems unlikely that a major difference in its properties would appear between one vertebrate and another. Secondly (ii), the

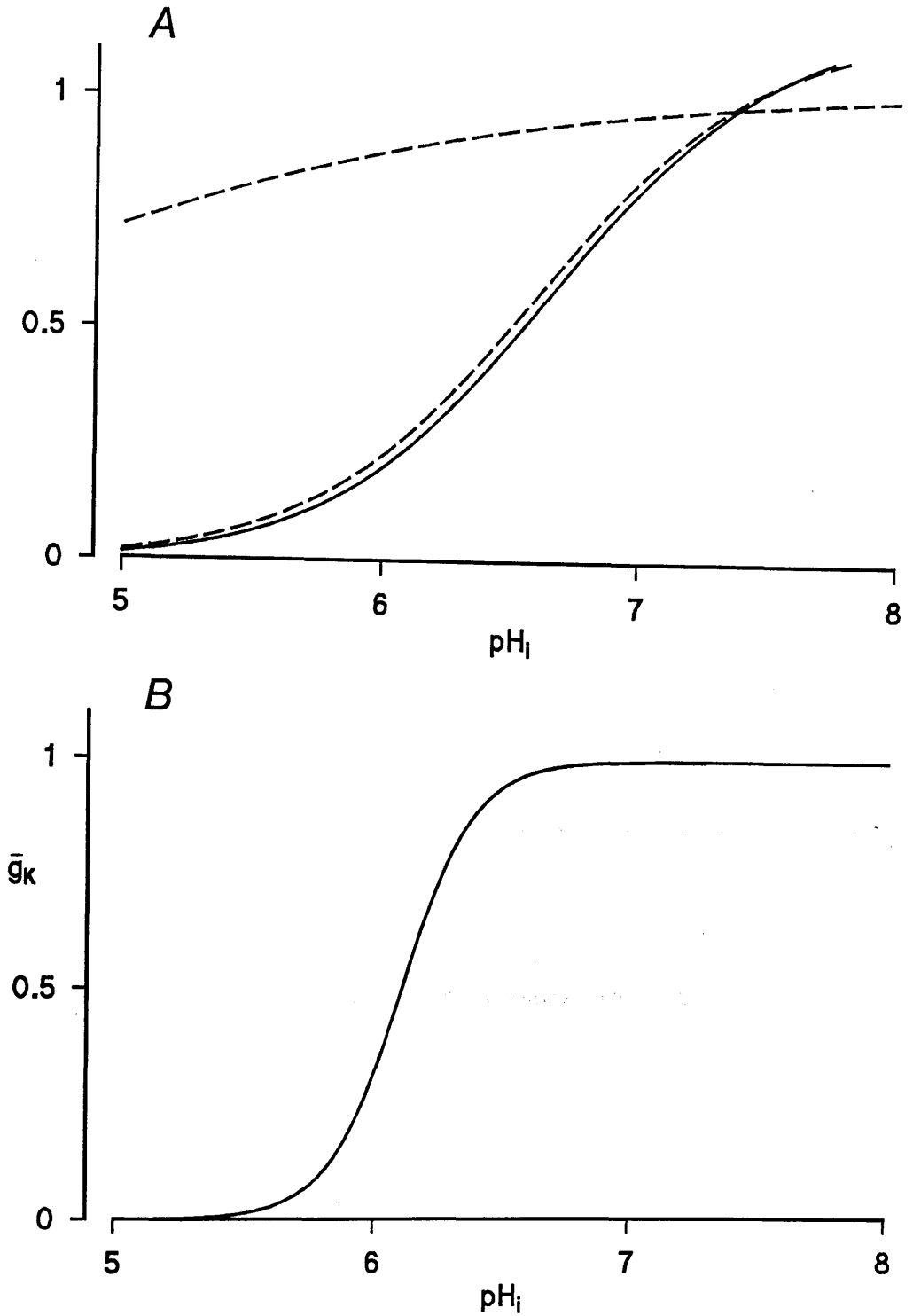


Figure 5.9. Combined  $P_o$ - $\text{pH}_i$  and  $i$ - $\text{pH}_i$  relationships for skeletal muscle  $K_{inw}$  channel. A, curves from Fig.5.2 and Fig.5.6 (dashed lines) were multiplied to obtain curve (solid line) representing overall reduction in current at different  $\text{pH}_i$ . B, normalized macroscopic conductance- $\text{pH}_i$  relationship from Blatz (1984). Curve is equation  $\bar{g}_k/\bar{g}_{k,7.0} = K^3/(K^3 + [H^+]_i^3)$  with  $\text{pK}=6.1$ .

present experiments were done on detached patches, which were therefore devoid of many intracellular components. But diffusible intracellular components would also be lost from cut muscle fibres in a vaseline-gap voltage-clamp apparatus such as was used by Blatz. Next (iii), we have to consider the difference in the geometry of the preparation. Inwardly rectifying K channels are known to be prevalent in the T-tubular membrane of muscle fibres, and in voltage clamp experiments on intact muscle such a distribution is liable to complicate the results through spatial attenuation of the applied voltage (DeCoursey, Dempster & Hutter, 1984). However, detailed consideration of this argument shows that it cannot account for a steeper pH-conductance relationship when the channels are so distributed; rather, the relation between  $\text{pH}_i$  and  $g_K$  is liable to be flattened as a result of the increase in the tubular space constant to be expected when  $\text{pH}_i$  is lowered.

There remains (iv) the circumstance that the present experiments were done with patches exposed to a constant flow of solution and that such treatment has been shown to have a major effect on the kinetics of the inwardly rectifying channel. This factor remains imponderable so long as the nature of the flow effect remains obscure. In cardiac muscle, where the inwardly rectifying K channel is not sensitive to flow (see next chapter) a moderate reduction in  $\text{pH}_i$  speeds the transitions between the open and a short-lived closed state with little fall in  $P_o$ . The steep fall in  $P_o$  seen below  $\text{pH}_i$  6.5 is due to entry of the channel into the long closed state, and the resulting relation between  $P_o$  and  $\text{pH}_i$  in cardiac muscle resembles that found in macroscopic experiments on skeletal muscle (compare Fig.5.9 with Fig.6.21).

Whether inwardly rectifying channels in skeletal muscle behave similarly to those in cardiac muscle when they are subjected to changes in  $\text{pH}_i$  in static solution is a question which to answer requires further experiments with a different technique.

Finally, it should be pointed out that in the macroscopic experiment of Blatz (1984)  $\text{pH}_i$  was lowered from 7.0 to 5.0 over a period of 75 mins, whilst in the present experiments  $\text{pH}_i$  was lowered only transiently for 30-40 seconds at a time. Supposing that there exists a multiplicity of closed states with long lifetimes, entry into which is favoured by low  $\text{pH}_i$ , channels would become absorbed into these closed states the more so the longer the exposure to low  $\text{pH}_i$ . This may well be another factor contributing to the steeper fall in  $P_o$  with lowered  $\text{pH}_i$  observed in macroscopic experiments.

#### Mode of action of lowered $\text{pH}_i$

The manner in which the  $P'_o$ -V relation for the rapid transitions in the  $K_{\text{inw}}$  channel is altered allows distinction between some of the possible modes by which lowering  $\text{pH}_i$  reduces  $P'_o$ . Characteristically, the  $P'_o$ -V relation never reaches unity even at strongly negative potentials in static solution (Fig.4.4, open symbols). Flow further depresses the open probability at negative potentials (Fig.4.4, filled symbols); and when  $\text{pH}_i$  is lowered the upper asymptote of the  $P'_o$ -V relation is depressed still more, as is implicit in Fig.5.2. Such a vertical shift in the gating curve cannot be attributed to a positive local potential such as might arise as a result of protonation of sites at the inner surface of the membrane: a change in the electrostatic conditions would produce a sideways displacement of

the gating curve. Rather, the indication is that protonation at the inner surface of the membrane somehow facilitates the transition from the open to the closed state by increasing the asymptotic value of the closing rate constant. The greater tendency for the channel to enter the long closed state at low  $\text{pH}_i$  could similarly be interpreted as a modification of intrinsic gating so as to favour the entry into that state.

An alternative interpretation of the channel closure promoted by low  $\text{pH}_i$  is that  $\text{H}^+$  blocks the open channel. This was the interpretation put forward by Moody & Hagiwara (1982) and by Blatz (1984) to account for the decrease in inward current in their macroscopic experiments. Block of  $K_{\text{inw}}$  channels by extracellular  $\text{Ba}^{2+}$ ,  $\text{Rb}^+$  and  $\text{Cs}^+$  (Hagiwara *et al.*, 1978; Standen & Stanfield, 1978; Hagiwara *et al.*, 1976; Gay & Stanfield, 1977; Standen & Stanfield, 1980), and by intracellular  $\text{Mg}^{2+}$  (Matsuda *et al.*, 1987; Vandenberg, 1987) is well documented. For all these ions it has been demonstrated that the block is voltage dependent, and this has been used to estimate the localization of the blocking site within the channel. By contrast, no voltage dependence has been demonstrated with  $\text{H}^+$ , neither in the macroscopic experiments of Moody & Hagiwara (1982) and Blatz (1984), nor in the present experiments. The case for  $\text{H}^+$  as a blocking ion can therefore only be sustained if it is supposed that the blocking site is outside the electric field at the inner mouth of the channel. The difference between the two hypotheses discussed above thereby becomes somewhat marginal. In this connection, it is noteworthy that although a blocking model is favoured by Matsuda and Stanfield (1989) as an explanation for the reduction in  $P_o$  produced by intracellular  $\text{Na}^+$ , they conclude

that even that voltage dependent decrease in  $P_o$  may equally well result from a modification of gating by the presence of  $\text{Na}^+$  within the channel.

As regards the origin of the decrease in single channel current produced by pH (Fig.5.6), this relatively small effect might be explicable as the consequence of a positive surface potential, too small to give rise to easily detectable changes in the position of the gating curve on the voltage axis. This is an attractive possibility in that it could explain also the reduction of similar magnitude also in the leak current by lowered  $\text{pH}_i$ . Unfortunately, analysis of the decrease in single channel conductance is made difficult by the limited  $\text{pH}_i$  range over which this effect can be explored, owing to complete channel closure as  $\text{pH}_i$  approaches 5.0. Furthermore, it would be difficult to study the phenomenon under conditions of low ionic strength, when the local potential should be larger, because single channel currents would then be so much attenuated as to become unresolvable from noise.

An alternative mechanism that could account for the decrease in single channel current is single channel block by  $\text{H}^+$ . Provided that the protonation-deprotonation reactions were fast ones, as has been reported in some instances (Attwell & Eisner, 1978), only a decrease in mean current amplitude would be detectable. The finding that the decrease in single channel amplitude shows no obvious voltage dependence (Fig.5.7) would again require that the blocking site is at the edge of the electric field. It should be noted, however, that on this hypothesis it becomes harder to account for the similarity in the

decrease in  $i_{K, \text{inw}}$  and in leak current. It would be necessary to suppose that the leak current flows through ungated channels that are subject to block by  $H^+$  in similar manner to  $K_{\text{inw}}$  channels, although they do not display the same rectifying properties and probably also different ionic selectivity.

Clearly, it is not possible for block by  $H^+$  to account for both (i) the changes in channel kinetics, which would require protonation and deprotonation to be relatively slow, and (ii) the decrease in single channel current which presupposes fast protonation and deprotonation reactions. Furthermore, both the above variants of channel block by  $H^+$  require subsidiary hypotheses to sustain them. For instance, it would be necessary to postulate two blocking states of greatly different lifetimes in order to account for the increase in both the short closed time  $t'_c$  and in the long lasting closed state prominent at low  $pH_i$ . On basis of economy of hypothesis then, it seems more likely that the decrease in open probability results from modification of gating by protonation of an allosteric site, and that the decrease in single channel current is due to a small positive surface potential owing to protonation of available sites at the inner surface of the membrane, whereby the local concentration of K ions is reduced.

#### Possible physiological role of fall in $K_{\text{inw}}$ conductance on intracellular acidification

Following severe exercise,  $pH_i$  of both human and frog skeletal muscle is known to fall from about pH 7.1 to pH 6.1 (Pan, Hamm, Rothman & Schulman, 1988; Renaud, 1989). Under such conditions, therefore, the  $K_{\text{inw}}$  conductance would be expected to

fall. The functional significance of this effect could be to counteract a decrease in tubular space constant which would otherwise be liable to develop during exercise through K accumulation in the tubular space, and which would reduce the depolarising efficiency of a surface action potential. In this connection, it might be noted that  $K_{inw}$  channels are not the only species of K channel subject to modulation by  $pH_i$ : recently,  $K_{ATP}$  channels have also been shown to be highly sensitive to  $pH_i$ , but in the reverse sense to  $K_{inw}$  channels, i.e.  $K_{ATP}$  channels open when  $pH_i$  falls (Davies, 1990). Supposing that  $K_{ATP}$  channels are present in the surface membrane of skeletal muscle fibres, as seems likely from their prevalence in sarcolemmal vesicles (Spruce *et al.* 1985, 1987; Chapter 2), a moderate fall of  $pH_i$  during exercise, and hence an increase in  $K_{ATP}$  current, would stabilize the membrane potential, provided that  $K^+$  accumulation at the surface of the fibre is less severe than in T-tubules. And a severe fall in  $pH_i$  might increase the permeability to a degree where this causes inexcitability and thus affords time for recovery. Whatever the validity of the above speculations may turn out to be, they serve to emphasize that in considering the physiological effect of change in  $pH_i$  on potassium permeability, the effects on the several types of K channels lying operationally in parallel need to be considered.

## CHAPTER 6

Sensitivity to  $\text{pH}_i$  of inwardly rectifying  
K channels in cardiac muscle.

## SUMMARY

1. Single channel currents through inwardly rectifying  $K^+$  channels were measured in attached and detached inside-out patches from guinea-pig ventricular cells. Patches were detached into 140mM KCl solution which contained 5mM added Mg or from which Mg was omitted. Pipettes also contained 140mM KCl.

2. Initially the properties of the channel in attached patches and in detached patches exposed to solutions of pH 7.4 were examined. The effects of lowering internal pH ( $pH_i$ ) to 6.5, 6.0 or 5.5 were then studied.

3. At  $pH_i$  7.4, the single-channel conductance was 21-25pS at room temperature (19-23°C). In cell-attached patches and patches detached into solutions containing about 0.7mM free  $Mg^{2+}$ , the channel rectified completely around  $E_K$ , passing no observable outward current at positive holding potentials. In addition to the open-closed transitions due to intrinsic gating seen at all negative potentials, rapid flickery closures appeared at potentials just negative to  $E_K$ .

4. In Mg-free solutions flickery closures were not observed and the channel was able to pass outward current at positive holding potentials. Intrinsic channel gating was strongly voltage dependent: open probability ( $P_o$ ) was voltage dependent: at +40mV  $P_o$  was <0.1; at more negative potentials  $P_o$  increased to a limiting value of about 0.9.

5. In contrast to the intrinsic gating of the inwardly rectifying channel in skeletal muscle, the cardiac channel was insensitive to the flow of solution.

6. When  $\text{pH}_i$  was lowered to 6.5, a small increase in frequency of brief closures was detected. When  $\text{pH}_i$  was lowered to 6.0, the frequency of these closures was much increased. However, unlike skeletal muscle, where the changes in intrinsic gating kinetics with low  $\text{pH}_i$  lead to a decrease in open probability, in cardiac muscle  $P_o$  was reduced very little.

7. When  $\text{pH}_i$  was lowered beyond 6.5, the channel tended to enter into a long lasting closed state. At  $\text{pH}_i$  5.5, the channel became inactive within a few seconds and remained inactive until  $\text{pH}_i$  was restored. This effect set a limit to the range over which the kinetic change described above could be studied.

8. With moderate acidification to  $\text{pH}_i$  6.5, single channel current decreased to about 0.9 times its value at  $\text{pH}_i$  7.8. When  $\text{pH}_i$  was lowered to 6.0, single channel current decreased to about 0.7 its value at  $\text{pH}_i$  7.3. This reduction showed no voltage dependence between -80 and +40mV.

9. The steep pH dependence of entry into the long closed state (7 above) will govern the magnitude of the macroscopic current when  $\text{pH}_i$  falls, as the effect of  $\text{pH}_i$  on open probability whilst the channel is still active (6 above) and on single channel conductance (8 above) are relatively small.

10. When  $\text{pH}_i$  is lowered the leak current decreased to a similar extent as the single channel current. The effect of low  $\text{pH}_i$  on leak current, and on the kinetic and conductive properties of the inwardly rectifying channel were readily reversed on restoring  $\text{pH}_i$ .

## INTRODUCTION

In cardiac ventricular cells, and to a lesser extent in atrial cells, an important component of the total current at the resting potential is the inwardly rectifying K current, termed  $I_{K1}$  by Hall, Hutter and Noble (1963). The channels responsible for  $I_{K1}$  were identified in 1981 by Trube, Sakmann and Trautwein. Since then, various properties of the channel have been studied at normal intracellular pH. The rationale for examining also the  $pH_i$  sensitivity of these channels was a set of reports based on records of whole cell currents which suggested that cardiac  $K_{inw}$  channels were at least as sensitive to a decrease in  $pH_i$  as their counterparts in skeletal muscle. Thus according to Harvey and Ten Eick (1988) a reduction in  $pH_o$  from 7.4 to 5.4, which would be expected to produce a fall in  $pH_i$  by 0.45 units (Deitmer & Ellis, 1980) caused inward K current to fall to about 0.6 of its initial value; and the removal of  $Na_o$ , which would be expected to produce a decrease in  $pH_i$  of similar magnitude (Allen *et al.*, 1986) also reduced inward K current to about one half. If the  $K_{inw}$  channel in cardiac muscle were indeed so highly sensitive to  $pH_i$ , changes in  $K_{inw}$  current might be important for the understanding of the behaviour of cardiac muscle in ischaemia, when  $pH_i$  is known to fall (Bailey *et al.*, 1981; Gasser & Vaughan-Jones, 1990). A direct study of the behaviour of single  $K_{inw}$  channels at different  $pH_i$  therefore seemed desirable.

## METHODS

Isolated ventricular cells were prepared as described in Chapter 1. Patch pipettes contained 140 mM-KCl, buffered to pH 7.3 or 7.8 with 5 mM-HEPES/KOH. Patches were detached into solution containing (mM): 140 KCl, 5  $K_2$ ATP, 1 EGTA, 0 or 5  $MgCl_2$  buffered to pH 7.3 or 7.8 with 5 mM-HEPES/KOH. In some experiments 120 mM-KAspartate + 20 mM-KCl was used in place of 140 mM-KCl. With 5 mM added  $MgCl_2$ , free  $[Mg^{2+}]$  was

estimated to be 0.75mM at pH 7.3, and 0.69mM at pH 7.8. These concentrations are within the normal physiological range; recent work suggest values between 0.4 and 1 mM (Blatter & McGuigan, 1986; Blatter *et al.*, 1989). Lowering the pH of the bath solution would increase  $[Mg^{2+}]_i$  to e.g. 2.2mM at pH 5.0. An increase of this order would occur *in vivo*, as ATP is by far the most important buffer of intracellular magnesium in cardiac myocytes, although the rise may be somewhat less due to buffering by mitochondria (Jung *et al.*, 1990).

## RESULTS

### Properties of inwardly rectifying $K^+$ channel in cell-attached patches and in patches detached into solution of pH 7.4

When a patch pipette is sealed against the sarcolemmal membrane of an isolated ventricular cell, inward current steps are observed at negative membrane potentials (Fig.6.1A). As  $V_h$  approaches the  $K^+$  equilibrium potential at about 0mV, the size of the current steps decreases until the steps become undetectable in the background noise. At positive potentials, no current steps are seen, that is, there is complete rectification around 0mV. The current-voltage (I-V) relation for this experiment is shown in Fig.6.1B. The chord conductance increases with hyperpolarization:  $g_K$  is about 21pS at -15mV and rises to 29.1pS at -120mV. The deviation from a linear relationship was unusually marked in this experiment. A similar hyperbolic shape of the I-V curve was noted by Vandenberg (1987) when external K concentrations were high; with low K concentrations, the curve was linear or slightly saturating.

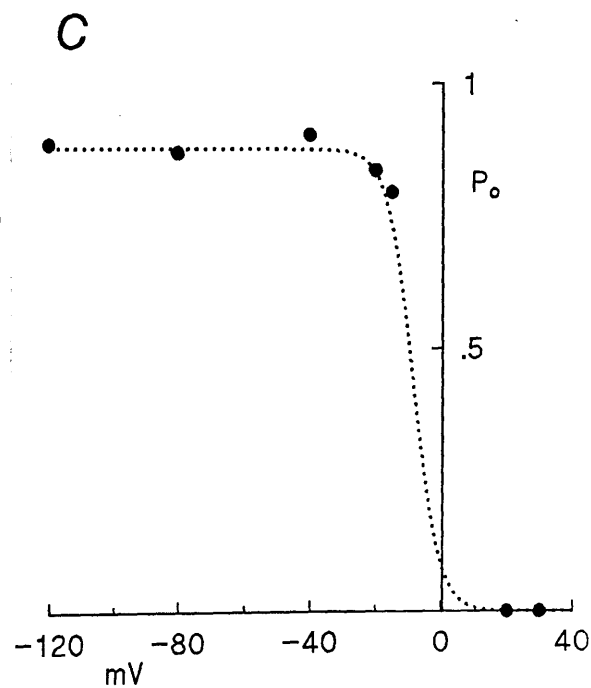
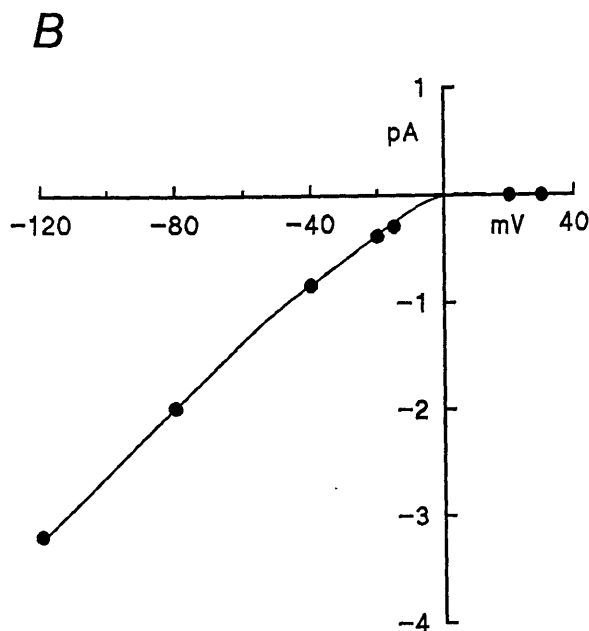
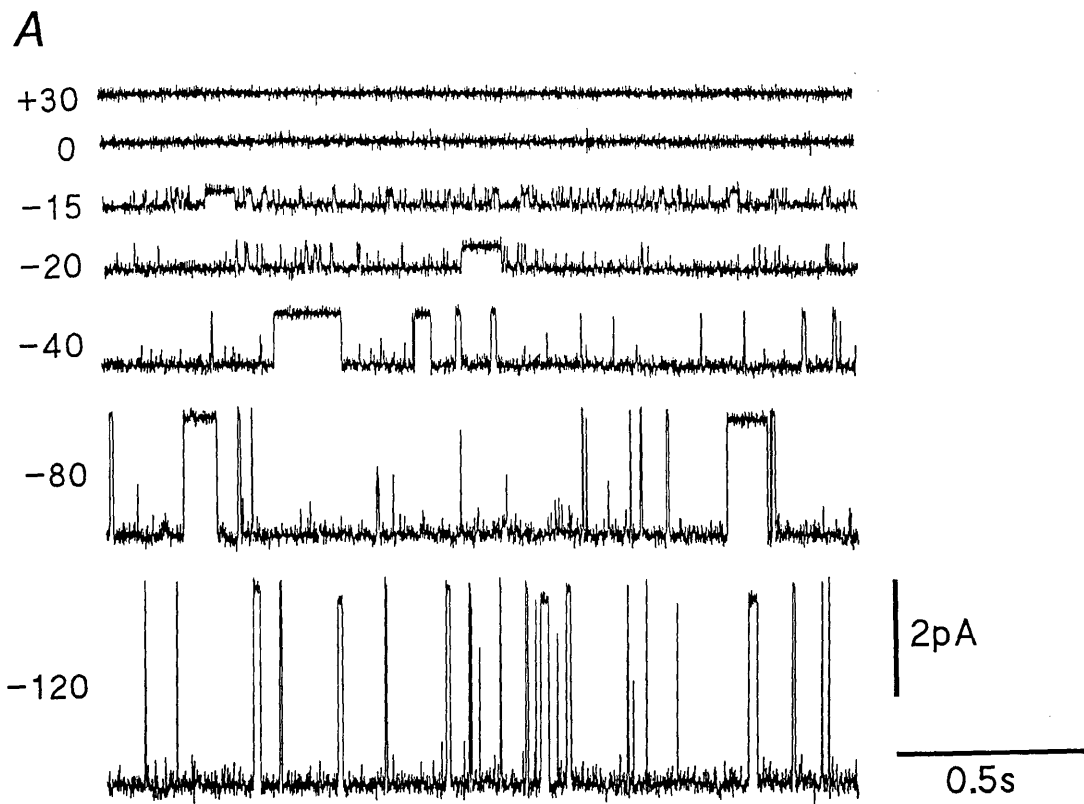


Figure 6.1. Inwardly rectifying K channel in cell-attached patch of guinea pig ventricular myocyte. Patch pipette contained 140 mM KCl and 5mM HEPES, pH 7.4. *A*, single channel currents at different holding potentials; 500Hz filter. Inward currents are downwards. *B*, current-voltage relation. *C*, open probability-voltage relation.

In recordings from attached patches, more frequent and rapid closures appear as  $V_h$  approaches 0mV. These are detectable in the trace at -20mV (Fig.6.1A) and they become more pronounced at -15mV. This behaviour is similar to the high frequency flicker (HFF) seen in cell-attached patches on skeletal muscle (Chapter 3, this thesis) and on cardiac muscle (Kurachi, 1985 Fig.3).  $Mg^{2+}$  must be involved in the generation of this fast activity because channels exposed to internal (bath) solutions containing a high concentration ( $\approx 0.7mM$ ) of free Mg also showed HFF, whereas no HFF was seen when Mg was omitted from the internal solution. The effect of this process on channel open probability is quite small at -20mV and -15mV (Fig.6.1C), but it may be largely responsible for the completeness of the rectification at positive potentials. At more negative potentials,  $P_o$  is voltage independent and remains high even with strong hyperpolarization.

When patches were detached into a  $Mg^{2+}$ -free solution, previously inwardly rectifying channels no longer rectified sharply around 0mV and outward currents could be recorded at positive potentials (Fig.6.2 inset). The single channel current-voltage relation for this experiment is shown in Fig.6.13. It is almost linear for negative potentials to -80mV, but rectifies slightly at positive potentials. As well as eliminating high frequency flicker near  $E_K$ , as mentioned above, the removal of  $Mg^{2+}$  reveals an intrinsic gating mechanism, as it did in skeletal muscle. Fig.6.2 shows the open probability-voltage relationship, which could be fitted with a Boltzmann curve with equation:

$$P_o = 0.89 / (1 + \exp((V-25.5)/5)).$$

This activation curve lies about 21 mV to the right of the corresponding one for skeletal muscle (Fig.3.11), and is slightly less

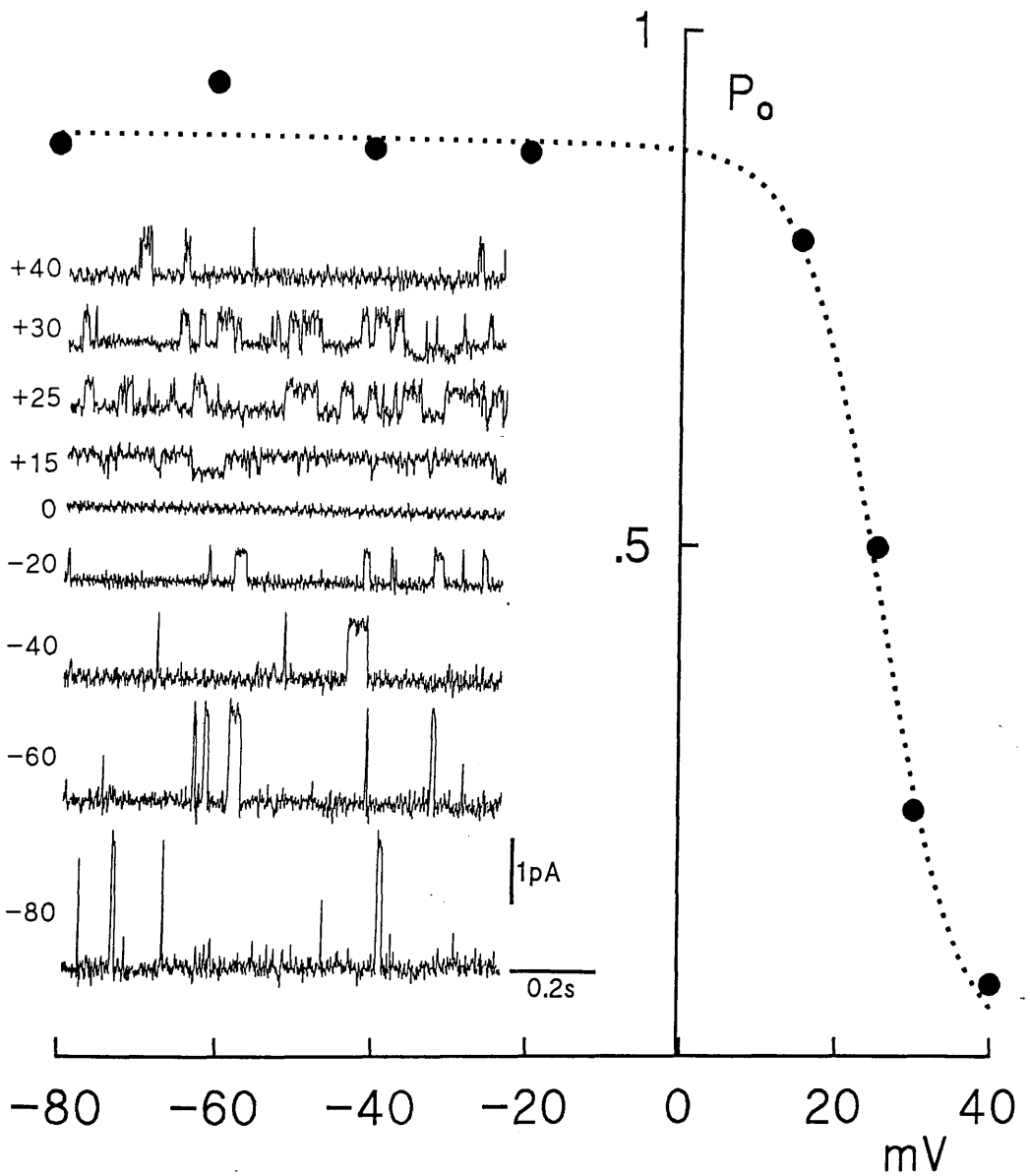


Figure 6.2. Open probability-voltage relationship of  $K_{inw}$  channel in patch detached into  $Mg^{2+}$ -free solution at pH 7.3. Inset shows current records at each holding potential; filter 500Hz.

steep. Also, the maximum activation (0.89) is somewhat less than in skeletal muscle (0.96).

The detailed kinetics of an inwardly rectifying channel in  $Mg^{2+}$ -free solution at  $-40mV$  were analyzed with the threshold crossing technique. Rare sublevels were treated as open states. The results are shown in Fig.6.3A,B. The open times could be fitted by a single exponential with a time constant of 143 ms (mean open time  $\hat{t}_o$  was 147 ms). Within the range 0-30 ms, the distribution of closed times were fitted by a sum of two exponentials with time constants 0.36 ms and 5.73 ms. 274 closing events out of 3000 total were longer than 30 ms, indicating the presence of at least another closed state. Overall mean closed time  $\hat{t}_c$  was 88.6 ms. During the 8 minute period analyzed, the longest closed interval was 589 ms, i.e. in this experiment there were no long closed periods (as defined for skeletal muscle,  $t_{closed} > 1s$ ). In other experiments, such long closures were observed at neutral pH, but infrequently.

Fig.6.4 shows the behaviour of a single inwardly rectifying  $K^+$  channel in response to exposure to a flowing solution. Both bath and flow solutions contained 0  $Mg^{2+}$ . No obvious effect of flow on channel activity can be seen. Furthermore, kinetics analysis of several periods before, during and after flow failed to show any systematic differences in  $\hat{t}_o$ ,  $\hat{t}_c$  or  $P_o$ . This lack of a flow effect is in marked contrast to the situation in skeletal muscle, and provides an opportunity to study the effects of lowering  $pH_i$  without the complications that beset the interpretation of the skeletal muscle results.

A subconductance state with approximately 2/3 the size of the unitary conductance was seen occasionally in both attached and detached

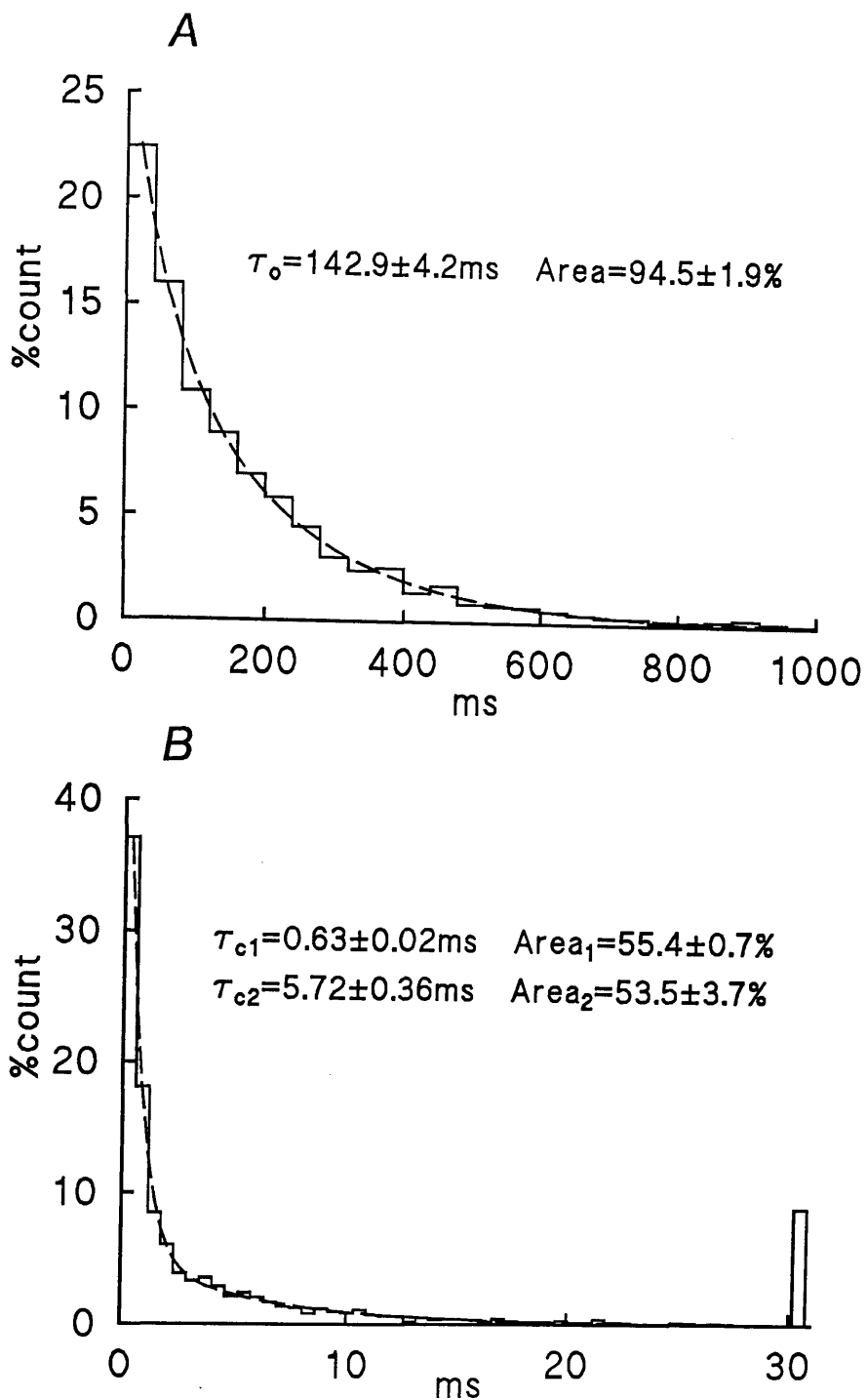


Figure 6.3. Kinetic behaviour of  $K_{inw}$  channel in  $Mg^{2+}$ -free solution at pH 7.4. 480s recording at  $V_h$  -40mV, filtered at 1kHz and sampled at 5kHz. A, open times histogram, with single exponential curve. B, close times histogram, with double exponential curve. Closed times greater than 30ms are indicated by the bin at the right of the graph. Parameters of fitted curve are given with each plot. (Time constants and area percentages are quoted  $\pm$  standard deviations as reported by the fitting routine, and are an indication only of relative uncertainty of parameter estimates.)

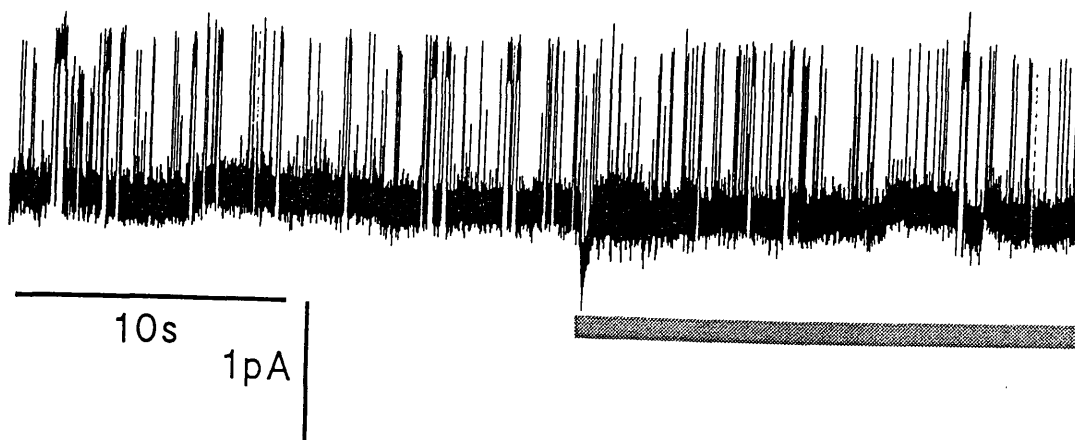


Figure 6.4. Inward rectifier channel activity in static and flowing solutions. Holding potential was  $-40\text{mV}$ . Bath and flow solutions contained  $5\text{mM}$  added  $\text{MgCl}_2$ ;  $\text{pH}$   $7.4$ . Period of flow indicated by shaded bar. In contrast to  $K_{\text{inw}}$  channels in skeletal muscle, flow itself had no effect on channel kinetics or conductance.

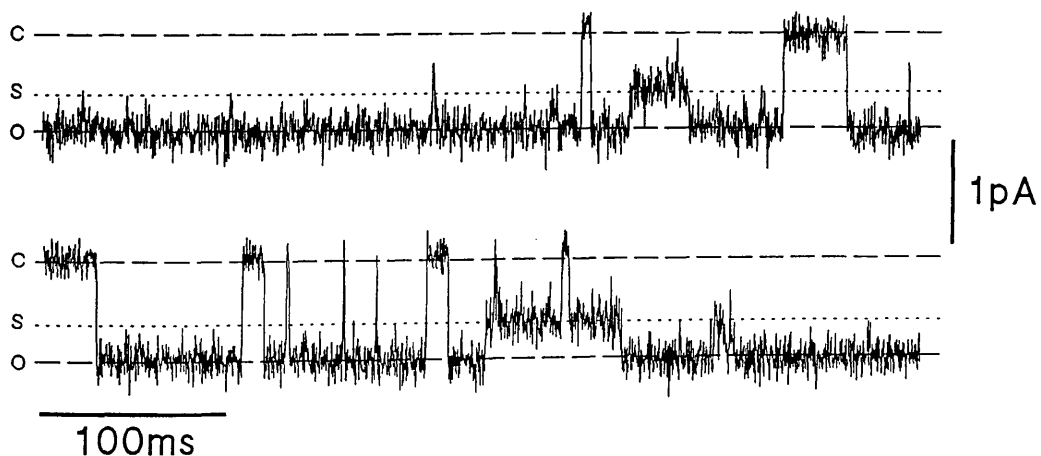


Figure 6.5. Subconductance states in cardiac inward rectifier channel. Same patch as above. Holding potential was  $-40\text{mV}$ ; filter  $1\text{kHz}$ . Open (O), closed (C) and substate (S) current levels are indicated.

patches (Fig.6.5). The substate was always entered from the fully open state, and returned to the open level, in all but one case (lower trace) where the channel briefly closed, then reopened to the substate. Despite a lack of quantitative data, the frequency of occurrence of substates seems to be less than reported elsewhere (Sakmann & Trube, 1984a; Matsuda, 1988).

#### Effects of lowering $pH_i$ on inward rectifier

Several changes in the activity of inwardly rectifying  $K^+$  channels in patches from ventricular cells are observed when  $pH_i$  is lowered. Both channel open probability and unitary current amplitude are reduced in low  $pH_i$ . Leak current is also decreased. These effects are graded with the degree of acidification, and are readily reversible.

In the experiment of Fig.6.6A,  $pH_i$  was lowered from 7.8 to 6.5. The most obvious effect is an upward shift in the trace due to a decrease in the leak current as pH was lowered. On return to  $pH_i$  7.8, the trace moved back to its original level. There was also a small decrease in single channel current. This degree of acidification did not produce a detectable change in  $P_o$ , though brief closures occurred with greater frequency. When  $pH_i$  was lowered from 7.3 to 6.0, the frequency of brief closures increased greatly as indicated by the density of the lower margin of the trace in Fig.6.6B. The reduction in single channel current was also more pronounced ( $i_{pH6.0}/i_{pH7.3} = 0.74$ ). The rapid activity at  $pH_i$  6.0 was interrupted by two long-lasting closures. During the second closure, the solution was switched back to pH 7.3. The channel remained shut until leak current had increased to nearly its previous level. When the channel reopened, its unitary current and kinetics were similar to that seen before the period in acid. When the patch was exposed to a solution at  $pH_i$  5.5 (Fig.6.6C),

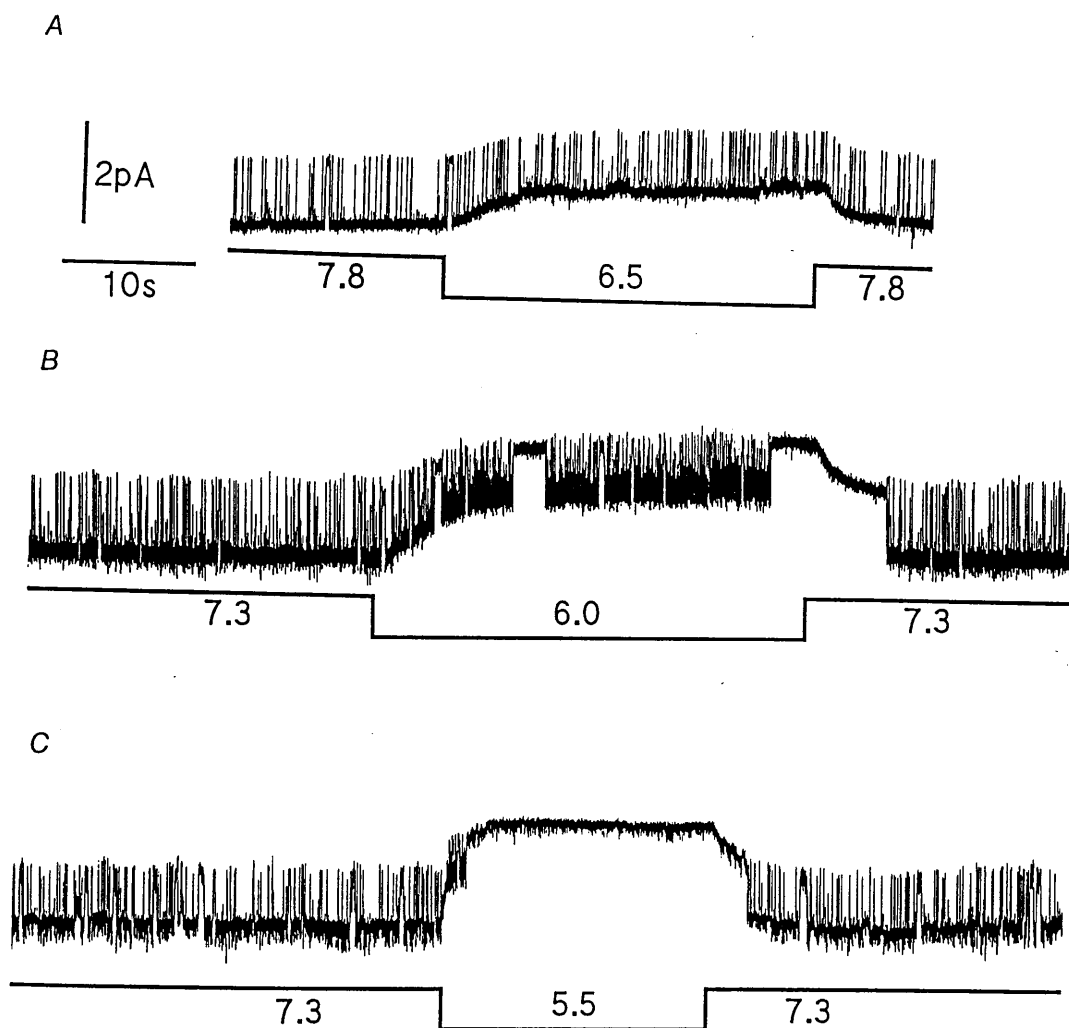


Figure 6.6. Inward rectifier current activity with changes in  $pH_i$ . In each of the three experiments, holding potential was  $-60\text{mV}$ . Filter  $500\text{Hz}$ . Upward shift in traces due to decrease in leak current as  $pH_i$  was lowered. A,  $pH_i$  7.8/6.5. B,  $pH_i$  7.3/6.0. C,  $pH_i$  7.3/5.5.

single channel current fell during the change to 0.65 its initial value at  $\text{pH}_i$  7.3, before total closure of the channel supervened. Return to  $\text{pH}_i$  7.3 rapidly restored channel activity.

Estimates of overall channel open probability ( $P_o$ ), during stable periods at different  $\text{pH}_i$  are plotted in Fig.6.7. (This graph is comparable with Fig.5.2 for skeletal muscle in the previous chapter, except that here unnormalized values for  $P_o$  have been plotted.) Again, the scatter in points at  $\text{pH}_i$  6.0 and 6.5 is due to the variability in the appearance of the long closed state during perfusion with acid solution. However, a marked effect on  $P_o$  over the range  $\text{pH}_i$  5.5 to 6.5 is evident. The Boltzmann curve plotted over the data has slope factor 3.13 and midpoint at pH 6.04.

#### Effect on channel kinetics

A feature common to the kinetics of inwardly rectifying channels from both skeletal and cardiac muscle is the presence of a long closed time component. In cardiac muscle, as in skeletal muscle, this component contributed very little to the overall closed time at  $\text{pH}_i$  7.3 or 7.8. With progressively lower  $\text{pH}_i$  the channel spent a greater proportion of time in the long closed state. An indication of the pH dependence of this effect may be obtained by calculating the ratio of total time that channels are active to the total recorded time, at any  $\text{pH}_i$ . This yields percentage time active: >99% at  $\text{pH}_i$  7.3 and 7.8, 94% at 6.5, 45% at 6.0, and 10% at  $\text{pH}_i$  5.5. Once a channel became inactive it tended to stay closed until  $\text{pH}_i$  was restored (see e.g. Fig.6.6C), so these figures depend to a large extent on the duration of exposure to acid solution. Therefore it is certain that they are overestimates. Another measure related to the probability of seeing the long closed state in any period of low  $\text{pH}_i$  (and so to overall  $P_o$ ) is the duration

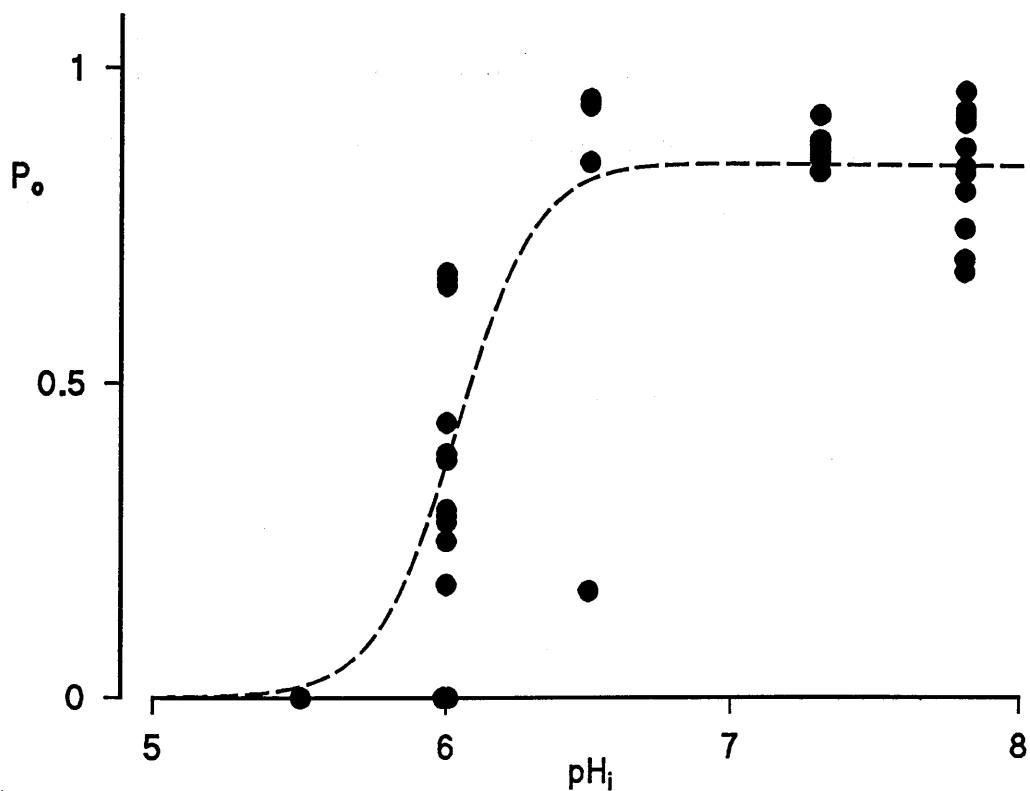


Figure 6.7. Overall open probability of cardiac inward rectifier at different  $\text{pH}_i$ . Open probability was determined from total open and closed times including periods of long lasting closure. Fitted curve has equation  $P_o = 0.86/[1+\exp(-7.19 \cdot (\text{pH}_i - 6.04))]$ .

of channel activity before the first appearance of the long closed state after  $\text{pH}_i$  is lowered. It is evident from these experiments that this latency is shorter on average after lowering  $\text{pH}_i$  to 5.5 (<1 - 3.5s) than to 6.0 (2 - >32s). However, the slow time course of the solution change in these experiments makes it impossible to quantify the shorter latencies with reasonable accuracy: for that to be done, some kind of "concentration jump" method would be required.

It was shown earlier that the channel can exist in at least two closed states with relatively short lifetimes, and that transitions between these and the open state predominate at  $\text{pH}_i \geq 7.3$ . That internal acidification has an effect on these transitions also is evident from Fig.6.6B which shows more rapid closures at pH 6.0. The results of a half-amplitude threshold analysis of 25 second periods from this experiment in which long closed states were excluded is shown in Fig.6.8A,B. At both  $\text{pH}_i$  7.3 and 6.0, open and closed time histograms were fitted with one and two exponentials respectively. Despite the small numbers of events, and hence the relatively greater uncertainty in the fitted parameters compared with the analysis of Fig.6.3, it is apparent that both closed times and the open time are significantly reduced, the latter due to the increase in frequency of closures.

Because periods in acid solution were short, a full analysis discriminating  $\tau_{c1}$  and  $\tau_{c2}$  was not done. Instead, we obtained the simpler measure of mean open time ( $\hat{t}_o$ ) and mean short closed time ( $\hat{t}'_c$ ), from which  $P'_o$  was calculated. When  $\text{pH}_i$  was lowered,  $\hat{t}_o$  always decreased, and, in most cases, there was also a decrease in  $\hat{t}'_c$ . However, the combined effect of these kinetic changes on  $P'_o$  was slight. In the experiment detailed above,  $P'_o$  fell from 0.94 at  $\text{pH}_i$  7.3 to 0.90 at  $\text{pH}_i$  6.0. Fig.6.9 shows that there was little effect of pH on  $P'_o$  in all

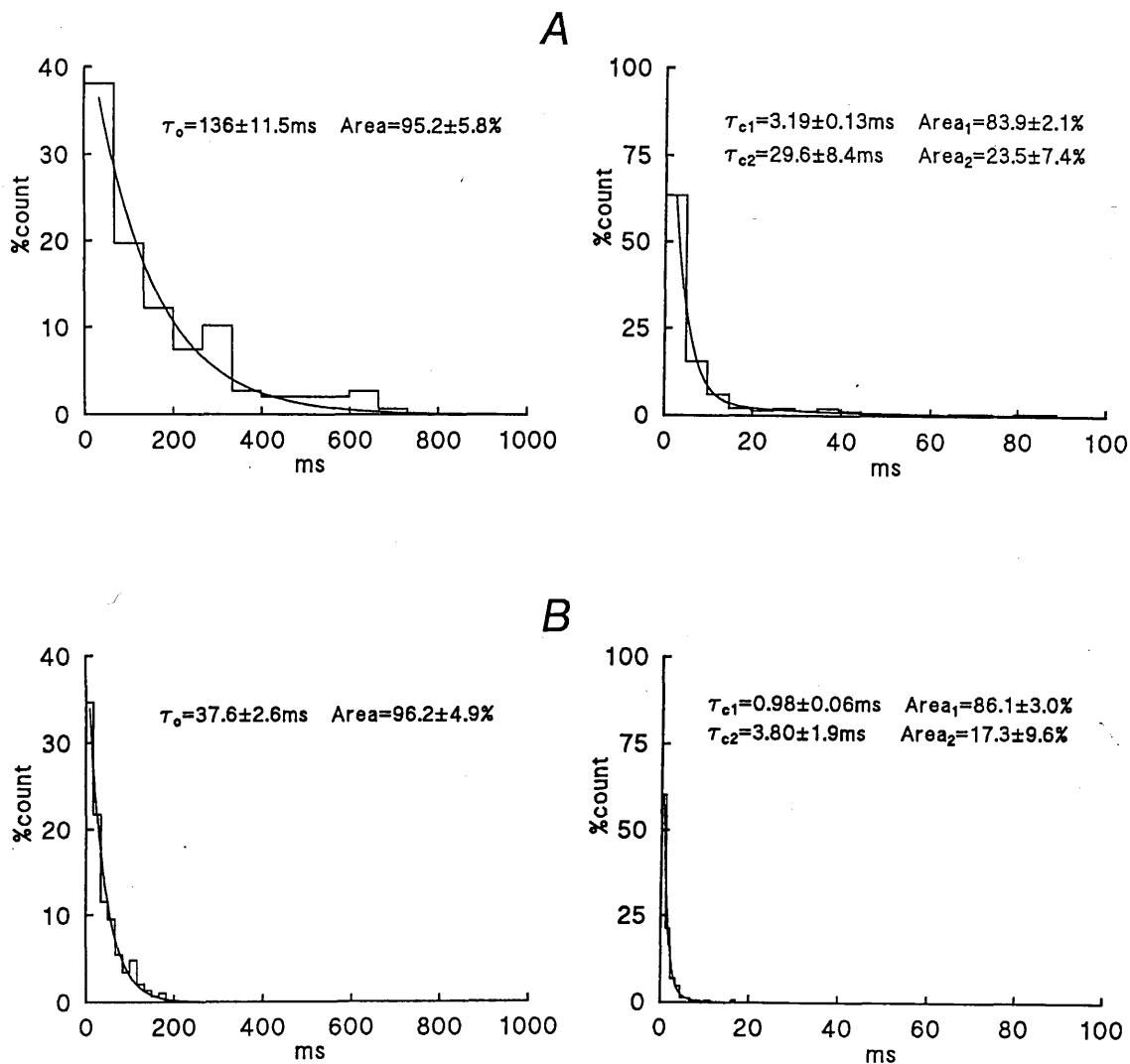


Figure 6.8. Kinetic analysis of  $K_{inw}$  channel at  $\text{pH}_i$  7.3 and 6.0. Same patch as Fig 6.6B. 25s of recording at  $V_h$  -80mV, filtered at 1kHz and sampled at 5kHz. A, open and closed time histograms at  $\text{pH}_i$  7.3. B, open and closed time histograms at  $\text{pH}_i$  6.0. Both open and both closed time histograms are plotted with the same axes for comparison; for binning and fitting, open and closed histograms at  $\text{pH}_i$  6.0 had ranges 0-250ms and 0-25ms respectively. Parameters of fitted exponential curves are given with each plot.

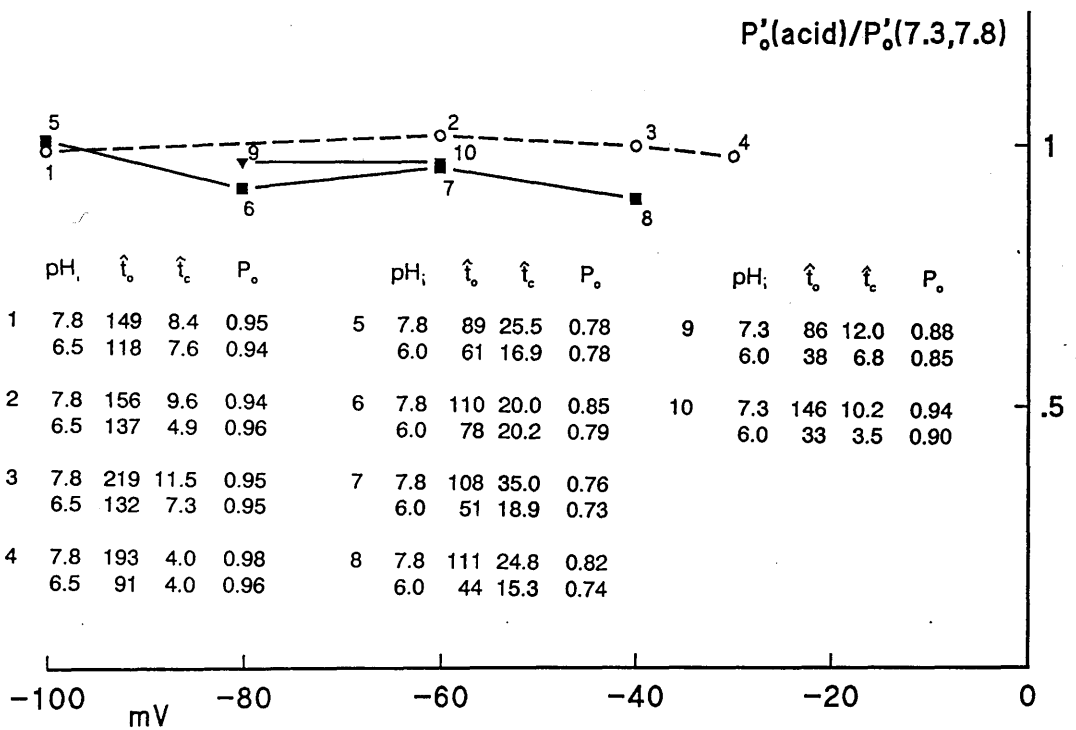


Figure 6.9. Effect on channel open probability of lowering  $pH_i$ . Results from three experiments.  $P'_o$  was determined from mean open and closed times (given in inset table), excluding closed periods longer than 1s.

experiments; in some cases  $P'_o$  increased slightly. This is in marked contrast to the effect of  $pH_i$  on  $P'_o$  in skeletal muscle, where  $P'_o$  always fell substantially, due to a decrease in  $\hat{t}_o$  and (mostly) an increase in  $\hat{t}'_o$ .

There was no discernible voltage dependence of the effect of low  $pH_i$  on either  $P_o$  or  $P'_o$  at negative potentials. In one experiment in which positive potentials were investigated at pH 7.3/6.0, the channel entered the long closed state within a few seconds of changing to acid solution at +15, +25, +30 and +40 mV (Fig.6.10). It is interesting to note that at +30mV and +40mV, when  $P_o$  at pH 7.3 was low,  $P'_o$  appeared to rise during brief bursts of activity before the channel closed completely. Unfortunately, these episodes were too short and noisy for  $P'_o$  to be measured; clearly more work needs to be done in this voltage range.

#### Effect on single channel current and leak current

On switching to an acid perfusion solution,  $i_K$  and  $i_{leak}$  fell concurrently. The time to reach a steady level after switching solutions (5-10s) is somewhat greater in these experiments than those on skeletal muscle, because of the comparatively low flow rates used here. After restoration of neutral pH, both currents increased again with the same time course. (In Fig.6.6A the first transition is faster than the second, because the flow rate was deliberately increased during perfusion with pH 6.5 solution.)

As before,  $i_K$  was measured by constructing amplitude histograms when sufficiently long (> about 10 sec), stable periods of activity could be recorded. When only short periods were available, e.g. when a channel quickly entered the long closed state, individual current

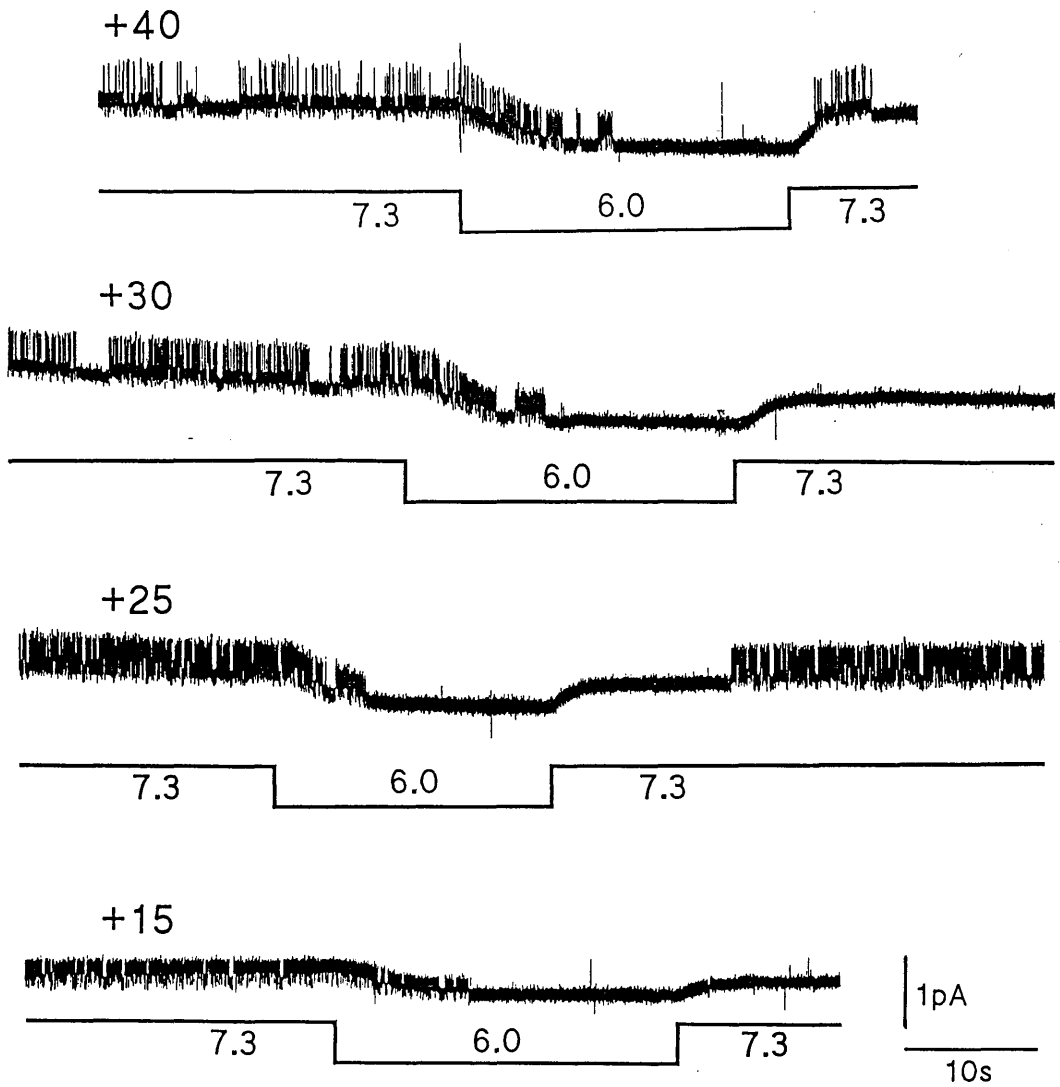


Figure 6.10. Outward current activity of  $K_{inw}$  channel at  $pH_i$  7.3 and 6.0. Traces at different potentials were recorded from the same patch as Fig.6.6B. Filter 500Hz. Downward shift in traces due to decrease in leak current when  $pH_i$  was lowered.

transitions were measured with a cursor to obtain a value of  $i_K$ . Figures 6.11 and 6.12 show amplitude histograms corresponding to the experiments of Fig.6.6 A&B. When  $\text{pH}_i$  is lowered from 7.8 to 6.5 (Fig.6.11) the peaks move closer together indicating a decrease in  $i_K$  from -1.28 to -1.16pA. The relative sizes of the peaks are not greatly different, reflecting little change in  $P_o$ . Lowering  $\text{pH}_i$  from 7.3 to 6.0 (Fig.6.12) produces a decrease in  $i_K$  from -1.39 to -1.03pA. Here, the height of the open channel peak is reduced, but the area under the peak remains constant indicating little fall in  $P_o$  despite the greater number of very short closures.

Fig.6.13A shows the current-voltage relation at  $\text{pH}_i$  7.3 and 6.0 for the same experiment as in Fig.6.6B. There was some rectification at positive potentials: the maximum chord conductance was about 25pS. When  $\text{pH}_i$  was lowered to 6.0, there was a reduction in single channel current over the whole voltage range. The ratio of  $i_K$  at 7.3 and 6.0 is plotted in Fig.6.13B. The relative decrease in  $i_K$  shows no obvious voltage dependence.

Pooled measurements from all experiments on cardiac inwardly rectifying  $\text{K}^+$  channels at different  $\text{pH}_i$  and  $V_h$  are plotted as conductance in Fig.6.14. In general, conductance is less at lower  $\text{pH}_i$ . The curve through the points is the upper end of a Boltzmann, with slope factor 1 and midpoint at pH 5.3. The three points at pH 5.5 must be considered upper limit estimates because the channels shut down before pH of the solution perfusing the patch reached its final value.

In experiments on cardiac muscle, the magnitude of the leak current,  $i_{\text{leak}}$ , varied between patches from about 1 to 2 times  $i_K$ . As Fig.6.6A-C showed, there is a reversible reduction of  $i_{\text{leak}}$  with  $\text{pH}_i$ . The

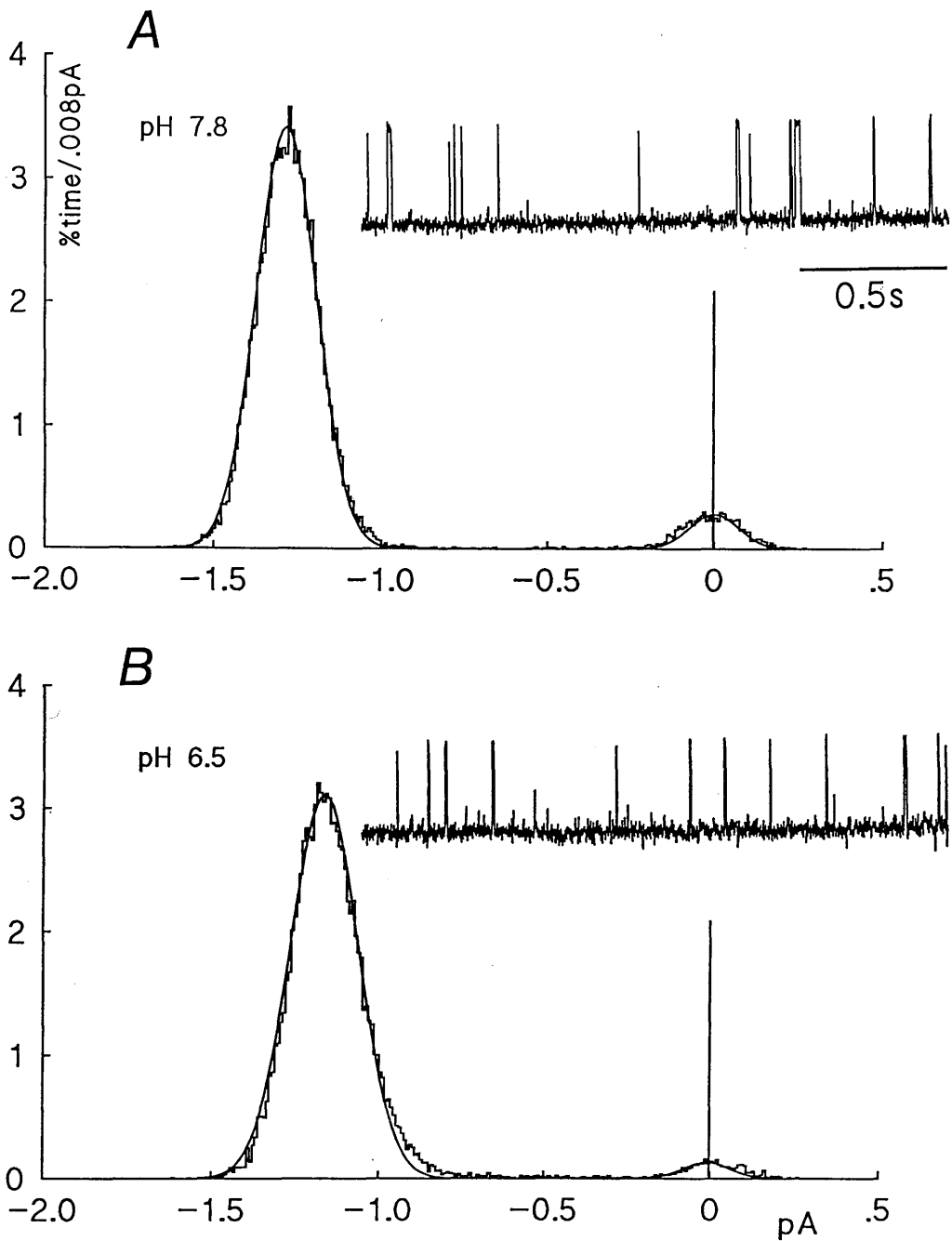


Figure 6.11. Amplitude histograms of  $K_{inw}$  channel currents at A,  $pH_i$  7.8, and B,  $pH_i$  6.5. 10s of recording, filtered at 400Hz and sampled at 2kHz. Insets show short sections of recording. Gaussian curves were fitted to open and closed current levels.

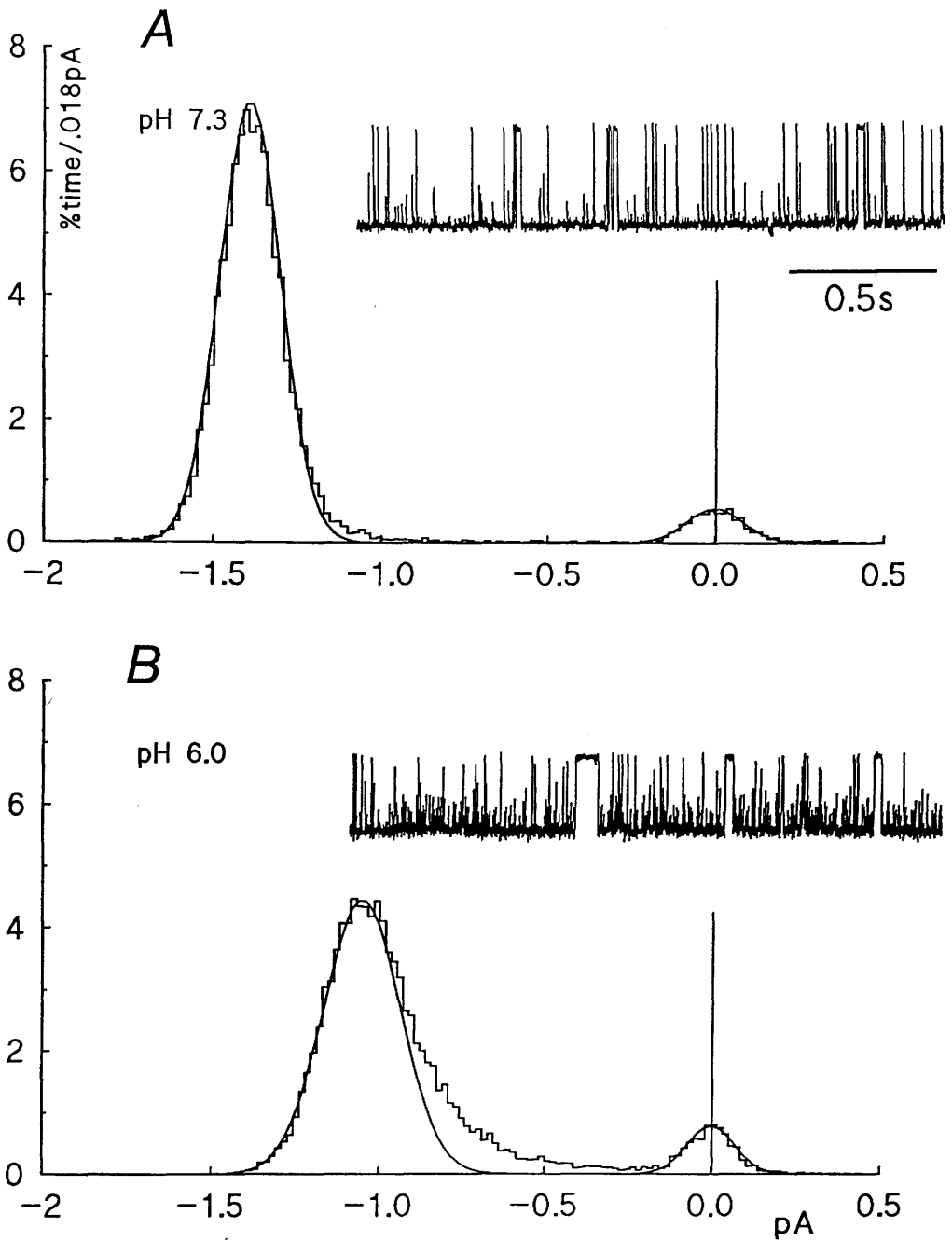


Figure 6.12. Amplitude histograms of  $K_{inw}$  channel currents at A,  $pH_i$  7.3, and B,  $pH_i$  6.0. 10s of recording, filtered at 400Hz and sampled at 2kHz. Insets show short sections of recording. Gaussian curves were fitted to open and closed current levels.

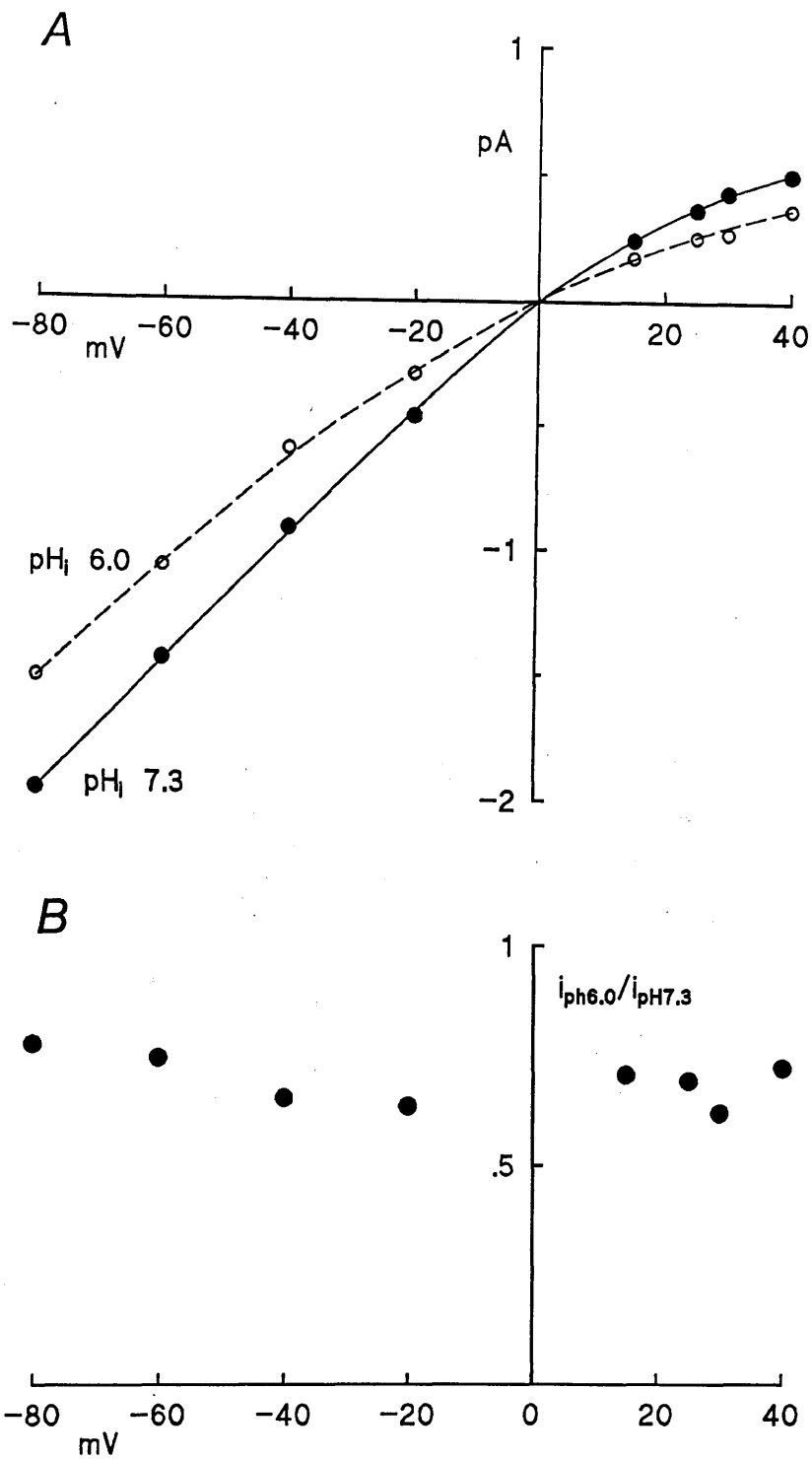


Figure 6.13. Reduction in single  $K_{inw}$  channel current when  $pH_i$  was lowered from 7.3 to 6.0 at different potentials. A, current-voltage relation at  $pH_i$  7.3 ( $\bullet$ , solid line) and 6.0 ( $\circ$ , dashed line). B, ratios of single channel currents.

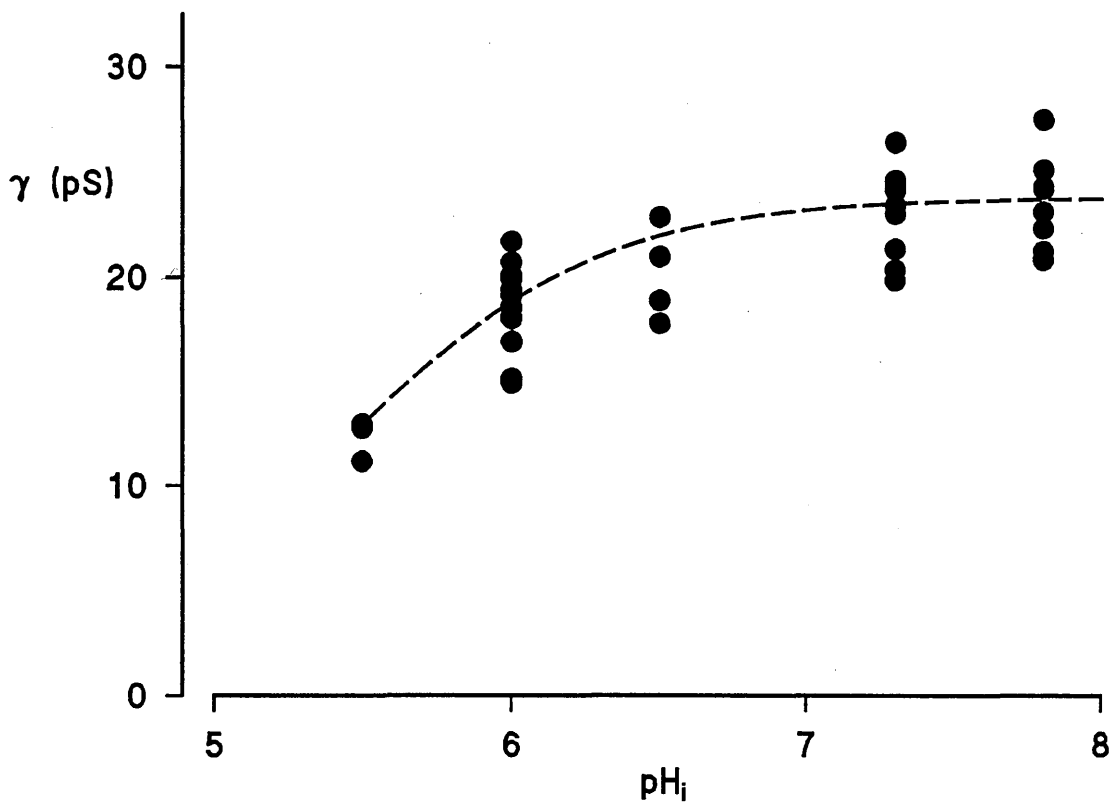


Figure 6.14. Single channel conductance of cardiac inward rectifier channels at different  $\text{pH}_i$ . Results from all experiments. Curve has equation  $\gamma = 24/[1+\exp(-2.3 \cdot (\text{pH}_i - 5.43))]$ .

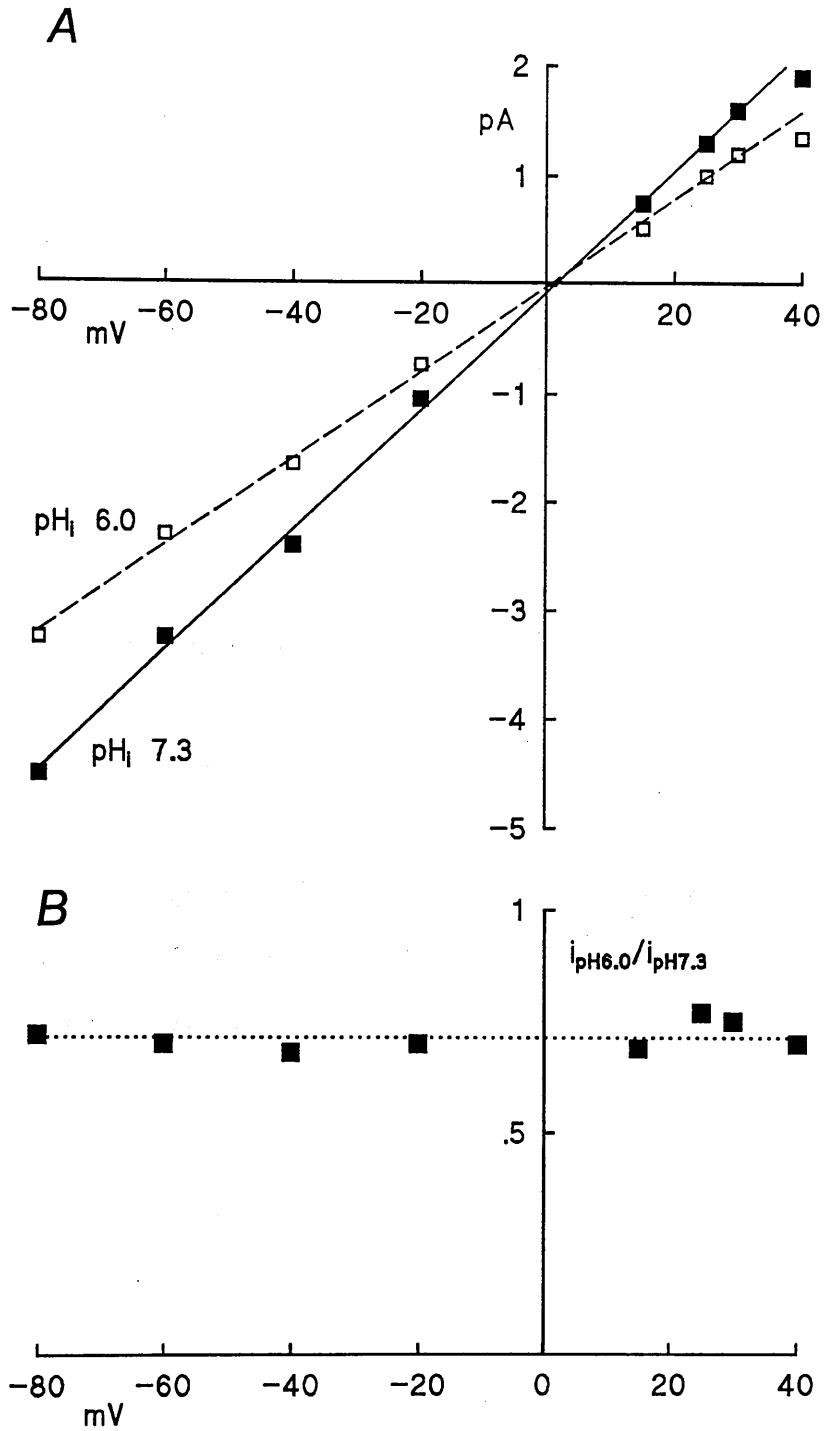


Figure 6.15. Reduction in leak current when  $\text{pH}_i$  was lowered from 7.3 to 6.0 at different potentials. Same patch as Fig.6.13. A, current-voltage relations at  $\text{pH}_i$  7.3 ( $\blacksquare$ , solid line) and 6.0 ( $\square$ , dashed line). B, ratios of leak currents.

current-voltage relation of  $i_{\text{leak}}$  for the same experiment as Fig.6.6B is shown in Fig.6.15A. The decrease in leak current is of the same magnitude as the decrease in single channel current; this decrease does not depend on voltage (Fig.6.15B).

## DISCUSSION

Before discussing the effects of lowering  $\text{pH}_i$  on the inwardly rectifying channel in cardiac muscle, I will briefly consider some aspects of the behaviour of the channel at  $\text{pH}_i$  7.4 in relation to previous findings.

### Contributions of internal $\text{Mg}^{2+}$ and intrinsic gating to inward rectification

The evidence for involvement of intracellular Mg in inward rectification, and the steepness of the rectification around 0mV are consistent with a voltage-dependent entry of  $\text{Mg}^{2+}$  ions into the open channel from one side of the membrane to cause channel block (Matsuda *et al.*, 1987; Vandenberg, 1987). In addition, we see that the channel closes in a voltage-dependent fashion in the absence of internal Mg by the operation of an intrinsic gate. Both of these mechanisms may contribute to the rectification of macroscopic current.

Vandenberg's view (1987) that all rectification can be explained in terms of voltage-dependent block by  $\text{Mg}^{2+}$  was based on single-channel I-V records obtained with rapid (100-200ms) linear voltage ramps. However, the relatively slow kinetics of the gating mechanism (Matsuda, 1988 Fig.3) meant that these experiments would not show the low steady-state activation at positive potentials. Block by intracellular  $\text{Mg}^{2+}$  was considered the major mechanism underlying inward rectification also in

other cardiac  $K^+$  channels (ATP-sensitive K channel, Horie *et al.*, 1987; muscarinic  $K^+$  channel, Horie & Irisawa, 1989).

Silver and DeCoursey (1990) found only small differences in whole-cell inward rectifier currents in endothelial cells, between cells with nominally zero and physiological concentrations of  $Mg^{2+}$ . They suggested that in these cells the intrinsic gating mechanism is responsible for most of the inward rectification.

The possibility that blocking and gating mechanisms may interact cannot be excluded. Matsuda (1988) showed that the presence of subconductance states produced by  $Mg^{2+}$  block of outwardly conducting channels is consistent with the notion of a channel composed of three identical subunits. A significant steady-state (averaged) outward current after positive voltage steps with  $2\mu M$  internal  $Mg^{2+}$  could be explained by supposing that a partially blocked channel is prevented from closing by gating. Oliva *et al.* (1990) have suggested that a model of this kind could explain the presence of a macroscopic outward  $I_{K1}$  current at potentials positive to  $E_K$ .

### Absence of inactivation

In contrast to other studies in cardiac muscle (see below), we find that the open probability of the channel does not fall with increased hyper-polarization. Inwardly rectifying  $K^+$  channels have been found to be blocked in a voltage-dependent fashion by extracellular sodium in egg cells (Ohmori, 1978; Fukushima, 1982) and in skeletal muscle (Hille & Schwarz, 1978; Standen & Stanfield, 1979; Matsuda & Stanfield, 1989). A similar inactivation is seen in cardiac muscle, even when  $Na^+$  is absent from the pipette solution (Kameyama *et al.*,

1983; Sakmann & Trube, 1984b; Kurachi, 1985). Sakmann & Trube (1984b) suggest two explanations: 1) either or both of the divalent cations present in their pipette solution (1.8mM Ca<sup>2+</sup>, 1mM Mg<sup>2+</sup>) may have similar but stronger blocking effects than Na<sup>+</sup>, or 2) the channel contains an intrinsic inactivating gate. That we find no inactivation with pipette solutions containing no added Ca<sup>2+</sup> or Mg<sup>2+</sup> would favour the first explanation, but it would be necessary to confirm that the presence of these ions does indeed cause channel block. In one of the first papers on single cardiac inward rectifier channels, Kameyama *et al.* (1983) show a voltage dependent inactivation, but [Ca<sup>2+</sup>]<sub>i</sub> is not clearly indicated: in some experiments they added 1.8mM CaCl<sub>2</sub> to the pipette solution to improve pipette-membrane sealing. Matsuda & Stanfield (1989) showed inwardly rectifying channels in rat or mouse myotubes to have a consistently high (>0.8) open probability, with 1.8mM CaCl<sub>2</sub> in the pipette solution.

#### Rarity of substates

We rarely saw subconductance states. This may be due to the extremely low (nanomolar) concentration of internal Ca<sup>2+</sup> in our experiments, as Mazzanti & DiFrancesco (1989) found that 0.1-10μM Ca<sup>2+</sup> increased the frequency and duration of partial closures. Only a single subconductance level at 66% was seen with any reliability. Various relative conductance levels have been reported elsewhere in cardiac cells: 65-85% (Kameyama *et al.*, 1983), 25%, 50% & 75% (Sakmann & Trube, 1984a; Mazzanti & DiFrancesco, 1989) and 33% & 67% (Matsuda, 1988; Matsuda *et al.*, 1989).

#### Absence of flow effect

No effects of flow on the gating properties of the inward rectifier in cardiac muscle were seen in these experiments. This

contrasts with the situation in skeletal muscle, where flow produces a marked decrease in  $P_o$ . If we assume that the structure of the membrane and any submembrane attachments are similar in patches detached from skeletal muscle vesicles and dispersed cells, and from cardiac myocytes, the possibility that the flow effect can be explained by a mechanism involving the local accumulation of potassium ions is made more unlikely.

Effect of lowering  $pH_i$  on inwardly rectifying channel:  
decrease in single channel conductance

Comparison of Fig.6.14 with Fig.5.6 shows that the decrease in single channel conductance found on lowering  $pH_i$  is greater in cardiac muscle than in skeletal muscle. On the view that the decrease in single channel conductance is due to a local positive (or less negative) potential at the inner surface of the channel, the greater sensitivity to low  $pH_i$  of the cardiac  $K_{inw}$  channel, as compared with the one in skeletal muscle, could arise from a small structural difference, e.g. in the distance between the protonation site and the channel pore mouth, or in pore mouth geometry. According to Jordan (1987) these factors have a powerful influence on the local potential produced at the pore mouth by a single charge. In this connection, it should be added that in the presence of a local potential, the  $pH$  at the pore mouth will differ from the bulk  $pH_i$ . In the present situation this means that the intrinsic  $pK_a$  of the protonation site is probably higher than the apparent  $pK_a$ .

As with skeletal muscle, an alternative hypothesis to account for the decrease in  $\gamma$  is block of the open channel by  $H^+$ . Again it would be necessary to suppose that the site at which block occurs is outside the electric field, for it is evident from Fig.6.13 that the block in

cardiac muscle also shows no detectable voltage dependence over a wide range.

### Effects of $pH_i$ on kinetic behaviour of cardiac channel

Earlier it was shown that the kinetics of the inwardly rectifying channel in cardiac muscle could be adequately described in terms of a model with one open and three closed states. However, at  $pH_i \geq 7.3$ , the longest closed state is entered only rarely and contributes very little to the overall  $P_o$ . In this section, rate constants will be derived for the two simplest three-state models which neglect the slowest and smallest component. It will be shown that channel activity simulated using these rate constants closely resembles observed channel activity. Lastly, I will show how the appearance on acidification of more frequent flickery closures may be explained in terms of changes in these rate constants.

The experiment of Fig.6.6B was most suitable as a starting point for this exercise, since after the reduction of  $pH_i$  to 6.0 the character of channel activity was more visibly different from that at  $pH_i$  7.3 than in experiments where  $pH_i$  was lowered only to 6.5. In this experiment also, relatively long periods of activity before the channel entered the long closed state were recorded. Exponential fits to dwell times from an analysis of a 30s period at -60mV before  $pH_i$  was lowered from 7.3 to 6.0 gave time constants: mean open time,  $\tau_o = 136ms$ , mean short closed time (1),  $\tau_{c1} = 3.3ms$  (84% of the total area under the p.d.f.) and mean short closed time (2)  $\tau_{c2} = 29.6ms$  (23% area);  $P_o$  was 0.935.

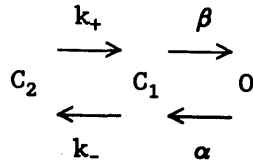
The two linear models with one open and two closed states are I:  $C \rightleftharpoons C \rightleftharpoons O$  and II:  $C \rightleftharpoons O \rightleftharpoons C$ . Both models have four independent rate constant parameters. A third possible three-state model with six rate

constants, in which all three states are interconnected circularly will not be considered, although such a scheme cannot be ruled out. The equations in Fig.6.16 were used to calculate rate constants for both models given  $\tau_o$ ,  $\tau_{c1}$ ,  $\tau_{c2}$  and  $P_o$ . Rate constants thus calculated are given in Table 4.

In order to verify that the two models and their corresponding rate constants represent reasonable descriptions of actual channel behaviour at  $\text{pH}_i$  7.3, simulations using these rate constants were performed in hardware using the QS-100 (see Chapter 1 for details). Since this device is limited to linear models with discrete state lifetimes and forward/backward transition probabilities, settings were chosen which yielded rate constants closest to the observed values. Examples of synthesized activity, produced by running these models, are shown in Fig.6.17. Gaussian noise from a different source was added to give artistic verisimilitude to otherwise bald and unconvincing traces, and all traces were low-pass filtered with  $f_c = 500\text{Hz}$ . The original trace is also reproduced here for comparison. That all three traces have a similar appearance suggests that the kinetic behaviour of the cardiac channel may be described by both models I (CCO) and II (COC) equally well. Simulated activity was analyzed in the same way as the original recording. The results, which are given in Table 5, show reasonably good agreement between real and model time constants.

When  $\text{pH}_i$  was lowered to 6.0, a rapid flickering of the cardiac channel away from the open channel current level was evident from both the original recording (Fig.6.6B) and from the skew in the corresponding amplitude histogram (Fig.6.12, lower panel). These altered kinetics were not associated with a significant fall in  $P_o$ . The question arises as to whether this pattern of activity could be

Model I:



$$\alpha = 1 / \tau_o$$

$$\beta = (1/\tau_{c1} + 1/\tau_{c2}) - (1-P_o) \cdot \tau_o / (P_o \cdot \tau_{c1} \cdot \tau_{c2})$$

$$k_+ = 1 / (\tau_{c1} \cdot \tau_{c2} \cdot \beta)$$

$$k_- = (1-P_o) \cdot \tau_o / (P_o \cdot \tau_{c1} \cdot \tau_{c2}) - k_+$$

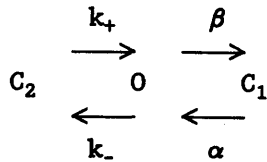
$$\tau_o = 1 / \alpha$$

$$\tau_{c1}, \tau_{c2} = (-b \pm \sqrt{(b^2 + 4 \cdot c)}) / 2$$

$$\text{where } b = -(\beta + k_+ + k_-), \quad c = \beta \cdot k_+$$

$$P_o = 1 / (1 + (\alpha/\beta) \cdot (1 + (k_-/k_+)))$$

Model II:



$$\alpha = 1 / \tau_{c1}$$

$$\beta = (\tau_o - P_o \cdot (\tau_o - \tau_{c2})) / (P_o \cdot \tau_o \cdot (\tau_{c2} - \tau_{c1}))$$

$$k_+ = 1 / \tau_{c2}$$

$$k_- = (P_o \cdot (\tau_o + \tau_{c1}) - \tau_o) / (P_o \cdot \tau_o \cdot (\tau_{c2} - \tau_{c1}))$$

$$\tau_o = 1 / (\beta + k_-)$$

$$\tau_{c1} = 1 / \alpha$$

$$\tau_{c2} = 1 / k_+$$

$$P_o = \alpha \cdot k_+ / ((k_+ + k_-) \cdot (\alpha + \beta) - \beta \cdot k_-)$$

Figure 6.16. Equations relating time constants and rate constants for linear kinetic models with open one and two closed states. Model I equations were taken from the Appendix in Kameyama *et al.* (1983). Model II equations were derived using the equation for  $P_o$  in Sakmann *et al.* (1984b, Eq.20).

Table 4. Rate constants derived from analysis of  $K_{inw}$  channel at  $pH_i$  7.3. Using equations of Fig.6.15, rate constants for CCO and COC kinetic models were calculated for time constants estimated from analysis of channel activity at -60mV. The closest model (simulated) rate constants are also given. Units of all value are  $s^{-1}$ .

|          |           | $k_-$ | $k_+$ | $\alpha$ | $\beta$ |
|----------|-----------|-------|-------|----------|---------|
| Model I  | real      | 50.4  | 41.5  | 7.4      | 255     |
|          | simulated | 59.3  | 59.2  | 7.4      | 178     |
| Model II | real      | 1.53  | 33.8  | 313      | 5.8     |
|          | simulated | 1.85  | 29.6  | 475      | 5.6     |

Table 5. Kinetic analysis of real and simulated channel activity at  $pH_i$  7.3. All recordings were filtered at 750Hz and digitized at 5kHz. 30s of real recording at -60mV and 120s of simulated activity was analyzed.

|          | $\hat{t}_o$<br>(ms) | $\hat{t}_c$<br>(ms) | $P_o$ | $\tau_o$<br>(ms) | $\tau_{c1}$<br>(ms) | Area <sub>1</sub><br>(%) | $\tau_{c2}$<br>(ms) | Area <sub>2</sub><br>(%) |
|----------|---------------------|---------------------|-------|------------------|---------------------|--------------------------|---------------------|--------------------------|
| Real     | 146                 | 10.2                | 0.935 | 136              | 3.19                | 84                       | 29.6                | 23                       |
| Model I  | 135                 | 11.4                | 0.92  | 135              | 4.04                | 58                       | 22.2                | 43                       |
| Model II | 131                 | 9.15                | 0.93  | 135              | 2.32                | 79                       | 38.7                | 24                       |

Table 6. Model rate constants for simulated activity at  $pH_i$  6.0. (Units  $s^{-1}$ ).

|          | $k_-$ | $k_+$ | $\alpha$ | $\beta$ |
|----------|-------|-------|----------|---------|
| Model I  | 61.0  | 59.2  | 118      | 3850    |
| Model II | 1.85  | 29.6  | 3910     | 57      |

Table 7. Mean open and closed times, and open probability of real and simulated activity at  $pH_i$  6.0. 25s of recording of real activity at -60mV was filtered at 750Hz and digitized at 5kHz. 30s of simulated activity was digitized at 5kHz without filtering.

|          | $\hat{t}_o$<br>(ms) | $\hat{t}_c$<br>(ms) | $P_o$ |
|----------|---------------------|---------------------|-------|
| Real     | 33.2                | 3.51                | 0.935 |
| Model I  | 8.98                | 0.551               | 0.94  |
| Model II | 18.8                | 1.33                | 0.93  |

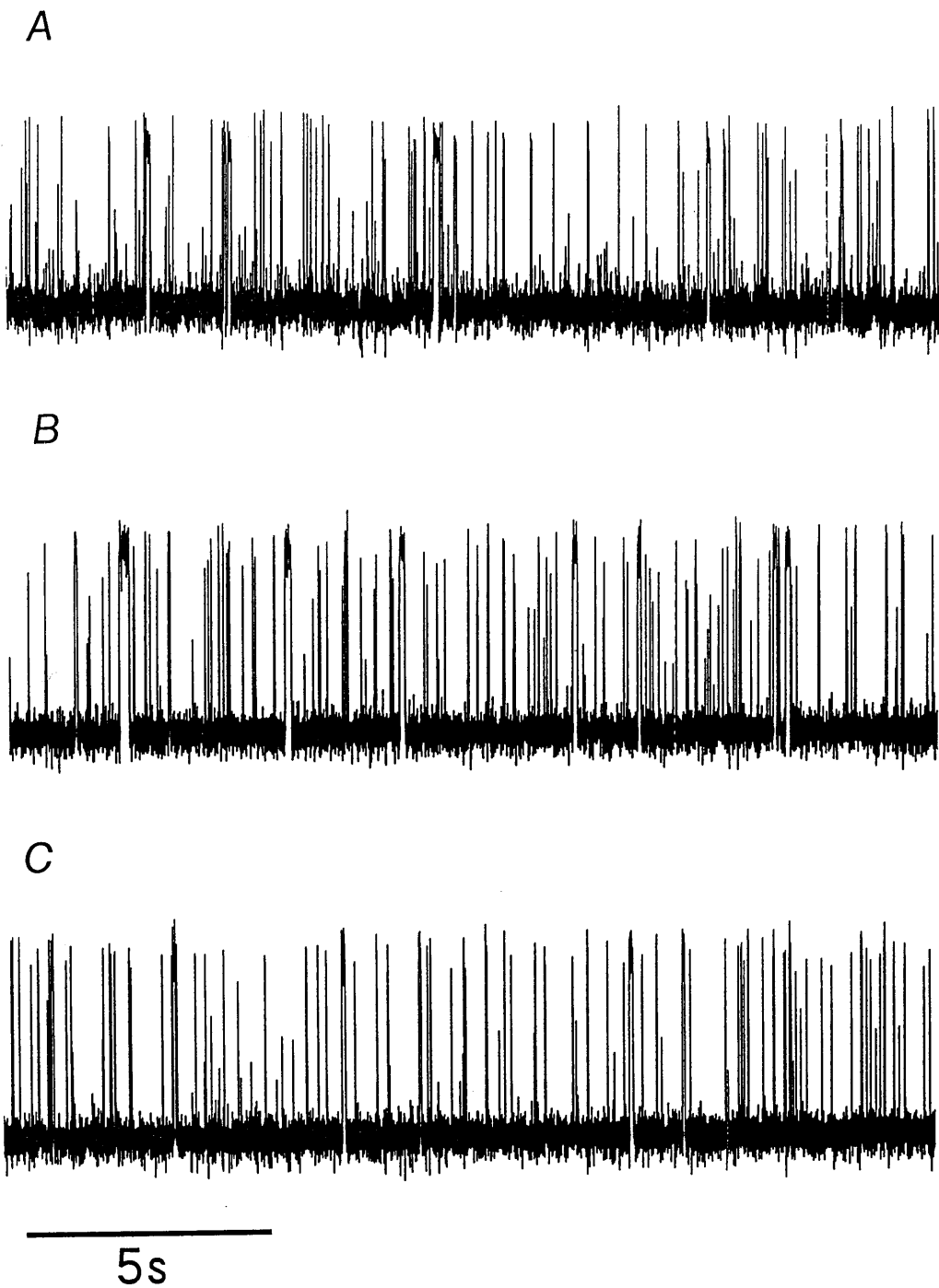


Figure 6.17. Real and simulated activity at  $\text{pH}_i$  7.3. A, section of recording of  $K_{\text{inw}}$  channel activity at  $V_h$  -60mV. B, channel activity simulated with CCO model. C, channel activity simulated with COC model. Model rate constants are given in Table 4.

produced by the two models above simply by changing one or more rate constants, or whether one would be required to introduce additional closed time components. Altering a single rate constant produces a change in  $P_o$ , so to maintain  $P_o$  the ratio of rate constants corresponding to forward and backward transitions were also kept as near constant as possible. After some experimentation, it was found that raising the pair of rate constants for transitions between the open state and the shorter lived closed state ( $C_1$ ) in both models ( $\alpha$  &  $\beta$ ) produced simulated activity which, after filtering, resembled the original recording at  $\text{pH}_i$  6.0. No adjustment of the rates of transition between 0 and the longer lived closed state ( $C_2$ ) ( $k_+$  or  $k_-$ ) was required. Example traces and corresponding rate constants are presented with the original trace in Fig.6.18. In model I,  $\alpha$  and  $\beta$  were increased by factors of 16 and 22 respectively; in the case of model II they were increased by a factors of 8 and 10 (Table 6).

Time constants estimated from simulated activity without filtering are given in Table 7. When  $\hat{t}_o$ ,  $\hat{t}_c$  and  $P_o$  obtained in this way are compared with the corresponding figures for the original experiment at  $\text{pH}_i$  6.0, a discrepancy between measured and actual kinetics is apparent: both  $\hat{t}_o$  and  $\hat{t}_c$  are overestimated by factors of 2-6. This is because most of the short closing events are attenuated below the half-amplitude detection threshold by the low-pass filter. However, the error in the estimate of  $P_o$  is less than 5%, because the missed gaps are so short. In general,  $P_o$  is relatively insensitive to the degree of filtering. At  $\text{pH}_i$  7.3, when channel kinetics are relatively slow, errors in the estimation of time constants are much smaller.

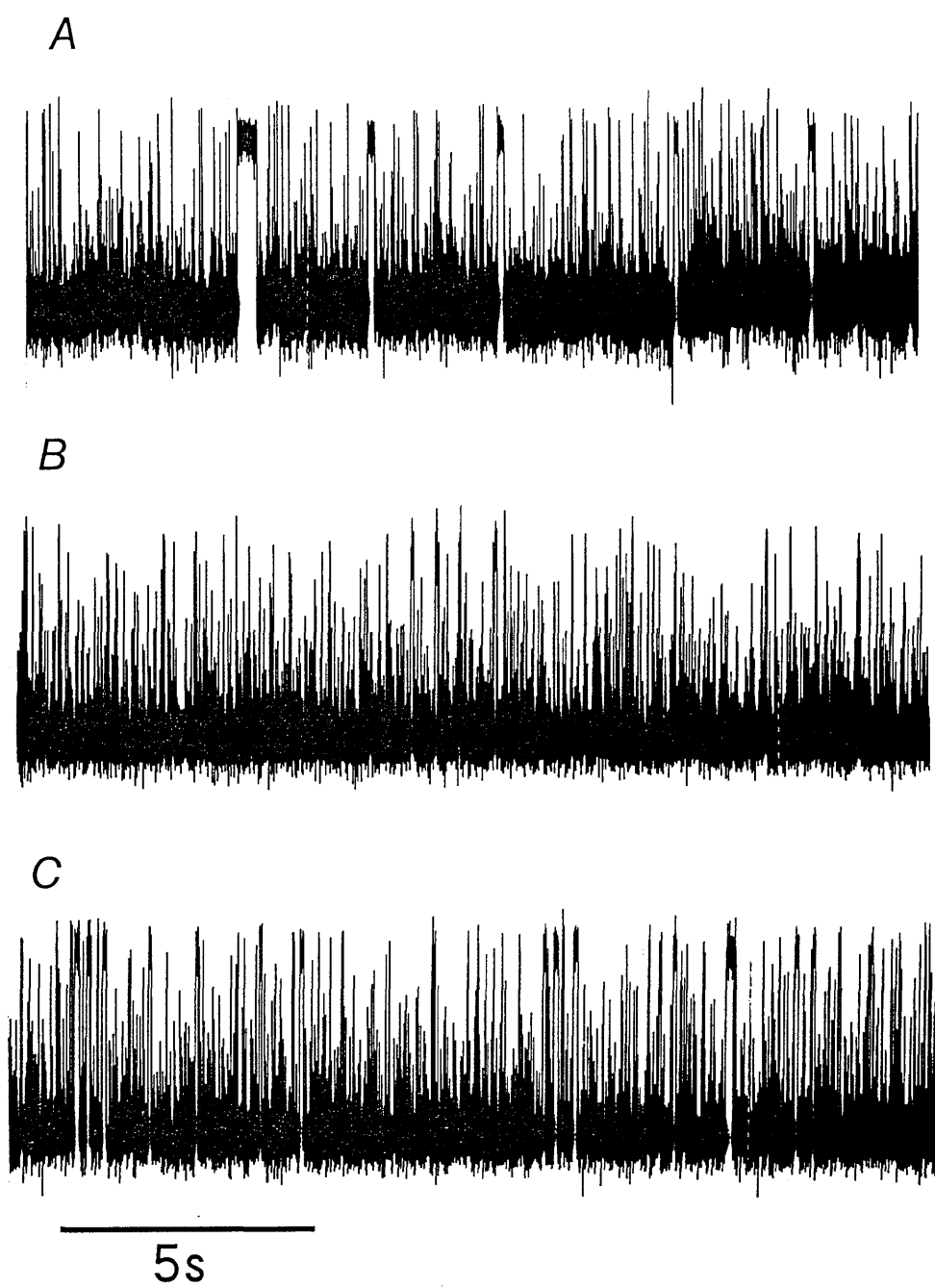


Figure 6.18. Real and simulated activity at  $pH_i$  6.0. A, section of recording of  $K_{inw}$  channel activity at  $V_h$  -60mV. B, channel activity simulated with CCO model. C, channel activity simulated with COC model. Model rate constants are given in Table 6.

The possibility that the reduction in the single channel current, seen when  $\text{pH}_i$  is lowered from 7.3 to 6.0, is due to the incomplete resolution, due to filtering, of rapid transitions between 0 and  $C_1$  described above was also investigated. Since the amplitude of the voltage steps produced by the simulator is a constant, any reduction in simulated  $i$  after filtering would be readily detected. However, there was no measurable reduction with  $f_c = 500\text{Hz}$ , and less than 3% reduction at  $f_c = 50\text{Hz}$ . Therefore, a component not included in the present kinetic model must be invoked to explain the decrease in single channel current seen in these experiments.

#### Functional role of pH-sensitivity of inwardly rectifying channels in cardiac muscle

The present experiments were initiated because the literature, already cited in the introduction to this chapter, suggested that the cardiac  $K_{\text{inw}}$  channel was highly sensitive to  $\text{pH}_i$ . In the event, the present measurements of single channel currents did not bear out the expectation based on the above macroscopic experiments: although the kinetic properties of the  $K_{\text{inw}}$  channels in cardiac muscle were found to be altered by reduction in  $\text{pH}_i$  to 6.5, the mean open probability was little altered by such moderate acidification and the small decrease in single channel conductance would by itself do little to decrease the macroscopic inward current (Fig.6.19). Only when  $\text{pH}_i$  was lowered towards 6.0 did a sizeable decrease in open probability manifest itself, owing to the entrance of channels into the long lasting closed state. It could be that  $K_{\text{inw}}$  channels respond differently in isolated patches than in intact cells; that some factor promoting channel closure in cells is absent in the detached cardiac patch. If so, that factor is unlikely to be of diffusible nature, for patches isolated from skeletal muscle did show a distinct fall in  $P_o$  on acidification even to only pH 6.9. In this

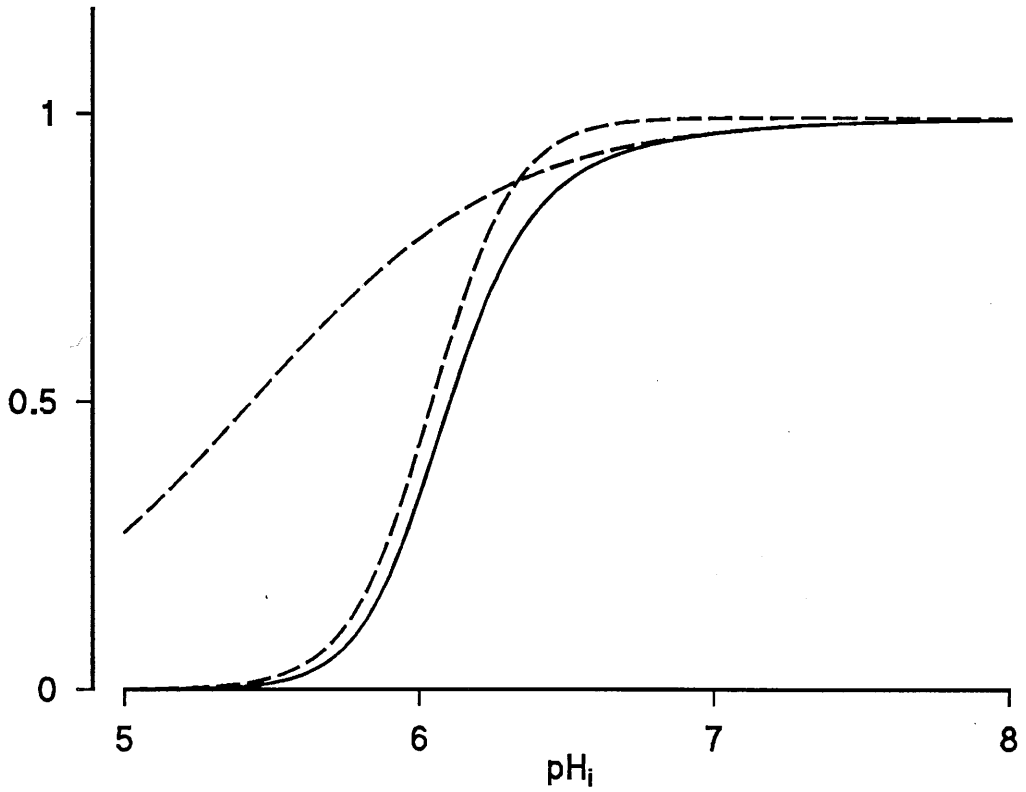


Figure 6.19. Combined  $P_o$ - $pH_i$  and  $i$ - $pH_i$  relationships for cardiac muscle  $K_{inw}$  channel. Curves from Fig.6.7 and Fig.6.14 (dashed lines) were multiplied to obtain curve (solid line) representing overall reduction in current at different  $pH_i$ .

connection, it might be recalled that in detached patches  $K_{inw}$  channels in cardiac muscle differ also from  $K_{inw}$  channels in skeletal muscle in lacking sensitivity to flow. Perhaps the different behaviour of K channels isolated from different muscles arise during patch formation from some difference in the point of detachment between the integral membrane protein which constitutes the channel and elements of the cytoskeleton connected to it. Much more needs to be known about the structure of membrane patches before such possibilities can be meaningfully considered.

Recent experiments on isolated guinea-pig ventricular muscle subjected to simulated ischaemia have shown that  $pH_i$  falls by 0.2 pH units under such conditions (Gasser & Vaughan-Jones, 1990). In total global ischaemia in rat heart intracellular acidification by 1.0 pH unit has been reported (Bailey *et al.*, 1981). In severe ischaemia, therefore, some reduction in  $g_{K,in}$  would be expected on the basis of both macroscopic and microscopic observations. By itself, such a reduction of  $g_K$  would tend to destabilize the membrane so as to promote arrhythmia. However, the tendency towards destabilization may be kept in check through the different response of other types of K channel to a fall in  $pH_i$ .  $K_{ATP}$  channels, for instance, are known to open in response to a fall in  $pH_i$ , both in ventricular myocytes (Lederer & Nichols, 1989) and in skeletal muscle (Davies, 1990). And the recently discovered fatty acid (arachidonic acid) activated K channel may also contribute towards an increase in  $g_K$  since intracellular levels of fatty acids increase during ischaemia and the opening of this channel is enhanced by a fall in  $pH_i$  (Kim & Clapham, 1989; Ordway *et al.*, 1989). The relative importance of these several in parallel K channels in the response of  $g_K$  to a fall in  $pH_i$  needs yet to be determined. As always in physiological research, analysis of the individual components of the

system is not enough: it has to be followed by studies designed to show how these components, in this case the global potassium conductance in the region of the resting potential, are synthesized into a functioning whole.

## REFERENCES

- ADRIAN, R.H. (1964). The potassium and rubidium permeabilities of frog muscle membrane. *Journal of Physiology* 175, 134-159.
- ADRIAN, R.H., CHANDLER, W.K. & HODGKIN, A.L. (1970a). Voltage clamp experiments in striated muscle fibres. *Journal of Physiology* 208, 607-644.
- ADRIAN, R.H., CHANDLER, W.K. & HODGKIN, A.L. (1970b). Slow changes in potassium permeability in skeletal muscle. *Journal of Physiology* 208, 645-668.
- ALLEN, D.G., EISNER, D.A., MORRIS, P.G., PIROLO, J.S. & SMITH, G.L. (1986). Metabolic consequences of increasing intracellular calcium and force production in perfused ferret hearts. *Journal of Physiology* 376, 121-141.
- ATTWELL, D. & EISNER, D.A. (1978). Discrete membrane surface charge distributions. *Biophysical Journal* 24, 869-875.
- BAILEY, I.A., WILLIAMS, S.R., RADDA, G.K. & GADIAN, D.G. (1981). Activity of phosphorylase in total global ischaemia in the rat heart. *Biochemistry Journal* 196, 171-178.
- BEELEER, G.W. & REUTER, H. (1970). Voltage clamp experiments on ventricular myocardial fibres. *Journal of Physiology* 207, 165-190.

- BLATTER, L.A., BURI, A. & McGUIGAN, J.A.S. (1989). Free intracellular magnesium concentration in isolated ferret ventricular muscle and in frog skeletal muscle measured with ion-selective micro-electrodes containing the new magnesium sensor ETH 5214. *Journal of Physiology* 418, 154P.
- BLATTER, L.A. & McGUIGAN, J.A.S. (1986). Free intracellular magnesium concentration in ferret ventricular muscle measured with ion selective micro-electrodes. *Quarterly Journal of Experimental Physiology* 71, 467-473.
- BLATZ, A.L. (1984). Asymmetric proton block of inward rectifier K channels in skeletal muscle. *Pflügers Archiv*. 401, 402-407.
- BLATZ, A.L. & MAGLEBY, K.L. (1983). Single voltage-dependent chloride-selective channels of large conductance in cultured rat muscle. *Biophysical Journal* 43, 237-241.
- BLATZ, A.L. & MAGLEBY, K.L. (1986). Correcting single channel data for missed events. *Biophysical Journal* 49, 967-980.
- BOLL, W. & LUX, H.D. (1985). Action of organic antagonists on neuronal calcium currents. *Neuroscience Letters* 56, 335-339.
- BOVELL, D., BURTON, F.L., HUTTER, O.F. & TIAN, L.J. (1990). Effects of decreased internal pH on inwardly rectifying K channels in guinea pig ventricular cell membrane. *Journal of Physiology* 429, 111P.

- BROWN, K.M. & DENNIS, J.S. (1972). Derivative free analogs of the Levenberg-Marquadt and Gauss algorithms for non-linear least squares approximation. *Numerische Mathematik* 18, 289-297.
- BURTON, F.L., DÖRSTELMANN, U. & HUTTER, O.F. (1988). Single-channel activity in sarcolemmal vesicles from human and other mammalian muscles. *Muscle & Nerve* 11, 1029-1038.
- BURTON, F.L. & HUTTER, O.F. (1988). The different actions of low intracellular pH and of formaldehyde on inwardly rectifying potassium channels from rat sarcolemmal vesicles. *Journal of Physiology* 410, 17P.
- BURTON, F.L. & HUTTER, O.F. (1990). Sensitivity to flow of intrinsic gating in inwardly rectifying potassium channel from mammalian skeletal muscle. *Journal of Physiology* 424, 253-261.
- CALDWELL, J.H., CAMPBELL, D.T. & BEAM, K.G. (1986). Na channel distribution in vertebrate skeletal muscle. *Journal of General Physiology* 87, 907-932.
- COLQUHOUN, D. & SIGWORTH, F.J. (1983). Fitting and statistical analysis of single-channel records. In: *Single-Channel Recording*, ed. SAKMANN, B. & NEHER, E. pp. 191-263. New York & London: Plenum.
- COULOMBE, A., DUCLOHIER, H., CORABOEUF, E. & TOUZET, N. (1987). Single chloride-permeable channels of large conductance in cultured cardiac cells of new-born rats. *European Biophysical Journal* 14, 155-162.

- DAVIES, N.W. (1990). Modulation of ATP-sensitive K<sup>+</sup> channels in skeletal muscle by intracellular protons. *Nature (Lond.)* 343, 375-377.
- DeCOURSEY, T.E., DEMPSTER, J. & HUTTER, O.F. (1984). Inward rectifier current noise in frog skeletal muscle. *Journal of Physiology* 349, 299-327.
- DEITMER, J.W. & ELLIS, D. (1980). Interactions between the regulation of the intracellular pH and sodium activity of sheep cardiac Purkinje fibres. *Journal of Physiology* 304, 471-488.
- EDSALL, J.T. & WYMAN, J. (1958). *Biophysical Chemistry Vol.1*. New York: Academic Press.
- FUKUSHIMA, Y. (1982). Blocking kinetics of the anomalous potassium rectifier of tunicate eggs studied by single channel recordings. *Journal of Physiology* 331, 311-331.
- GASSER, R.N.A. & VAUGHAN-JONES, R.D. (1990). Mechanism of potassium efflux and action potential shortening during ischaemia in isolated mammalian cardiac muscle. *Journal of Physiology* 431, 713-741.
- GAY, L.A. & STANFIELD, P.R. (1977). Cs causes a voltage-dependent block of inward K currents in resting skeletal muscle fibres. *Nature (Lond.)* 267, 169-170.
- GRAY, P.T.A, BEVAN, S. & RITCHIE, J.M. (1984). High conductance anion-selective channels in rat cultured Schwann cells. *Proceedings of the Royal Society of London.B.* 221, 395-409.

- GUHURAY, F. & SACHS, F. (1984). Stretch-activated single ion channel currents in tissue-cultured embryonic chick skeletal muscle. *Journal of Physiology* 352, 685-701.
- HAGIWARA, S., MIYAZAKI, S., MOODY, W. & PATLAK, J. (1978). Blocking effects of barium and hydrogen ions on the potassium current during anomalous rectification in the starfish egg. *Journal of Physiology* 279, 167-185.
- HAGIWARA, S., MIYAZAKI, S. & ROSENTHAL, N.P. (1976). Potassium current and the effect of cesium on this current during anomalous rectification of the egg cell membrane of the starfish. *Journal of General Physiology* 67, 621-638.
- HAGIWARA, S. & TAKAHASHI, K. (1974). The anomalous rectification and cation selectivity of the membrane of a starfish egg cell. *Journal of Membrane Biology* 18, 61-80.
- HAGIWARA, S. & YOSHII, M. (1979). Effects of internal potassium and sodium on the anomalous rectification of the starfish egg as examined by internal perfusion. *Journal of Physiology* 292, 251-265.
- HALL, A.E., HUTTER, O.F. & NOBLE, D. (1963). Current-voltage relations of Purkinje fibres in sodium-deficient solutions. *Journal of Physiology* 166, 225-240.
- HAMILL, O.P., MARTY, A., NEHER, E., SAKMANN, B. & SIGWORTH, F.J. (1981). Improved patch-clamp techniques for high-resolution

- current recording from cells and cell-free membrane patches. *Journal of Physiology* 391, 85-100.
- HAMILL, O.P. & SAKMANN, B. (1981). A cell-free method for recording single channel currents from biological membranes. *Journal of Physiology* 312, 41-42P.
- HARVEY, R.D. & TEN EICK, R.E. (1989). On the role of sodium ions in the regulation of the inwardly-rectifying potassium conductance in cat ventricular myocytes. *Journal of General Physiology* 94, 329-348.
- HESTRIN, S. (1981). The interaction of potassium with the activation of anomalous rectification in frog muscle. *Journal of Physiology* 317, 497-508.
- HILLE, B. & SCHWARZ, W. (1978). Potassium channels as multi-ion single-file pores. *Journal of General Physiology* 72, 409-442.
- HORIE, M. & IRISAWA, H. (1989). Dual effects of intracellular magnesium on muscarinic potassium channel current in single guinea-pig atrial cells. *Journal of Physiology* 408, 313-332.
- HORIE, M., IRISAWA, H. & NOMA, A. (1987). Voltage-dependent magnesium block of adenosine-triphosphate-sensitive potassium channel in guinea-pig ventricular cells. *Journal of Physiology* 387, 251-272.
- HUTTER, O.F. & NOBLE, D. (1960). The chloride conductance of frog skeletal muscle. *Journal of Physiology* 151, 89-102.

- HUTTER, O.F. & WARNER, A.E (1972). The voltage dependence of the chloride conductance of frog skeletal muscle. *Journal of Physiology* 151, 89-102.
- ISENBERG, G. & KLÖCKNER, U. (1982). Calcium tolerant ventricular myocytes prepared by preincubation in a "KB medium". *Pflügers Archiv.* 395, 6-18.
- JORDAN, P.C. (1987). How pore mouth charge distributions alter the permeability of transmembrane ionic channels. *Biophysical Journal* 51, 297-311.
- JUNG, D.W., APEL, L. & BRIERLEY, G.P. (1990). Matrix free  $Mg^{2+}$  changes with metabolic state in isolated heart mitochondria. *Biochemistry* 29, 4121-4128.
- JUNG, F., SONG, M.J. & SACHS, F. (1987). Patch clamp anatomy: high voltage electron microscopy of in vivo patches. *Biophysical Journal* 51, 517a.
- KAMEYAMA, M., KIYOSUE, T. & SOEJIMA, M. (1983). Single channel analysis of the inward rectifier K current in the rabbit ventricular cells. *Japanese Journal of Physiology* 33, 1039-1056.
- KANDEL, E.R. & TAUC, L. (1966). Anomalous rectification in the metacerebral giant cells and its consequences for synaptic transmission. *Journal of Physiology* 183, 287-304.
- KATZ, B. (1949). Les constantes électriques de la membrane du muscle. *Archives des Sciences Physiologiques* 2, 285-299.

- KIM, D. & CLAPHAM, D.E. (1989). Potassium channels in cardiac cells activated by arachidonic acid and phospholipids. *Science* 244, 1174-1176.
- KIRBER, M.T., ORDWAY, R.W., SINGER, J.J. & WALSH, J.V.JR. (1990). Flow and extracellular  $Ca^{++}$  activate a  $K^+$ -channel in smooth muscle cells. *Biophysical Journal* 57, 309a.
- KIRBER, M.T., ORDWAY, R.W., WALSH, J.V.JR. & SINGER, J.J. (1989). A potassium-selective ion channel in gastric smooth muscle cells is activated by flow and  $Ca^{2+}$  at the extracellular surface. *Journal of General Physiology* 94, 36-37a.
- KURACHI, Y. (1985). Voltage-dependent activation of the inward-rectifier potassium channel in the ventricular cell membrane of guinea-pig heart. *Journal of Physiology* 366, 365-385.
- LAMB, T.D. (1984). A digital tape-recorder suitable for fast physiological signals. *Journal of Physiology* 360, 5P.
- LEDERER, W.J. & NICHOLS, C.G. (1989). Nucleotide modulation of the activity of rat heart ATP-sensitivity  $K^+$  channels in isolated membrane patches. *Journal of Physiology* 419, 193-211.
- LEECH, C.A. & STANFIELD, P.R. (1981). Inward rectification in frog skeletal muscle fibres and its dependence on membrane potential and external potassium. *Journal of Physiology* 319, 295-309.

- MAGLEBY, K.L. & PALLOTTA, B.S. (1983). Burst kinetics of single calcium-activated potassium channels in cultured rat muscle. *Journal of Physiology* 344, 605-623.
- MARTELL, A.E. & SMITH, R.M. (1974). *Critical Stability Constants*, Vol. 1. New York: Plenum.
- MATSUDA, H. (1988). Open-state substructure of inwardly rectifying potassium channels revealed by magnesium block in guinea-pig heart cells. *Journal of Physiology* 397, 237-258.
- MATSUDA, H., SAIGUSA, A. & IRISAWA, H. (1987). Ohmic conductance through the inwardly rectifying K channel and blocking by internal  $Mg^{2+}$ . *Nature (Lond.)* 325, 156-159.
- MATSUDA, H. & STANFIELD, P.R. (1989). Single inwardly rectifying potassium channels in cultured muscle cells from rat and mouse. *Journal of Physiology* 414, 111-124.
- MAZZANTI, M. & DIFRANCESCO, D. (1989). Intracellular Ca modulates K-inward rectification in cardiac myocytes. *Pflügers Archiv.* 413, 322-324.
- McMANUS, O.B., BLATZ, A.L. & MAGLEBY, K.L. (1987). Sampling, log binning, fitting, and plotting durations of open and shut intervals from single channels and the effects of noise. *Pflügers Archiv.* 410, 530-553.
- MILLER, C. (1985). Charybdotoxin, a protein inhibitor of single  $Ca^{2+}$ -activated  $K^+$  channels from mammalian skeletal muscle. *Nature (Lond.)* 313, 316-318.

- MOODY, W.J. & HAGIWARA, S. (1982). Block of inward rectification by intracellular  $H^+$  in immature oocytes of the starfish *Mediaster aequalis*. *Journal of General Physiology* 79, 115-130.
- MORRIS, C.E. (1990). Mechanosensitive ion channels. *Journal of Membrane Biology* 113, 93-107.
- NELSON, D.J., TANG, J.M. & PALMER, L.G. (1984). Single-channel recordings of apical membrane chloride conductance in A6 epithelial cells. *Journal of Membrane Biology* 80, 81-89.
- OHMORI, H. (1978). Inactivation kinetics and steady-state current noise in the anomalous rectifier of tunicate egg cell membranes. *Journal of Physiology* 281, 77-99.
- OHMORI, H., YOSHIDA, S. & HAGIWARA, S. (1981). Single  $K^+$  channel currents of anomalous rectification in cultured rat myotubes. *Proceedings of the National Academy of Sciences USA* 78, 4960-4964.
- OLESEN, S-P., CLAPHAM, D.E. & DAVIES, P.F. (1988). Haemodynamic shear stress activates a  $K^+$  current in vascular endothelial cells. *Nature (Lond.)* 331, 168-170.
- OLIVA, C., COHEN, I.S. & PENNEFATHER, P. (1990). The mechanism of rectification of  $i_{K1}$  in canine Purkinje myocytes. *Journal of General Physiology* 96, 299-318.

- ORDWAY, R.W., WALSH, J.V. & SINGER, J.J. (1989). Arachidonic acid and other fatty acids directly activated potassium channels in smooth muscle cells. *Science* 244, 1176-1179.
- PAN, J.W., HAMM, J.R., ROTHMAN, D.L. & SHULMAN, R.G. (1988). Intracellular pH in human skeletal muscle by <sup>1</sup>H NMR. *Proceedings of the National Academy of Sciences USA* 85, 7836-7839.
- POWELL, T., TERRAR, D.A. & TWIST, V.W. (1980). Electrical properties of individual cells isolated from adult rat ventricular myocardium. *Journal of Physiology* 302, 131-153.
- RENAUD, J.M. (1989). The effect of lactate on intracellular pH and force recovery of fatigued sartorius muscles of the frog, *Rana pipiens*. *Journal of Physiology* 416, 31-47.
- ROUGIER, O., VASSORT, G. & STÄMPFLI, R. (1968). Voltage clamp experiments on frog atrial heart muscle fibres with the sucrose gap technique. *Pflügers Archiv*. 301, 91-108.
- ROUX, B. & SAUVÉ, R. (1985). A general solution to the time interval omission problem applied to single channel analysis. *Biophysical Journal* 48, 149-158.
- SAKMANN, B. & TRUBE, G. (1984a). Conductance properties of single inwardly rectifying potassium channels in ventricular cells from guinea-pig heart. *Journal of Physiology* 347, 641-657.

- SAKMANN, B. & TRUBE, G. (1984b). Voltage-dependent inactivation of inwardly-rectifying single-channel currents in the guinea-pig heart cell membrane. *Journal of Physiology* 347, 659-683.
- SCHWARZ, W. & KOLB, H-A. (1984). Voltage-dependent kinetics of an anionic channel of large unit conductance in macrophages and myotube membranes. *Pflügers Archiv.* 402, 281-291.
- SILVER, M.R. & DeCOURSEY, T.E. (1990). Intrinsic gating of inward rectifier in bovine pulmonary artery endothelial cells in the presence or absence of internal  $Mg^{2+}$ . *Journal of General Physiology* 96, 109-133.
- SMITH, G.L. (1983). A functional and structural study of cardiac muscle subjected to membrane disruption techniques. Glasgow University: PhD.Thesis.
- SPRUCE, A.E., STANDEN, N.B. & STANFIELD, P.R. (1985). Voltage-dependent ATP-sensitive potassium channels of skeletal muscle membrane. *Nature (Lond.)* 316, 736-738.
- SPRUCE, A.E., STANDEN, N.B. & STANFIELD, P.R. (1987). Studies of the unitary properties of adenosine-5-triphosphate-regulated potassium channels from frog skeletal muscle. *Journal of Physiology* 382, 213-236.
- STANDEN, N.B. & STANFIELD, P.R. (1978). A potential and time-dependent blockade of inward rectification in frog skeletal muscle fibres by barium and strontium ions. *Journal of Physiology* 280, 169-191.

- STANDEN, N.B. & STANFIELD, P.R. (1979). Potassium depletion and sodium block of potassium currents under hyperpolarization in frog sartorius muscle. *Journal of Physiology* 294, 497-520.
- STANDEN, N.B. & STANFIELD, P.R. (1980). Rubidium block and rubidium permeability of the inward rectifier of frog skeletal muscle fibres. *Journal of Physiology* 304, 415-435.
- STANDEN, N.B., STANFIELD, P.R., WARD, T.A. & WILSON, S.W. (1984). A new preparation for recording of single-channel currents from skeletal muscle. *Proceedings of the Royal Society of London.B.* 221, 455-464.
- TRUBE, G., SAKMANN, B. & TRAUTWEIN, W. (1981). Inward rectifying potassium channels recorded from isolated heart cells by the patch clamp method. *Pflügers Archiv.* 391, R28.
- VANDENBERG, C.A. (1987). Inward rectification of a potassium current in cardiac ventricular cells depends on internal magnesium. *Proceedings of the National Academy of Sciences USA* 84, 2560-2564.
- WOLL, K.H., LEIBOWITZ, M.D. & HILLE, B. (1986). Chloride channels in adult frog skeletal muscle. *Biophysical Journal* 49, 413a.
- WOLL, K.H., LEIBOWITZ, M.D., NEUMCKE, B. & HILLE, B. (1987). A high-conductance anion channel in adult amphibian skeletal muscle. *Pflügers Archiv.* 410, 632-640.
- YELLEN, G. (1982). Single  $\text{Ca}^{2+}$ -activated nonselective cation channels in neuroblastoma. *Nature (Lond.)* 296, 357-359.